

The Messenger



No. 142 – December 2010

Improving network links to Paranal
The VLT Adaptive Optics Facility
Multiple populations in globular clusters
Dissecting the super cluster Westerlund 1



Enabling Virtual Access to Latin-American Southern Observatories

Giorgio Filippi¹

¹ ESO

EVALSO (Enabling Virtual Access to Latin-American Southern Observatories) is an international consortium of nine astronomical organisations and research network operators, part-funded under the European Commission FP7, to create and exploit high-speed bandwidth connections to South American observatories. A brief description of the project is presented. The EVALSO Consortium inaugurated a fibre link between the Paranal Observatory and international networks on 4 November 2010 capable of 10 Gigabit per second.

It should come as no surprise that the remoteness which makes a site excellent for optical–near-infrared astronomy also conflicts with the need for good connections to a fast communications infrastructure. With the constant increase in data rates and, more generally, in communications needs, limits in bandwidth may impede the efficiency of operations, and hinder future expansion. For the ESO Paranal Observatory and the Ruhr-Universität Bochum Observatorio de Cerro Armazones (OCA), this conflict will soon cease to exist. On 4 November 2010, at the ESO Vitacura offices in Santiago, the EVALSO Consortium formally inaugurated a fibre-based system capable of 10 Gigabit per second (Gbps) to connect the two observatories to the international academic networks.

The partners of EVALSO are the Università degli Studi di Trieste, Italy; the European Southern Observatory; Ruhr-Universität Bochum (RUB), Germany; Consortium Gestione Ampliamento Rete Ricerca (GARR), Italy; Universiteit Leiden, the Netherlands; Istituto Nazionale di Astrofisica (INAF), Italy; Queen Mary, University of London, United Kingdom; Cooperación Latino-Americana de Redes Avanzadas (CLARA), Uruguay; and Red Universitaria Nacional (REUNA), Chile. More details of the overall project and its members are available at the EVALSO website¹.

The project focuses on two aspects:
 – building an infrastructure to connect observatory sites efficiently to the European astronomical community by linking to the network infrastructures created in recent years with EC support (in particular ALICE² and GEANT³);
 – promoting research activities to enable and validate new ways to interact with the remote facilities made available by high-bandwidth communications. More details can be found in Filippi et al. (2010).

The present article focuses on the communications infrastructure, which is broken down into two major components: the optical paths and the communications equipment. The locations served by the new high capacity infrastructure are: the ESO Paranal Observatory and OCA, about 1200 km north of Santiago; the REUNA offices in Antofagasta (about 120 km from Paranal); and the ESO and REUNA offices in Santiago de Chile.

The communications technology

To guarantee current needs while making provision for future performance demands, the EVALSO project has opted for optical fibre network paths that could be procured from commercial installations or, where none existed, created new ones. The use of dark fibres (i.e. physical fibres whose full capacity is available) and, where this is not economically possible, use of reserved wavelengths, provides an optimal and flexible infrastructure for the traffic management needs of today, with a clear potential for future growth. In order to exploit these optical communications most effectively, DWDM (dense wavelength division multiplexing) technology was selected for the communications equipment.

The optical path infrastructure (numbers refer to Figure 1) consists of:

- new fibre cables (1 and 4) that serve the Paranal Observatory and OCA sites up to Ruta 5 at La Varilla;
- a pair of fibres from the existing installation along Ruta 5 to relay from La Varilla to Antofagasta;
- fixed wavelength communication (2) between the telecommunications provider Point of Presence (TELCO PoP) in Antofagasta and Santiago;
- dark fibres (5) between the TELCO PoP and the end points in Santiago, namely ESO's Vitacura offices and the REUNA office in Providencia;
- and housing space for EVALSO equipment at the TELCO PoP in Antofagasta (6) and Santiago (3).

In order to connect the two observatories to the Chilean TELCO infrastructure, new cables had to be installed in the Atacama Desert for a total of about 100 km. The cables were of the type used for direct underground installation and the first cable, approximately 80 km long, was laid down between Paranal and the point of connection to the telecommunications provider's backbone, situated along the Panamericana (Ruta 5, the Pan-American Highway) at La Varilla. The second, approximately 20 km long, is between OCA and an intermediate point on the first cable. These installations established an optical fibre path between the two observatories and, together with the portion of fibre procured from the commercial network, to Antofagasta.

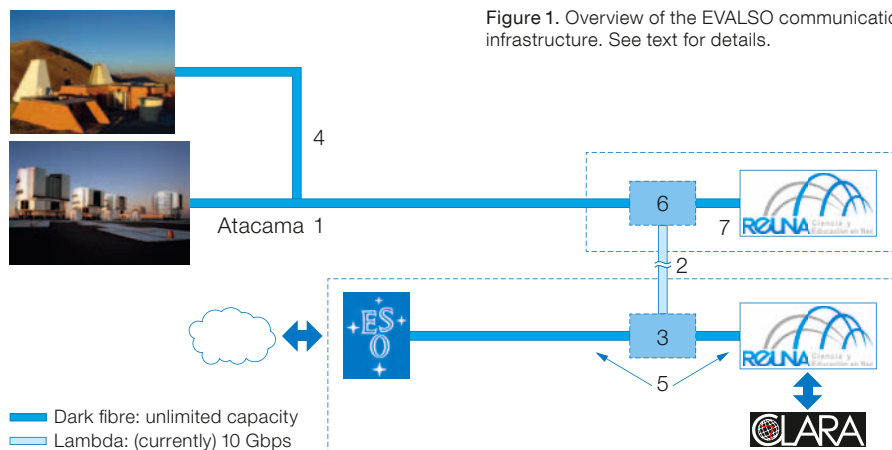


Figure 1. Overview of the EVALSO communications infrastructure. See text for details.

Underground installation is not only more secure, but limits the visual impact on the pristine desert environment. A special machine cuts a trench about 20 cm wide and 80 to 120 cm deep, depending on the nature of the soil (see Figure 2). The cable is suitable for direct installation without ducts (Figure 2). As reels of 4 km length are used, splicing boxes have to be placed in chambers at the same distance. The construction also crosses existing roads and a gas pipeline. A movie of the cable-laying process is included in the ESO podcast⁴. The distance from the end of the new cable, at the La Varilla crossroads, to the nearest installation of the telecommunications provider in Antofagasta is about 50 km. This distance has been covered by procuring a fibre pair from the existing facility. A fixed wavelength channel (LAMBDA), capable of carrying 10 Gbps, links Antofagasta and Santiago.

EVALSO equipment is installed at five nodes. At Paranal this node receives the traffic to and from both observatories. For each user community separate sub-channels are used to transport the traffic to its final destination. The aggregation point for the traffic handled by REUNA and from the observatories is sited at Antofagasta. Here the bundled (but not mixed!)



Figure 2. Two views of the work involved in laying the EVALSO optical cable from Paranal to link with the existing network infrastructure; upper image: cutting the trench; lower: laying the cable in the trench.

traffic is passed to the provider equipment for the approximately 1200 km section over the LAMBDA cable to Santiago. The LAMBDA termination in Santiago is the distribution point for the traffic coming from the northern region of Chile. Using local dark fibres, the Paranal traffic is delivered to the ESO Vitacura offices and the REUNA traffic to the REUNA offices in Santiago, and from there to the commercial and academic networks.

Project history and inauguration

The EVALSO project team (SA1 work package) began work in 2008 by taking over an initial market survey, which gave enough confidence in terms of technical and economic feasibility to continue with the project. Based on this input, the SA1 team detailed the specification of the final system and entered the procurement phase, assigning the optical paths to ESO (in coordination with OCA for their part of the connectivity) and the DWDM equipment to REUNA. The complex procurement phase took nearly the whole of 2009, leading to the final decision and the start of engineering in the last quarter. The installation of the new cables as well as the configuration and integration of the existing commercial parts, both paths and DWDM equipment, kept the team busy until October 2010, when the first transmission test could be made.

The EVALSO formal inauguration took place in a ceremony at the ESO Offices in Santiago (see the picture on the *Astronomical News* section page 40). The event was attended by a number of ambassadors and diplomats from EU countries, a very large delegation from the EC, high level officials from ESO, ALMA and other organisations. The event was opened by a short speech by the ESO Director General, Tim de Zeeuw, and there were speeches from Josè Palacios (REUNA president), Rolf Chini (RUB-OCA), Massimo Tarengi (ESO representative in Chile), Mario Campolargo (EC) and Ambassador Fernando Schmidt Ariztía (vice-minister of Foreign Affairs of Chile). Fernando Liello, Università degli Studi di Trieste, EVALSO Project Coordinator, explained the EVALSO framework and its relations with the overall academic research networks. The technical aspects of the EVALSO infrastructure were

illustrated by Giorgio Filippi, ESO, for the optical paths, and Sandra Jaque, REUNA, for the DWDM equipment.

The overall system is now available for the research activities of the EVALSO Consortium. There are three key areas that the project will develop:

- Fast and efficient access to data: at present, data collected at the Paranal Observatory can take anywhere from hours to weeks before it becomes available for use in Europe. EVALSO will allow data to be transferred in near real time.
- Virtual presence at the observatories: the bandwidth offered by EVALSO makes a “virtual presence” at the observatories possible.
- New possibilities in observing: EVALSO can serve several of the needs of its partner members, for example, by operating robotic telescopes on Cerro Armazones, supporting their use for educational purposes and improving the scientific exploitation of the capabilities of both observatories through innovative operations schemes, which will act as pathfinders for the operation of future facilities like the European Extremely Large Telescope.

As a member of the Consortium, ESO is planning to integrate the system into its communications infrastructure in the coming months, leading to its use in regular operation of the telescopes on Paranal.

Results of these developments will be reported in a future article.

References

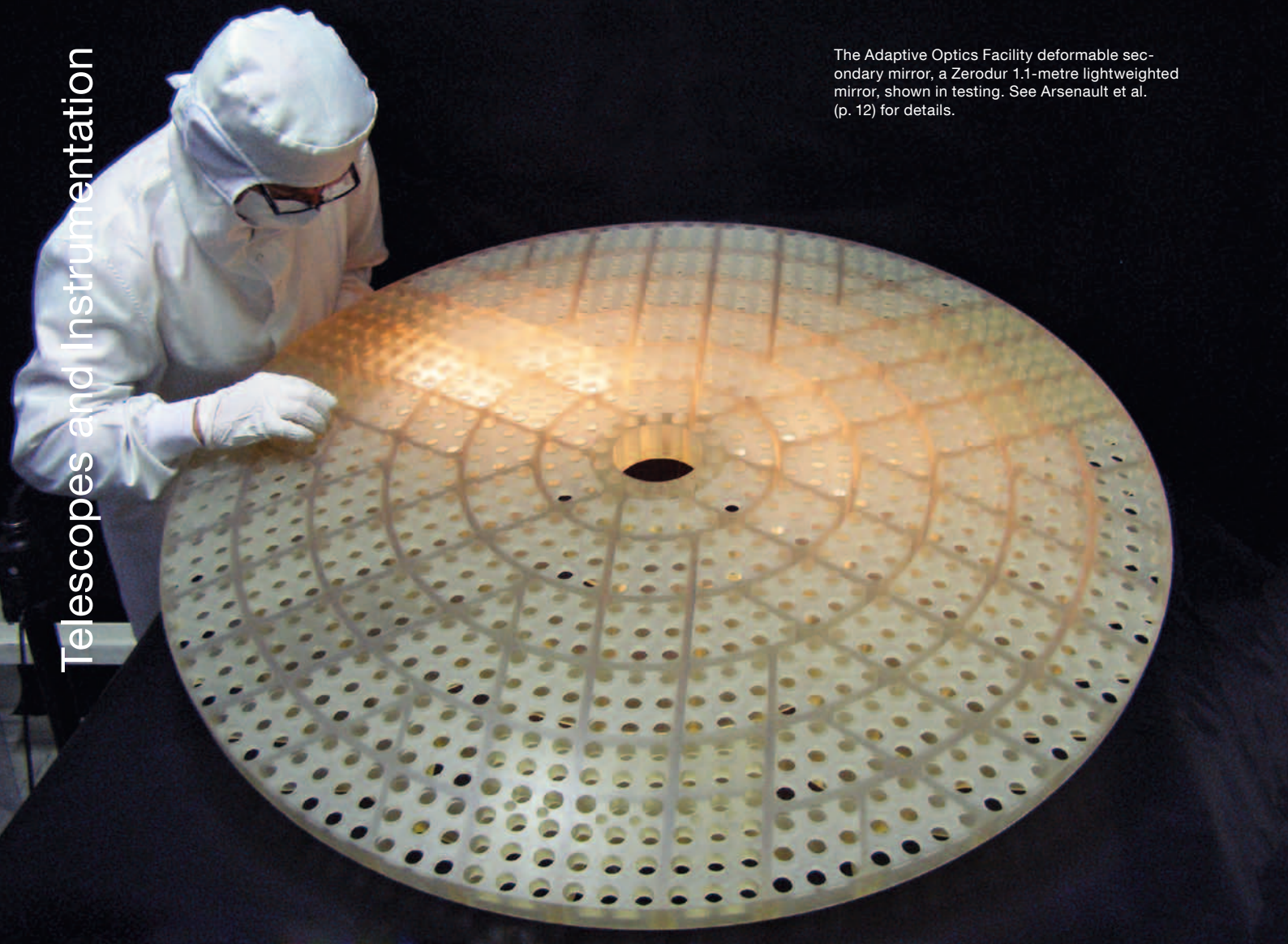
Filippi, G. et al. 2010, *Proc. SPIE*, 7740, 77401G

Links

- ¹ EVALSO web page: <http://www.evalso.eu>
- ² ALICE network: <http://www.redclara.net>
- ³ GEANT pan-European network: http://www.geant.net/About_GEANT/pages/home.aspx
- ⁴ ESO Podcast: <http://www.eso.org/public/videos/eso1043a/>



The Adaptive Optics Facility deformable secondary mirror, a Zerodur 1.1-metre lightweighted mirror, shown in testing. See Arsenault et al. (p. 12) for details.



Eight ALMA antennas observing as an interferometer at the high site on the Chajnantor plateau. See Testi et al. (p. 17) for more details.

On the Instrumental Polarisation of NAOS–CONICA

Gunther Witzel¹
 Andreas Eckart¹
 Rainer Lenzen²
 Christian Straubmeier¹

¹ I. Physikalisches Institut, Universität
 Köln, Germany

² Max-Planck-Institut für Astronomie,
 Heidelberg, Germany

As expected for a Nasmyth instrument, NAOS–CONICA shows a significant instrumental polarisation that is strongly dependent on the parallactic angle of the source and can reach up to 4% in the degree of linear polarisation. Detailed modelling of the polarimetric properties of the optical components of NAOS–CONICA using the Stokes/Mueller formalism allows the instrumental polarisation to be corrected with an accuracy of better than 1% in linear polarisation. In addition we propose an observation strategy that is expected to allow instrumental polarisation effects to be corrected to an accuracy of about 0.1%.

Polarimetric measurements can provide important information on the nature of radiative processes, which completes the picture obtained from total intensity observations. In particular this is the case for the supermassive black hole at the centre of the Milky Way and its associated variable near-infrared source Sagittarius A* (Sgr A*). Here, as for other targets, the interpretation of the polarimetric data depends crucially on the quality of the polarisation calibration and the knowledge of instrumental systematic errors. The majority of polarimetric observations of Sgr A* have been conducted with the near-infrared imager NAOS–CONICA (NACO) at the VLT, and we report here the results of a comprehensive analysis of the instrumental polarisation (IP) of this instrument. Full numerical details can be found in Witzel et al. (2010).

NACO and its polarimetric mode

NACO is the adaptive optics near-infrared imager at VLT Unit Telescope 4 (UT4, Yepun), consisting of the adaptive optics

module NAOS and the camera CONICA. This instrument provides a mode for polarimetric differential imaging combining a Wollaston prism and a $\lambda/2$ wave plate (a half-wave plate, HWP). The Wollaston prism separates the incoming partially polarised light into two orthogonal, linearly polarised outgoing beams (the ordinary and extra-ordinary beams). The HWP enables the observer to change the angle at which the measurement is conducted without rotating the Wollaston prism with respect to the detector and thus without changing the field of view. Intensity measurements over at least four angles (0° , 45° , 90° and 135°) in two integrations (two orthogonal beams simultaneously) are necessary to obtain information about linear polarisation. Circular polarisation cannot be measured, since the polarimetric mode of NACO does not include a $\lambda/4$ wave plate.

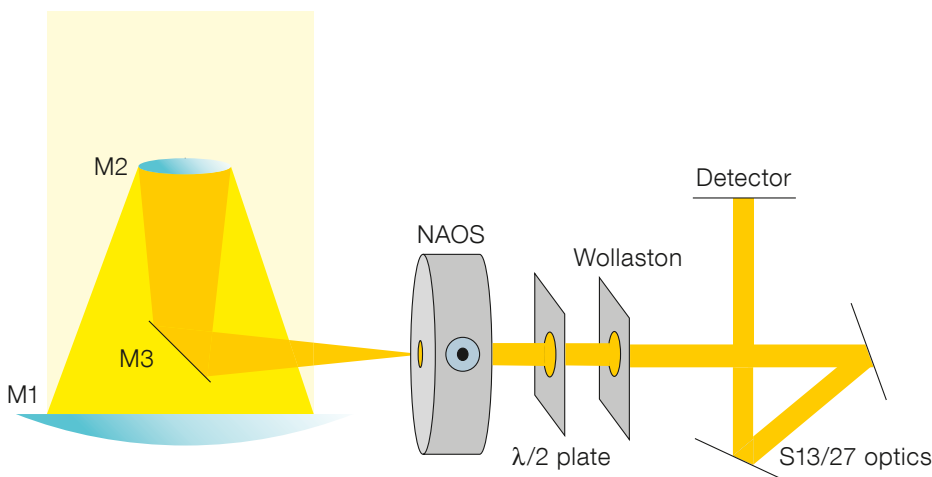
After about eight years of successful operation of NACO and plenty of polarimetric observations of the Galactic Centre (GC), Sgr A*, and of many other targets, it now seemed plausible to analyse the polarimetric mode on the basis of public ESO archive data. Long polarimetric light curves of bright sources at the GC have been especially useful in investigating the dependency of the IP on the telescope position, and in determining the accuracy achieved to date and attainable for future observations.

A model of the instrumental polarisation

To understand the IP of NACO we have developed a model of the instrumental effects within the Stokes/Mueller formalism. The polarisation of the incoming light is mainly affected by reflections at metallic coatings of mirrors within the light path of NACO. Each reflection causes crosstalk between the four Stokes parameters that describe the polarisation state. For unpolarised incoming light this crosstalk generates, for example, linear polarisation orthogonal to the plane of incidence. The magnitude of the crosstalk depends strongly on the angle of incidence: only mirrors with an inclination of $> 20^\circ$ will contribute significantly to the IP. All polarimetric effects of the optical elements and their relative orientation can be described by linear operations on the Stokes vector, the so-called Mueller matrices.

As a Nasmyth focus instrument, NACO shows an instrumental polarisation that depends strongly on the parallactic angle of the observed source. The cause of the variable part of the IP is the folding mirror M3 that is tilted at 45° (see Figure 1). While NACO itself is de-rotated with respect to the source, the orientation of M3 and, therefore, also the orientation of its IP with respect to the polarisation of the observed source, changes with the parallactic angle. As shown in Figure 1, other mirrors within NAOS and CONICA

Figure 1. Optical elements of VLT UT4, NAOS and CONICA and their relative orientation are sketched at the moment of the meridian transit.



contribute as well. Since these mirrors are part of the de-rotated instrument their contribution is, however, constant.

An important effect is caused by the HWP. A maintenance inspection revealed that the actual reference system for the HWP position angle is turned by $-6.6 \pm 0.2^\circ$ with respect to the reference assumed in the NACO manual. This results in an angle offset of -13.2° for measurements of the polarisation angle that has to be compensated for.

A simulation of the polarisation degree of the IP as a function of hour angle (for a source at the position of Sgr A*) is shown in Figure 2. The maximum instrumental polarisation is about 4% (all effects, including the optical elements of CONICA) and drops significantly at the time of meridian transit. A comparison of our model with the observed time series of the Stokes parameters of bright sources at the GC and with standard star observations confirms the model (see Figure 3). The polarisation of standard stars can be calibrated with an accuracy of better than $\sim 0.5\%$ for the Q and U Stokes parameters.

To our knowledge our results for the IRS16 stars at the GC are the first polarimetric measurements of sources within the central parsec of the GC, since Knacke & Capps (1977), that are independently calibrated using a method that goes beyond “boot-straping” procedures. An example is shown in Figure 3. The accuracy for sources of this brightness ($m_k > 9.5$ mag) is better than $\sim 1\%$ in linear polarisation and better than $\sim 5^\circ$ in polarisation angle for polarisation degrees higher than $\sim 4\%$.

A strategy for high precision polarimetry

The remaining systematic uncertainties of about 1% in linear polarisation result from insufficient knowledge of the characteristics of the Wollaston prism (such as the relative transmission of the orthogonal channels) and the effects of the flat-field calibration (the calibration light for the flat field is potentially polarised intrinsically up to 1%). A common calibration method to circumvent problems like this is “channel-switching”. In this method, at four

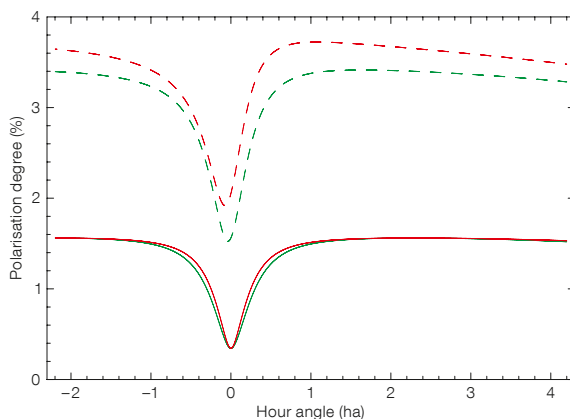


Figure 2. The polarisation degree of the instrumental polarisation as predicted by the model is shown as a function of hour angle. Linear polarisation (in green) and total polarisation (including the circular polarisation, in red) are shown for an unpolarised source with (dashed line) and without (solid line) the systematic effects of the analyser and flat-fielding.

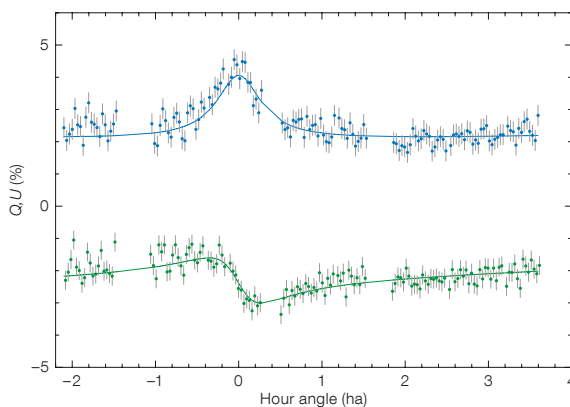


Figure 3. Stokes Q (in blue) and U (in green) parameters as a function of hour angle for IRS16C (linear polarisation 4.6% at PA_{18° , $m_k = 9.55$). The solid line is the best χ^2 -fit of the model and the points represent observations from 2009. The fitting confirms the time dependency of the instrumental polarisation as predicted by the model and additionally allows the apparent polarisation of this star to be determined.

additional angles — with a 90° -offset with respect to the above-mentioned four angles — intensities are measured. With this additional information Stokes parameters that are corrected for parts of the IP can be calculated. In particular, the effects of the Wollaston and the flat-fielding can be compensated for by this strategy.

Unfortunately this calibration is not suitable to correct all instrumental effects. In particular, the effects of reflections at metallic surfaces cannot be eliminated completely and reference offsets as caused by the HWP remain uncompensated. But we can show that this method is very useful if: 1) the HWP offset is already compensated for during observation; 2) the HWP is used to switch between the $0^\circ/90^\circ$ and $45^\circ/135^\circ$ angle pairs (respectively between their corresponding orthogonal pairs); and 3) NACO as a whole is rotated to switch by 90° for the measurement of the additional four angles. With this strategy the number of parameters of our model can be reduced

to three, mainly describing the variable part of the IP that is known with an accuracy of about 0.1% (see Figure 3). A disadvantage is the alteration of the field of view that results from a rotation of NACO as a whole as compared to the full field.

Polarised emission of Sgr A*

Figure 4 shows the derived total and polarised flux, linear polarisation and polarisation position angle for Sgr A* measured with NACO in June 2006. As a result of our analysis we can show that the common boot-straping calibration of time series of Sgr A* on the basis of the average foreground polarisation as determined by Knacke & Capps (1977) is in good agreement with our new calibration. The main reason is that the statistical errors of the photometry dominate the described instrumental effects for short integrations of faint sources like Sgr A*. Only at the lowest states of polarisation do both methods deviate significantly in polarisation angle, an effect that can

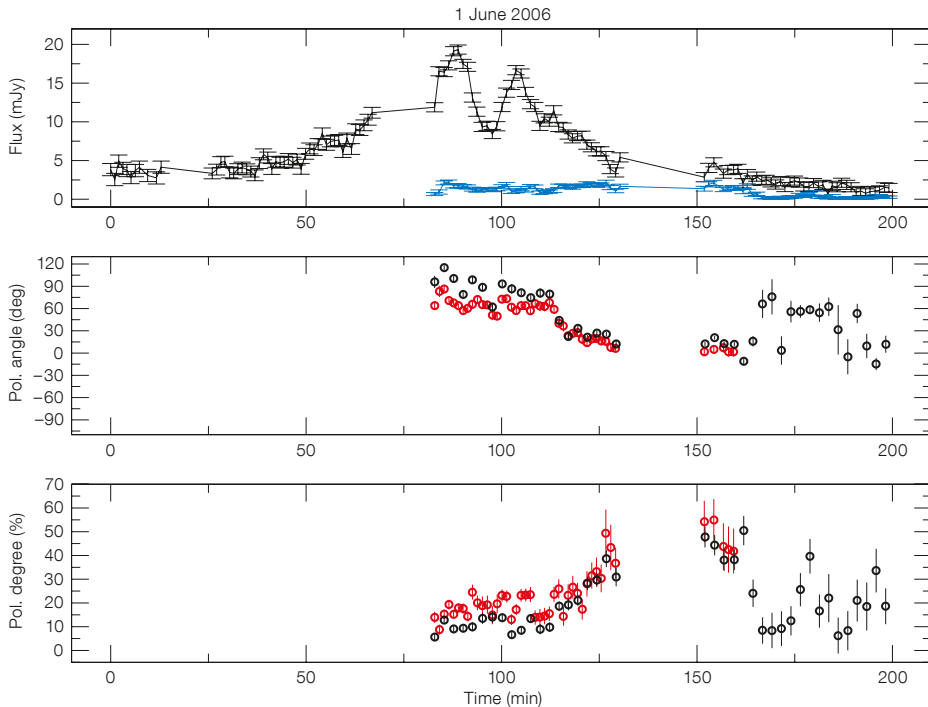


Figure 4. Light curve of Sgr A* observed with NACO in June 2006. Upper panel: total flux (black) and polarised flux (blue); middle panel: polarisation position angle; lower panel: linear polarisation. For the polarimetric parameters, the results of both calibration methods are shown: boot-strapping (red points) and the model described here (black points).

be explained by the interplay of the HWP offset and the boot-strapping method that cannot correct for it. In these polarisation states a reliable estimation of the polarisation angle is impossible anyway, and we can conclude that for Sgr A* in its bright flare phases the boot-strapping calibration yields the same results within the statistical uncertainties as a calibration with our more elaborate polarisation model. Only these bright phases have been interpreted in the framework of the relativistic modelling (Zamaninasab et al., 2010; Eckart et al., 2006; Meyer et al., 2006) that highlights the influence of strong gravity in the vicinity of the $4 \times 10^6 M_{\odot}$ supermassive black hole at the centre of the Milky Way.

Acknowledgements

We gratefully acknowledge fruitful discussions with Christian Hummel and the ESO User Support Department.

References

- Eckart, A. et al. 2006, A&A, 455, 1
- Knacke, R. F. & Capps, R. W. 1977, ApJ, 216, 271
- Meyer, L. et al. 2006a, A&A, 460, 15
- Meyer, L. et al. 2006b, A&A, 458, L25
- Witzel, G. et al. 2010, A&A, in press
- Zamaninasab, M. et al. 2010, A&A, 510, A3+



Image of NACO at the Nasmyth focus of VLT UT4 (Yepun). NACO consists of the adaptive optics module NAOS mated with the near-infrared imager and spectrograph CONICA.

Upgrading VIMOS

Peter Hammersley¹
 Lise Christensen²
 Hans Dekker¹
 Carlo Izzo¹
 Fernando Selman¹
 Paul Bristow¹
 Pierre Bourget¹
 Roberto Castillo¹
 Mark Downing¹
 Nicolas Haddad¹
 Michael Hilker¹
 Jean-Louis Lizon¹
 Christian Lucuix¹
 Vincenzo Mainieri¹
 Steffen Mieske¹
 Claudio Reinero¹
 Marina Rejkuba¹
 Chester Rojas¹
 Rubén Sánchez-Janssen¹
 Alain Smette¹
 Josefina Urrutia Del Rio¹
 Javier Valenzuela¹
 Burkhard Wolff¹

¹ ESO

² Excellence Cluster Universe, Technische Universität München, Germany

The high multiplex of the VLT visible imager and multi-object/integral-field spectrometer, VIMOS, makes it a powerful instrument for large-scale spectroscopic surveys of faint sources. Following community input and recommendations by ESO's Science and Technology Committee, it was decided to upgrade the instrument in phases. The first phase of the upgrade is described and included changing the shutters, installing an active flexure compensation system, replacing the detectors with CCDs with a far better red sensitivity and less fringing, and improving the data reduction pipeline.

VIMOS (Figure 1) is a powerful visible (360 nm to 1000 nm) imager and multi-object/integral-field spectrometer mounted on VLT Unit Telescope 3 (Melipal). Following a workshop on spectroscopic surveys¹ and recommendations by the ESO Science and Technology Committee, it was decided that the instrument, which entered operation in 2002, should be upgraded. In order to minimise downtime, it was decided to

complete the upgrade in phases. This article describes the activities of the first upgrade and the resulting improvement in performance.

The instrument and upgrades

VIMOS has four identical arms, each with a 7×8 arcminute field of view on the sky with a gap between the fields of 2 arcminutes. The instrument offers three main observing modes:

- *U*-, *V*-, *B*-, *R*-, *I*- and *z*-band imaging covering four fields each 7×8 arcminutes in size.
- Slit-based multi-object spectroscopy with spectral resolutions from a few hundred to 2500 in each of the four imaging fields.
- Integral-field unit (IFU) spectroscopy with fields of view between 13×13 and 54×54 arcseconds.

After eight years of operations, and to extend its useful life, it became necessary to upgrade the instrument in order to address various issues. The first upgrade included:

- 1) replacing the shutters, which were worn out, and improving the reliability of the instrument;
- 2) replacing the CCD detectors;
- 3) reducing the instrument flexure;
- 4) improving the data reduction pipeline.

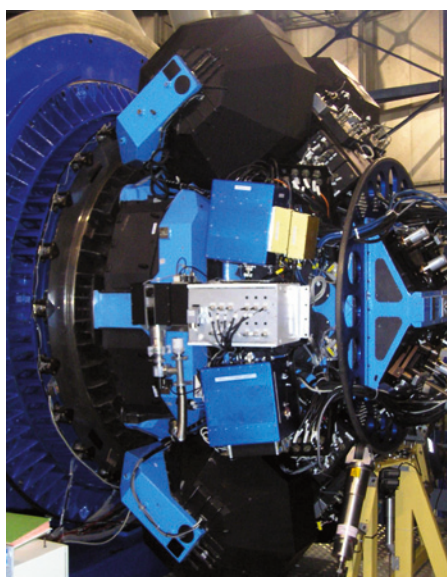


Figure 1. VIMOS is shown on the Nasmyth platform of VLT UT3.

Following tests on the instrument in November 2009 and February 2010, VIMOS was removed from the telescope between May and July 2010, so that the first stage of the upgrades could be made. The instrument was re-commissioned at the end of July. Making fine adjustments and optimising the system, then took a few more weeks.

New shutters and other measures to improve reliability

The exposure is controlled by 100 mm iris shutters manufactured by the Prontor company. Due to the size and speed requirements, these shutters are subject to considerable wear that has led to occasional failures. A failure occurring at the end of science integration is especially frustrating because it means that the exposure is lost and must be counted as technical downtime. Analysis of night reports from the last two years shows that the technical downtime due to shutter or detector controller failures has been 0.9% on average, a non-negligible fraction of the total VIMOS downtime which varied between 6% (Q4/2009) and 10% (Q4/2008).

Since this type of shutter is no longer commercially available, ESO has reverse-engineered the Prontor shutters and built ten copies. A new shutter controller was also designed, which has no dissipation in the open or closed condition and has an electromagnetic braking function to reduce the mechanical loads. Prototypes have survived lifetime tests of up to 200 000 operations without degradation. Four of these new shutters have been mounted and no technical downtime due to shutter failures has been experienced since then.

The Mask Exchange Unit (MEU) of each of the four VIMOS arms consists of four mechanisms (mask selector/gripper/translator/blocker) that must be precisely aligned for reliable operation. About half of the total technical downtime of VIMOS is due to MEU failures. In the first quarter of 2010 we began performing daytime dry runs with the MEU whenever new masks were mounted. The idea was to detect possible failures during daytime, when they can still be corrected.

Apart from the extra manpower to perform the daytime tests, the experience with dry runs is encouraging, although more statistics are needed.

The new detectors

The original VIMOS detectors were thinned back-illuminated CCDs made by e2v. These were cosmetically very clean and gave a good performance in the blue and visible wavelength ranges. At wavelengths longer than about 700 nm, however, the detectors had strong fringing, which meant that near 850 nm the quantum efficiency (QE) of the detector could change by up to 40% for changes in wavelength of about ten nanometres, or a movement across the detector of a few pixels. This made obtaining high quality spectroscopy very difficult in this wavelength range, particularly when there was flexure present.

The new detectors are also e2v devices. These are the same format as the original but the silicon is more than twice as thick. This has dramatically reduced the fringing so that now the maximum change in QE is at most 2% and cannot be seen at all with the LR-Red grating or in imaging. Figure 2 shows two raw stellar spectra near 850 nm taken with the old (red) and new (black) detectors using the HR-Red grating. With the old detector the fringing is so large that none of the stellar features can be recognised, and so careful reduction is required to produce usable results (Scodreggio et al., 2009). The raw spectrum taken with the new detector, however, is almost good enough to use, so simplifying the reduction and improving the quality of the results, especially on faint red objects.

Figure 3 shows the change in imaging zero points between the old and new detectors. The significant improvement in the *R*-, *I*- and *z*-bands can be clearly seen, however there is a slight decrease in sensitivity in the *U*-band. The data used for calculating the zero point with the new detectors were taken just before the primary mirror of Melipal was recoated, which has improved the zero points by 0.05 to 0.1 magnitudes.

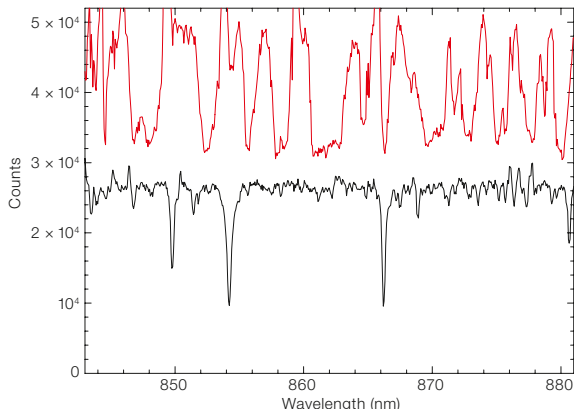


Figure 2. Raw stellar spectra taken with the old (red) and new (black) detectors using the HR-red grism. The star observed with the old detector was over a magnitude brighter than the star observed with the new detector. The “noise” in the red spectrum is caused by the fringing which makes the detector response vary rapidly with wavelength. This fringing has almost disappeared with the new detector so that the absorption features, such as the CaII triplet lines, can be easily seen.

The active flexure compensation

VIMOS is a large instrument, weighing three tonnes, and suffers from 12–20 pixels of flexure between the focal plane and the detector, when the instrument is rotated to follow the field rotation. This flexure causes the image to smear during long exposures, makes calibration more difficult, and reduces the accuracy of object position measurements taken in the imaging mode, necessary for MOS mask production. The instrument was delivered with a passive (mechanical) flexure compensation system. Its performance was improved by ESO to about four pixels, but the system is not easy to maintain or adjust, and in 2009 some arms exhibited flexures of nearly six pixels when the instrument rotated. These flexures had a major impact on operations. The spectroscopic flat and arc calibrations had to be taken immediately after the science observations to ensure that the flexures affecting science and calibrations were as similar as possible. Furthermore, the relative pointing of the four arms between pre-image and spectroscopic observation could change, thus offsetting the sources in the slit. This was particularly annoying, as observers could never optimally position the targets in all four quadrants at the same time.

Therefore, it was decided to install an active flexure compensation system (AFC). Two motors were placed on the fold mirror of each arm, allowing the

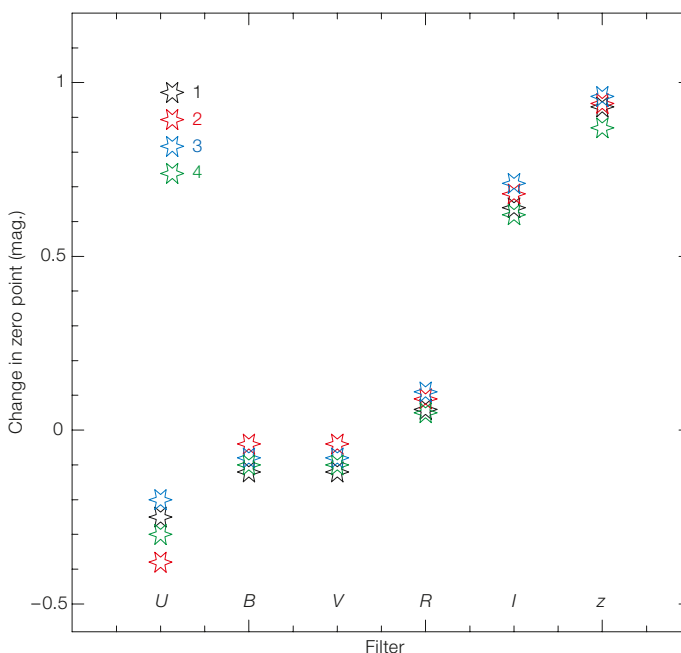


Figure 3. The change in imaging zero point (in magnitudes) between the old and new detectors is shown. The results for each of the four arms (indicated 1-4) are shown by separate points.

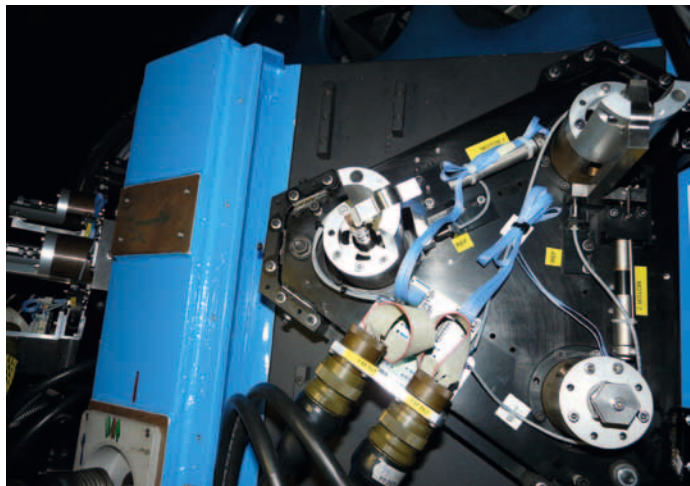


Figure 4. A close-up of the motors of the active compensation system.

image of the focal plane to be displaced in X and Y on the detector. A fibre in the focal plane, but just outside the nominal imaging field, then acts as a reference source and so before an observation is started the image of the focal plane can be correctly positioned on the detector. Any flexure during an observation is corrected by driving the motors using a look-up table. With the current system the target positioning can be done with approximately one pixel accuracy, while the registration between science and calibration observations is approximately

two pixels, the latter degraded by hysteresis. During the commissioning it was gratifying to be able to see all targets centred in all quadrants at the same time!

The new MOS pipeline

In the new release of the pipeline data reduction software (version 2.5.0, delivered to the users in October 2010) two new MOS recipes have been added; one for processing the calibration frames, and another for reducing the scientific

exposures. Using the new recipes is mandatory for reducing data obtained after the VIMOS CCD upgrade, and they can also be used for reducing older data. This new software, developed at ESO, is intended to replace the original set of five MOS recipes.

The new calibration recipe uses a calibration approach, based on pattern recognition, which was already applied successfully to the FORS1/2 and EFOSC2 pipelines (Izzo et al., 2007). This greatly reduces the software maintenance workload as it no longer requires any preliminary optical and spectral modeling of the instrument. This approach has been adopted in order to cope with the mechanical instabilities affecting any real-world instrument, a problem which was especially felt with VIMOS. Supporting the new VIMOS mosaic commissioning would have been impossible using the old MOS pipeline. VIMOS, with its four quadrants and six grisms, required the manual recomputation of at least 72 spectral distortion models at each major instrument intervention. With the new recipes, this is no longer necessary.

The new recipes also significantly improve the accuracy of the wavelength calibration, the quality of the sky subtraction,

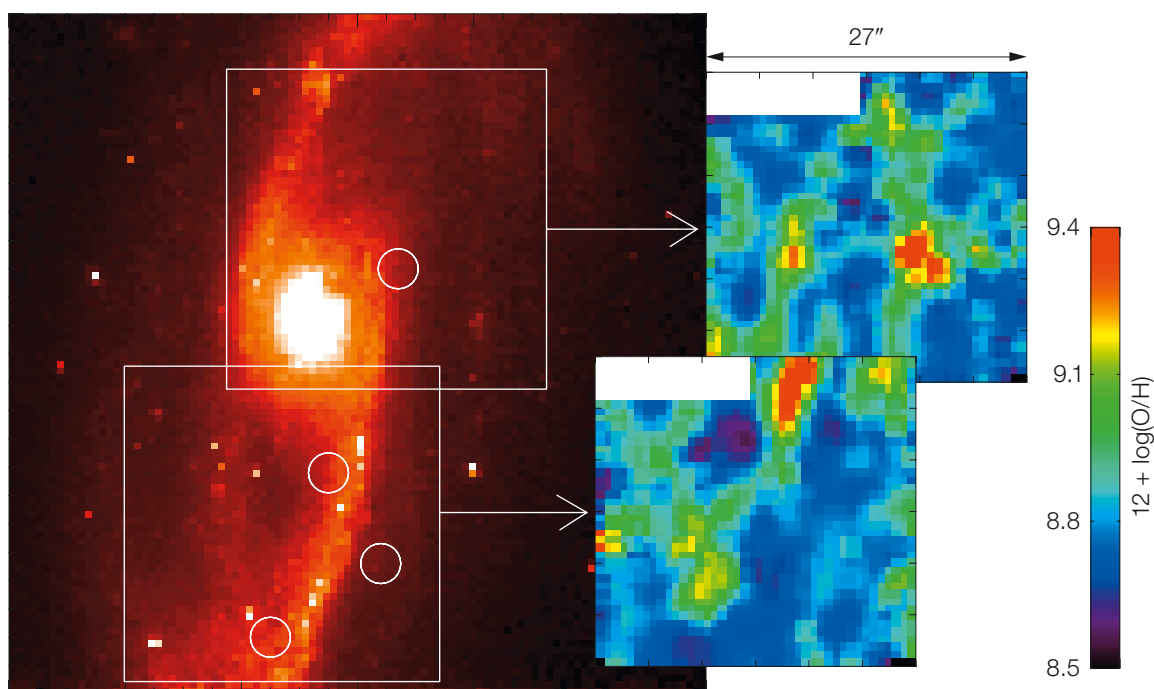


Figure 5. The image shows the galaxy NGC 6754 observed with the HST/NICMOS in the J-band. From the two IFU pointings the oxygen abundance was determined in the regions corresponding to where four SNe exploded (shown as open circles).

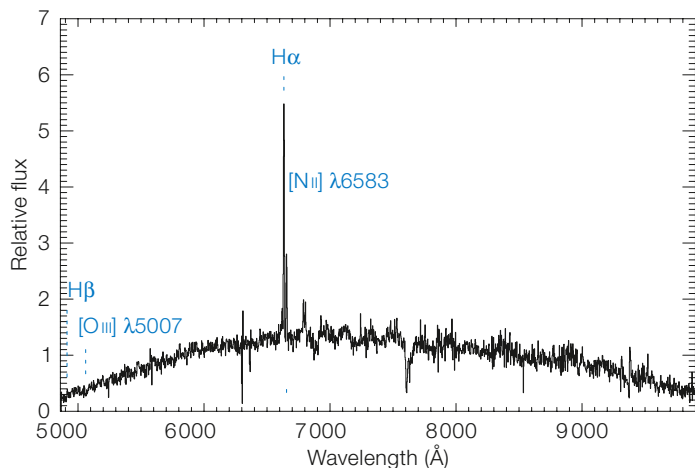


Figure 6. The VIMOS spectrum of one single spaxel of the IFU observation of NGC 6754.

colour maps on the right-hand side of Figure 5 illustrate this abundance, where the dark blue colour corresponds to solar metallicities, green and red to super-solar metallicities, and violet and black to sub-solar metallicities. Figure 6 shows an extracted spectrum from a single spaxel identifying the lines used, but also demonstrating fewer systematic sky subtraction residuals beyond 700 nm, thanks to the absence of detector fringes. The signal-to-noise ratio for continuum emission is 50 % higher, while in the region of strong sky emission lines the improvement is a factor of two, relative to the old detectors.

the optimal extraction of the detected objects, and the sky fringing correction. The new pipeline and the manual can be downloaded².

The commissioning

The commissioning of an instrument as complex as VIMOS needs to be carefully planned. There are many modes, and the tree of dependencies has become even more complex with the introduction of the AFC system. The AFC reference source is at the edge of the field and so focusing is now even more critical if defocus is not to cause the centroids to move. The conversion from pixel coordinates to millimetres at the mask plane, is now tied to the coordinates of the AFC reference pixel. Any change to the reference pixel means that the mask-to-CCD matrix must be re-determined.

VIMOS has three reference systems which must be aligned to a few pixels in 4000; the detector xy in pixels, the focal plane XY in mm and the spectral dispersion direction. This last alignment is particularly important for multiplexed observations with the low resolution gratings, as the reduction pipelines assume that the contaminating zero or second orders are well aligned with the first order spectrum (we thank Luigi Guzzo, Bianca Garilli, and Marco Scoddeggio for strongly insisting on this point). There are four arms, and six gratings per arm, each of which needs to be aligned, and so realignment of all gratings is a lengthy process. The re-characterisation of the instrument

after any intervention that causes a displacement of the image of the focal plane on the detector, takes a minimum of a week. During the commissioning, which was also a time to become familiar with the newly installed hardware, we had to repeat this re-characterisation a few times. Although this led to a loss of efficiency during the first two months of service observing, the stability achieved in the coefficients of the mask-to-CCD matrix are now outstanding, with daily positioning variations well below a pixel.

Performance validation

As part of the commissioning, performance validation observations were made to help characterise the MOS and IFU modes and provide a taste of the performance after the upgrade. Figures 5 and 6 show the results from the IFU observations. Figure 5 shows the HST/NICMOS J -band image of NGC 6754 where four supernovae were observed between 1998 and 2005. Two belonged to massive stars that exploded in core collapse events (Type II SNe) and the other two to white dwarf star explosions (Type Ia SNe). NGC 6754 is dominated by numerous H II regions and widespread star formation over the face of the galaxy. The strong optical emission lines in the spectra at the two VIMOS-IFU pointings allows the oxygen abundance in the regions where the SNe exploded to be derived, as well as in other regions of the galaxy. The oxygen abundance was calculated from the $H\alpha/[N II]$ ratio using the calibration of Pettini & Pagel (2004). The

Next steps

The first stage of the upgrade has significantly improved the performance of VIMOS in the red and reduced the amount of flexure to values close to the initial specifications of the instrument. Even so, further improvements are being planned for 2011 and 2012:

1. Replace the high resolution blue grism by a volume phase holographic grating with almost double the efficiency.
2. Improve the reliability and accuracy of the grism placement, mask insertion and focus mechanisms.
3. Increase the speed of the grism exchange unit (expected increase in overall operational efficiency is 2%).
4. Eliminate the need to perform pre-imaging with VIMOS before masks can be made. Potentially this could increase operational efficiency by 10 to 15 %.

After these changes we expect to have an instrument with a much improved stability, reliability, and efficiency that will permit more ambitious science to be attempted.

References

- Izzo, C., Jung, Y. & Ballester, P. 2007, in *The 2007 ESO Instrument Calibration Workshop*, 191
 Pettini, M. & Pagel, B. E. J. 2004, *MNRAS*, 348, 59
 Scoddeggio, M. et al. 2009, *Messenger*, 135, 13

Links

- ¹ Conference web page including presentations: www.eso.org/sci/meetings/ssw2009/
² VIMOS reduction pipeline available at: <http://www.eso.org/pipelines>

Progress on the VLT Adaptive Optics Facility

Robin Arsenault¹
 Pierre-Yves Madec¹
 Jérôme Paufigue¹
 Stefan Ströbele¹
 Jean-Francois Pirard¹
 Élise Vernet¹
 Wolfgang Hackenberg¹
 Norbert Hubin¹
 Liselotte Jochum¹
 Harald Kuntschner¹
 Andreas Glindemann¹
 Paola Amico¹
 Miska Lelouarn¹
 Johann Kolb¹
 Sébastien Tordo¹
 Robert Donaldson¹
 Christian Sönke¹
 Domenico Bonaccini Calia¹
 Ralf Conzelmann¹
 Bernard Delabre¹
 Mario Kiekebusch¹
 Philippe Duhoux¹
 Ivan Guidolin¹
 Marco Quattri¹
 Ronald Guzman¹
 Bernard Buzzoni¹
 Mauro Comin¹
 Christophe Dupuy¹
 Jutta Quentin¹
 Jean-Louis Lizon¹
 Armin Silber¹
 Paul Jolly¹
 Antonio Manescau¹
 Peter Hammersley¹
 Javier Reyes¹
 Andreas Jost¹
 Michel Duchateau¹
 Volker Heinz¹
 Clémentine Bechet¹
 Remko Stuik²

¹ ESO

² Huygens Laboratory, University of Leiden, the Netherlands

The Very Large Telescope (VLT) Adaptive Optics Facility is a project that will transform one of the VLT's Unit Telescopes into an adaptive telescope that includes a deformable mirror in its optical train. For this purpose the secondary mirror is to be replaced by a thin shell deformable mirror; it will be possible to launch four laser guide stars from the centrepiece and two adaptive optics modules are being developed to feed the instruments HAWK-I and

MUSE. These modules implement innovative correction modes for seeing improvement through ground layer adaptive optics and, for high Strehl ratio performance, laser tomography adaptive correction. The performance of these modes will be tested in Europe with a custom test bench called ASSIST. The project has completed its final design phase and concluded an intense phase of procurement; the year 2011 will see the beginning of assembly, integration and tests.

Overview

The ESO VLT Adaptive Optics Facility (AOF) is upgrading one of the Unit Telescopes (UTs) with a new secondary mirror (M2) unit. This unit includes an adaptive secondary mirror (with 1170 actuators), four laser guide stars (LGS) formed by four 22 W sodium beacons launched from the telescope centrepiece and a dedicated adaptive optics (AO) instrument park to provide users with optimised AO correction modes. The two AO components are GALACSI, the AO module for MUSE that will provide ground layer adaptive optics (GLAO) correction and a laser tomography correction for MUSE's narrow-field mode for high Strehl ratio correction in the visible spectral range, and GRAAL, the AO module for HAWK-I, which will provide only ground layer adaptive optics correction. The Adaptive Secondary Simulator and Instrument Testbed (ASSIST) will be used for a complete test phase of the AOF in Europe. This project constitutes a major stepping stone towards the European Extremely Large Telescope (E-ELT).

GALACSI is a module mounted at the Nasmyth focus; it contains four LGS wavefront sensors (WFS), a natural star tilt sensor and an infrared low-order sensor. The laser guide stars and WFSs can be tuned to two different fields of view: a 1-arcminute field of view for GLAO correction, producing a gain of two in ensquared energy at 750 nm; and a 7.5-arc-second field of view for laser tomography correction, providing a high Strehl ratio in the visible (5% at 650 nm) on-axis.

GRAAL is similar in design to GALACSI, but only applies a GLAO correction to

improve the ensquared energy in the K-band by a factor of two over the 7.5-arcminute field of view of HAWK-I. The four LGS WFSs are mounted on a rotating bearing inside the Hawk-I housing, while a natural guide star tilt sensor picks up a star in a ring outside the Hawk-I field of view. An additional natural guide star WFS is used for calibration and maintenance operations of the deformable secondary mirror (DSM).

The GALACSI and GRAAL real-time computers share identical SPARTA hardware architecture and most software features. SPARTA is a standard platform for real-time applications developed by ESO's Adaptive Optics Department and uses a hybrid architecture of a field programmable gate array, digital signal processor and central processing unit. It is designed to be flexible by offering sophisticated software control and post-processing features while accommodating various combinations (numbers) of WFSs and deformable mirrors. All WFS cameras and tilt sensor cameras are identical and use as detectors e2v CCD220 devices controlled by the New General Controller (NGC; Baade et al., 2009) developed by the ESO Optical Detector Team.

Status of the project

GALACSI

The GALACSI AO module design and manufacture is led by the ESO AO Department with the support of other ESO divisions (the Technology Division, Integration Department of the Instrumentation Division and Software Development Division). The main mechanical structure and optics have been outsourced to industry and off-the-shelf components are being purchased for the electro-mechanisms. The control software is being developed in-house and integration will be undertaken by the Integration Department. The mechanisms are controlled via the remote motor controller switching system based on the controller area network protocol. The final design review was held in June 2009 and several important procurements were launched at that stage. GALACSI's main structure, manufactured by Bossenkool (the Netherlands), has gone through final

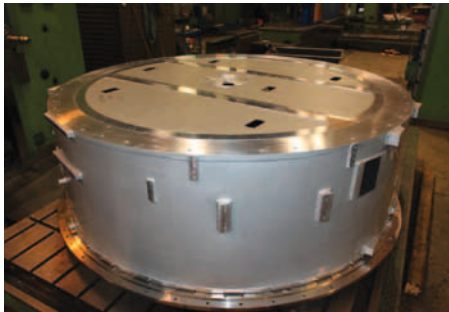


Figure 1. GALACSI's main mechanical structure is shown during acceptance at Bossenkool (the Netherlands) in September 2010.

acceptance and was delivered to ESO in October 2010; it is shown in Figure 1. The optics is being manufactured by SESO (France) and delivery is expected in December 2010. Several smaller mechanical components have already been received and are being tested and some are shown in Figure 2. The field selector is a critical key system and the positioning stages manufactured by Physik Instrumente have been received and are currently being tested. The electronic control is progressing steadily and several VME racks are complete and have been integrated into the cabinets.

The assembly and integration of GALACSI started in the ESO integration hall during the autumn of 2010 and will continue throughout 2011. The stand-alone test for the GALACSI module (without the DSM) will begin in 2011 to validate the whole assembly without the other major subsystems of the AOF. The complete system test phase for GALACSI with the DSM on ASSIST is expected to start in early in 2013 after GRAAL has completed its corresponding phase.

GRAAL

The GRAAL module is also led by the AO Department with support from the same departments as GALACSI, but with one main difference: a major contract has been issued for the important task of manufacturing and integrating the main structure and opto-mechanics, including all stages (provided by ESO) and the WFS co-rotator. This contract is being undertaken by NTE SENER S.A. (Spain) and will be completed in early 2011. This scheme will give the integration activities a strong start in Garching. The optics

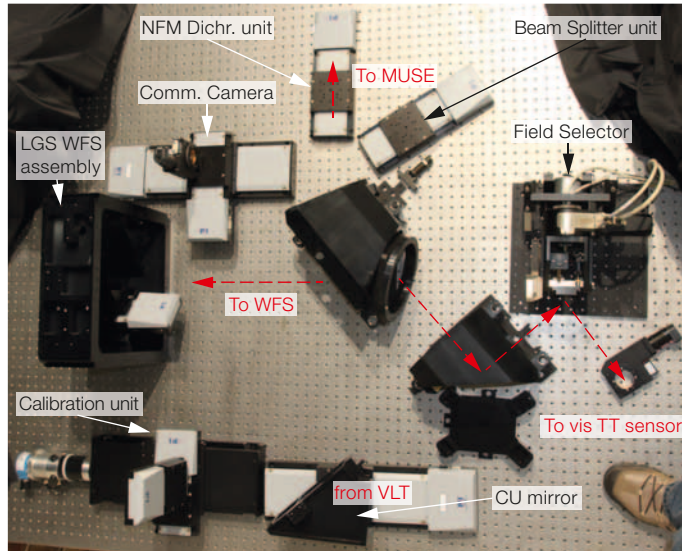


Figure 2. Several smaller mechanical components of GALACSI's optical train are shown.

is also being manufactured by SESO and delivery is expected in December 2010. Several software modules are being developed in common for GRAAL and GALACSI and there are synergies between both. During summer 2010, a VLT standard software module was delivered to NTE SENER S.A. with the corresponding hardware to control the co-rotator (consisting of an internal bearing and drive system to rotate the four LGS WFSs) and is being used by NTE SENER S.A. for their integration and testing process, as shown in Figure 3.

When the GRAAL main structure is delivered to Garching early in 2011, the optics will be integrated with the rest of the electronics and software. GRAAL tests in

stand-alone mode should start by late 2011 to prepare for a system test phase with the DSM on ASSIST in 2012.

Deformable secondary mirror

The deformable secondary mirror is being outsourced to MicroGate and ADS (Italy) and is the heart of the Adaptive Optics Facility. This contract completed its final design review in December 2007 and assembly started at the end of 2009. Several key components have been received by the suppliers and work is progressing along two parallel paths at MicroGate, where the electronics and software are being developed, and at

Figure 3. GRAAL's main structure is shown being integrated and tested at NTE SENER S.A. in Spain.

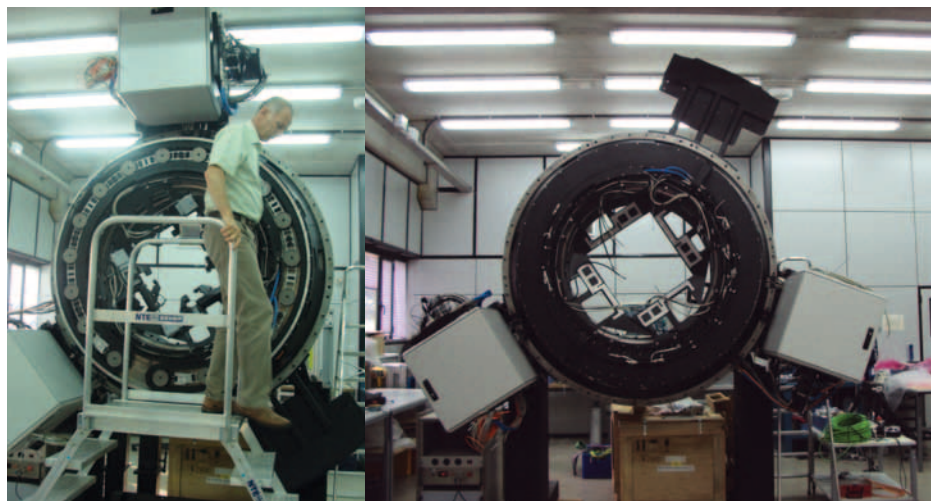


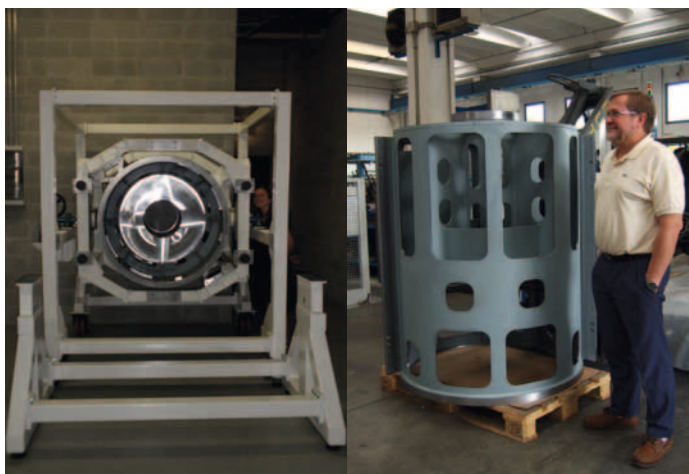


Figure 4. Part of the DSM reference body made by SESO in France (see the image on p. 4, upper, for the whole DSM). The intricate rib structure is literally sculpted from a monolithic block of Zerodur. The 1170 circular holes allow passage for the actuators. This process, known as lightweighting, reduces the mass by 80% to a mere 35 kg.

ADS where the electro-mechanics is being assembled and manufactured. The main highlight of 2010 has been the delivery of the reference body, a Zerodur 1.1-metre lightweighted optical component that provides the reference surface for the thin shell mirror, shown in Figure 4 (and featured in an ESO announcement¹).

SAGEM (France) is continuing its efforts on the thin shell contracted to them by MicroGate. The convex side has been polished successfully to specifications and the thinning process from the back-side is starting. Note that SAGEM is proceeding carefully and made a detailed analysis of the thinning process before finalising the details. Figure 5 shows the integration and service stand for the DSM and M2 hub. Figure 6 shows some of the electronic control boards for the

Figure 5. Integration and service stand for the DSM. The M2 hub, including the DSM, is mounted inside.



DSM. The next step is a milestone in mid-2011 to review the progress of the integration. Delivery of the DSM to Garching is planned for early 2012, when the system test phase in Europe will begin.

The Four Laser Guide Star Facility

The Four Laser Guide Star Facility (4LGSF) project includes two important contracts contributing to the design and manufacturing of this system. TOPTICA Photonics, a company located near Munich, is responsible for the laser design and manufacture. TOPTICA has been selected as the preferred supplier after an initial call for tender and a competitive preliminary design with another supplier. The manufacturing contract was signed in June 2010. A final design review will be conducted in June 2011 and six months later a pre-production unit will be ready so that all the laser specifications can be verified. Then the four units will be produced. They

consist of 1178 nm infrared fibre Raman lasers, doubled in frequency by second harmonic generation to 589 nm (see Bonaccini Calia et al. [2010] for details); Figure 7 shows the test laser setups. These lasers have very few components, require minimal optical alignment and occupy a small volume, all contributing to a greater reliability. This represents a major milestone in terms of simplicity, compactness and improved reliability. The current LGS system uses the PARSEC laser, which delivers 5 W of Na power and sits on a large optical bench located in the laser cleanroom below the Nasmyth platform of UT4. In contrast the TOPTICA 22W laser fits in a volume of half a cubic metre (excluding the electronics cabinets)!

TNO Science & Industry (the Netherlands) holds the second important contract. They will finalise the reference design provided by ESO and manufacture the optical tube assembly, which is the telescope part of the launch telescope system (see Figure 8). This is based on a two-lens design, the largest being 40 cm in diameter while a 30 cm beam is launched into the atmosphere. A 45-degree mirror steers the beam and allows the laser guide star to be pointed to the appropriate off-axis distance.

The ESO 4LGSF team is focusing on the rest of the laser system design: beam diagnostics and jitter control for fast beam pointing; optical and mechanical design; electronic and software design; and analysis of the whole system. Interfacing the 4LGSF with the UT and the

Figure 6. Electronic control boards for digital signal processing for the DSM. Each board controls 16 channels.

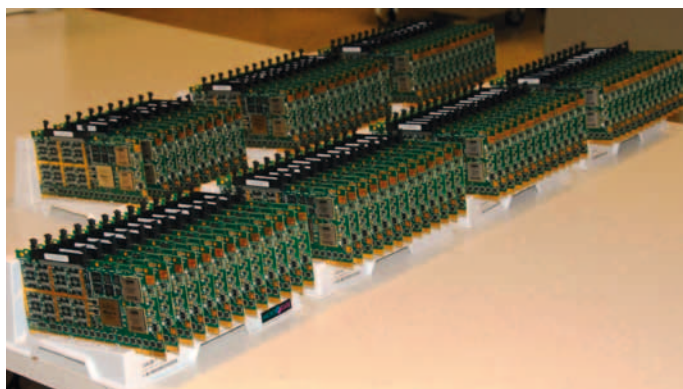




Figure 7. Left: The ESO Raman fibre laser used to test laser optics coatings for the launch telescope. Right: The single arm Raman fibre amplifier from MPB/TOPTICA showing the required 37.4 W of infrared 1178 nm power for the proper Na wavelength output power (image from April 2010).

unit is expected for the summer of 2011 and the final design of the laser will be reviewed in mid-2011.

ASSIST

The ASSIST test bench is a key component of the Adaptive Optics Facility. It will allow full characterisation of the AOF in Europe before installation and commissioning in Paranal. It also offers stable, known and reproducible conditions of turbulence (simulated by phase screens) to establish whether the whole assembly (wavefront sensors, real-time computer, deformable mirror and the algorithms implemented) meet the performance specifications.

The most striking feature of ASSIST is that it requires a large 1.7-metre main mirror to feed the light onto the M2 convex deformable mirror. This mirror is manufactured by AMOS (Belgium) and is in the last stages of aspheric polishing (see Figure 9). Acceptance is planned for late 2010.

The bench consists of a tower with the 1.7-metre mirror at the base and the new generation M2 unit (hosting the DSM) on top (see Figure 10). A system of 45-degree mirrors will feed artificial sources from the side. A star simulator and turbulence generator feeds ASSIST with sources simulating natural and laser guide stars (with different focus positions) and three phase screens located at different altitudes. This setup allows realistic testing of the AO modules and complete testing of all the functionalities. ASSIST will be delivered to Garching in spring 2011 for integration in the large tower with the mirrors well in advance of the arrival of the DSM, planned for early 2012.

Unit Telescope upgrade

In April 2008 it was recognised by the project and upper management that the scope of modifications required to the UT that will receive the AOF were substantial and needed detailed planning and careful

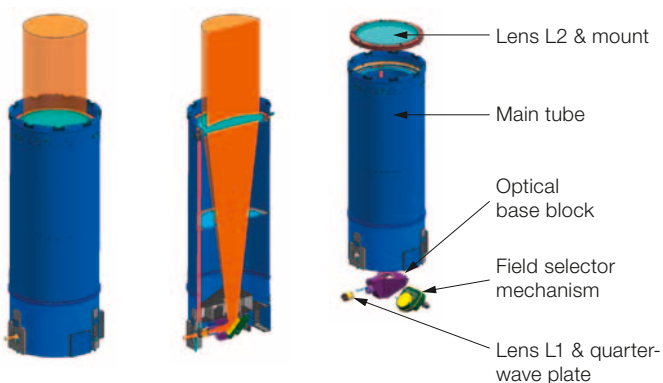


Figure 8. The optical tube assembly being developed by TNO Science & Industry. Together with the beam control and diagnostics system this assembly makes up the launch telescope system for the 4LGSF. Four similar units are mounted on the centrepiece of the UT to launch the four laser guide stars at 90 km altitude.

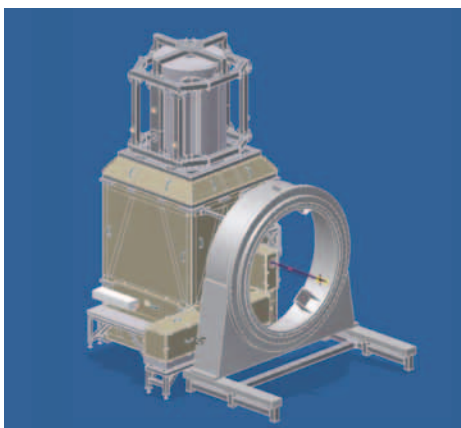
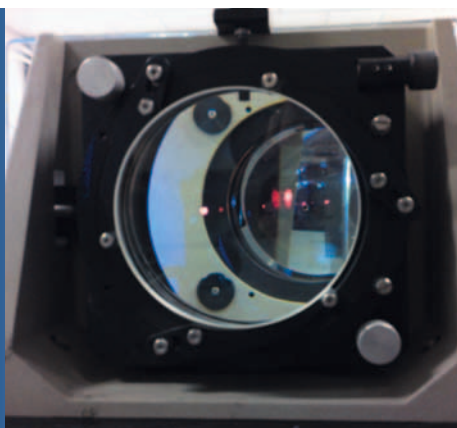


Figure 9. The ASSIST test bench (left) with the new generation M2 unit on top of the structure. The large 1.7-metre mirror is at the bottom (hidden by the light covers in this illustration) and the Nasmyth adaptor/rotator test bench can be seen on the right-hand side to allow the AO modules to be mounted. On the right is the secondary mirror (AM2), a 140 mm convex aspherical mirror manufactured by ASTRON, that completes the main tower optics of ASSIST.

mechanical design of the lasers and optical tube assembly interfaces also requires the team's full attention. Safety is important when designing with 22 W



lasers as components and is taken very seriously by the team. A consultant has been contracted to provide support to the safety analysis and much has been learnt during the design of the current 4LGSF system.

The final design documentation for the 4LGSF is complete and the final design review will take place in January 2011. Procurement will then start for the optomechanical and electronic system assembly. A first optical tube assembly

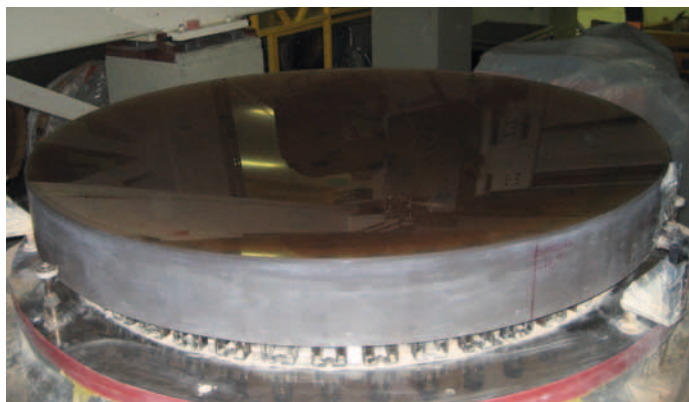


Figure 10. The main 1.7-metre mirror of ASSIST is shown at AMOS in Belgium during the last step of aspherical polishing.

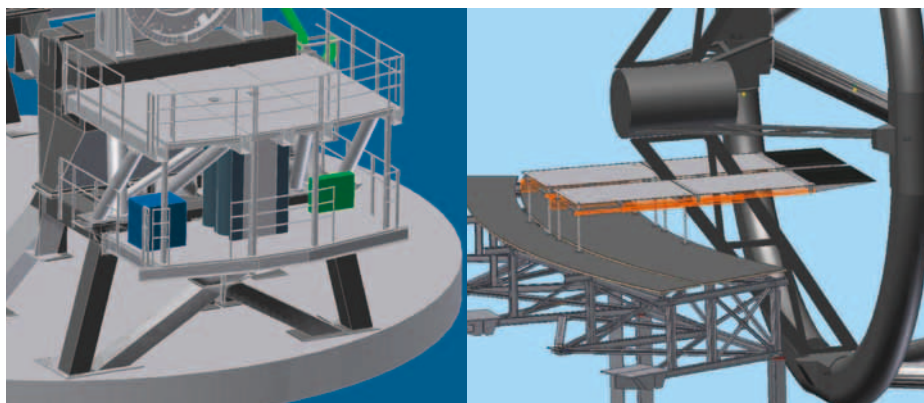


Figure 11. Left: Concept of a Nasmyth platform extension for the 4LGSF electronic cabinets and heat exchangers below the existing platform. Right: One of the two concepts for a deployable M2 maintenance platform to enable quick maintenance work on the new generation M2 unit.

implementation. A specific branch of the AOF project was created to manage this effort. At the AOF system final design review, held in April 2010, a large number of documents focused on this aspect and received the approval of the review board and the Paranal management. This review constituted the kick-off for this sub-project. The basis for the definition of the requirements is all the non-conformances identified in the Interface Control Document between the AOF and the VLT. This sub-project will implement: mechanical interfaces between the UT and the 4LGSF electronics cabinets and launch telescopes on the UT centrepiece (see Figure 11 left); overhaul of the cooling system and electrical supply; implementation of platform extensions to accommodate all the electronics cabinets; modification to the Nasmyth guider arm to accommodate the longer back focal

distance of GALACSI–MUSE; definition of all cable (for power, signals, fibres, etc.) routing in the UT; development and implementation of a new, easier to deploy, M2 maintenance platform (see Figure 11 right); and specification of all the required assembly, integration and testing facilities needed in Paranal.

Complementary systems

There are a few important components of the AOF that are being developed as sub-contracts to other firms or to ESO departments. The real-time computer SPARTA for GRAAL and GALACSI is managed by a sub-group of the AO Department. The two identical real-time computers will be delivered to the AOF after SPHERE is delivered. SPHERE is a single conjugate AO system using a natural guide star on axis; the required functionalities will be re-used by the maintenance mode of GRAAL (for the natural guide star on-axis). The GLAO functionalities will build on this for the GLAO mode of GRAAL and GALACSI. These aspects will be completed by laser tomography AO functionalities for the

MUSE narrow-field mode of GALACSI. The ESO Optical Detector Team is using the fast readout OCam (developed by LAOG, LAM and OHP; see Release eso0922²) to develop an NGC controller for the e2v CCD220 detector that will be used for the WFS cameras. Fifteen units have been ordered for SPHERE and the AOF.

Project outlook

The year 2011 will be an exciting one during which all the AOF project subsystems will start assembly and testing. The first science thin shell mirror and the GRAAL main assembly should be delivered during the first quarter of the year. GALACSI integration will already be underway and preliminary tests of the two AO module subsystems will take place in the course of the year. ASSIST will be delivered to Garching and integrated during the second half of 2011.

The AOF system test phase will start when the DSM is delivered in the first quarter of 2012 and will proceed with optical testing of the DSM, full system tests of GRAAL and then GALACSI. This will last for slightly more than one year. The 4LGSF integration and test proceeds in parallel to these activities and the first shipments to Paranal and the beginning of the commissioning activities will take place during the second half of 2013. This shipment will trigger intense commissioning activities involving the whole AOF team until the end of 2014, which is the project goal for provisional acceptance Chile.

References

- Arsenault, R. et al. 2010, Proc. SPIE, 7736, 0L
- Baade, D. et al. 2009, The Messenger, 136, 20
- Bonaccini Calia, D. et al. 2010, The Messenger, 139, 12
- Feautrier, P. et al. 2010, Proc. SPIE, 7736, 0Z
- Paufique, J. et al. 2010, Proc. SPIE, 7736, 1P
- Stuik, R. et al. 2010, Proc. SPIE, 7736, 3M

Links

- ¹ Deformable secondary mirror: <http://www.eso.org/public/announcements/ann1056/>
- ² OCam: <http://www.eso.org/public/images/eso0922b/>

ALMA Status and Progress towards Early Science

Leonardo Testi¹
 Richard Hills²
 Robert Laing¹
 Stefano Stanghellini¹
 Wolfgang Wild¹

¹ ESO

² Joint ALMA Observatory

We report on the status and progress of the ALMA project and the expected timeline and capabilities for Early Science. Over the past year, the progress on ALMA construction and on the commissioning activities has been huge. At the time of writing the observatory is progressing on the initial phases of science verification and preparing to open to external users to begin Early Science observations.

The year 2010 has seen extraordinary progress in the ALMA project. At the beginning of the year, with three fully equipped antennas working as an interferometer, Commissioning and Science Verification (CSV) activities officially started at the Array Operations Site (AOS) on the Chajnantor plateau at an elevation of 5000 metres (Testi, 2010). Under the leadership of Richard Hills and Alison Peck at the Joint ALMA Office, the CSV team has been steadily working to test and improve the performance of the whole ALMA system. This process has culminated in the production of the first ALMA test images in the second part of the year (see Figure 1 for an early example). At the time of writing the CSV

team is working to obtain science demonstration data with the eight-antenna interferometer at the high site and is focusing on refining the calibration plan, in addition to continuing the commissioning activities on the equipment that is constantly being delivered.

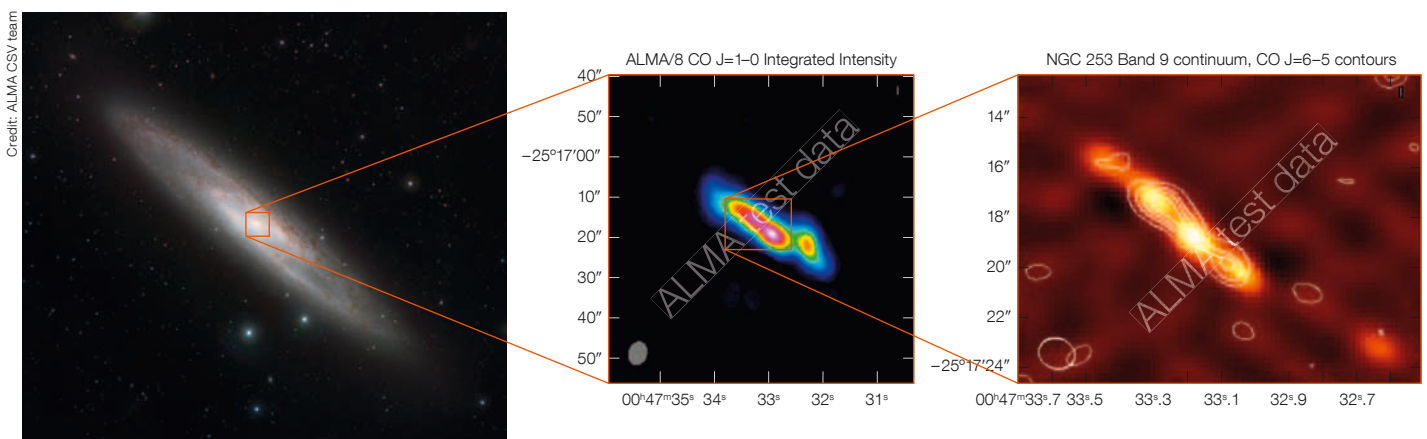
On the hardware construction side, there has been steady progress throughout the year thanks to the tremendous effort from the project teams in all regions and the work of the Assembly Integration and Verification group in Chile. In particular, focusing on deliverables from the European side, the ALMA front-end cartridges for Band 7 (275–373 GHz, produced at IRAM in France) and Band 9 (602–720 GHz, produced by NOVA in the Netherlands) as well as the water vapour radiometers (produced by the Swedish company Omnisys) are in a very advanced stage of production and more than half of the total number of units have been delivered to the project. The test data shown in Figure 2 were obtained with the Band 7 and Band 9 cartridges. Phase correction using the water vapour radiometers (see Nikolic et al., 2009) has been demonstrated as part of commissioning; this represents a key step towards validating the ALMA calibration strategy for high frequency and high angular resolution observations.

Naturally, the most visible pieces of hardware of the ALMA system are the antennas. ALMA has provisionally accepted fourteen antennas. Eight antennas are fully equipped and working as an interferometer at the high site (see the image on the Telescopes and Instru-

mentation section page, p. 4); the remainder are partly equipped and under test or in the process of being outfitted with ALMA front-end and back-end systems at the Operations Support Facility (OSF). Many more antennas are in various stages of assembly in the contractor camps at OSF. Among these are the first European antennas from the AEM consortium; five of these have been fully assembled at the time of writing (see Figure 3) and the first ones are undergoing performance tests and tuning with the goal of being delivered to the ALMA project in early 2011.

Initial results of the all-sky pointing tests have been excellent with the root mean square on pointing accuracy below 1 arc-second (see Figure 4 for an example of a pointing run). The surface accuracy of the European antenna tested so far is also excellent. The panels are mounted and aligned in the assembly procedures to a good initial accuracy. Preliminary tests on the first antenna have shown that, following a partial initial cycle of holography measurements and panel adjustments, the surface can be brought within the ALMA specifications (see example in Figure 5). Testing of many aspects, such as the dependence of the antenna performance on environmental conditions and of the final figure and stability of the surface accuracy, are starting at the time of writing.

Figure 1. ALMA test data obtained in Bands 3 and 9 on the nearby star-forming galaxy NGC 253. The large image is a VISTA infrared image of NGC 253 (see ESO PR 1025). The data shown is the CO(1–0) integrated emission; at right the CO(6–5) integrated emission contours are overlaid on the 0.45 mm continuum emission.



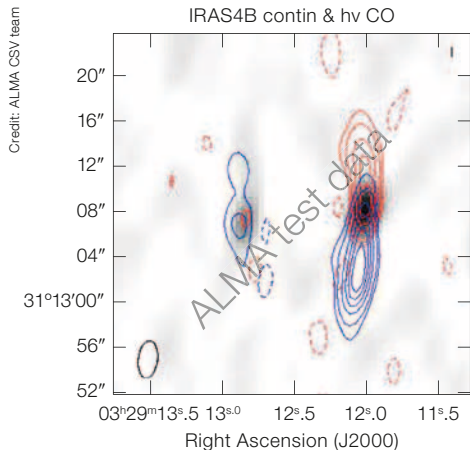


Figure 2. ALMA test data in Band 7 of the molecular outflow in the star-forming region NGC 1333. The red and blue contours show the high velocity CO(3–2) emission while the 0.85 mm continuum emission is shown as greyscale.



Figure 3. The AEM antenna camp at the OSF. Five antennas are fully assembled while a sixth is inside the temporary shelter on the right ready for the installation of the main reflector assembly; parts of the seventh antenna are also being assembled.

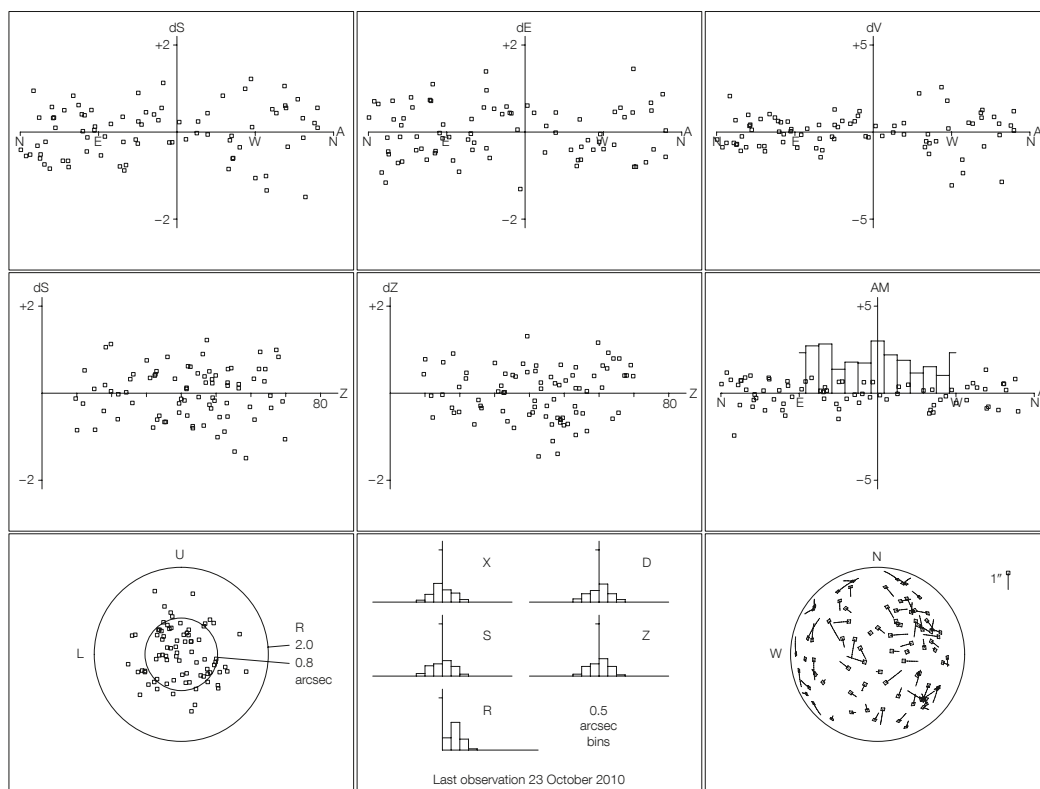


Figure 4. Example of all-sky optical pointing session for the first AEM antenna. The top panels show the pointing errors as a function of azimuth and elevation of the observed stars. The bottom right circular diagram shows the position of the observed stars on the sky. The bottom left circular panel shows the pointing error distribution, which in this case corresponds to an all sky rms accuracy of 0.8 arcseconds.



Figure 5. Adjusting panels on the AEM antennas using the manual panel adjuster tools. Note that this operation can be performed walking on the reflector surface when the antenna is stowed; the hole on the dish surface to the rear of the image is used for the optical pointing telescope.

During the autumn of 2010, the ALMA project has been going through a series of external reviews that have focused on the progress and current results of the CSV activities and the readiness for operations, culminating in the ALMA Annual External Review. These reviews scrutinised all the aspects of the ALMA project and provided advice to the ALMA Director and the ALMA Board on the status and progress of ALMA construction. The main focus of the reviews has been to assess the readiness of ALMA for Early Science. The conclusion of the reviews is that hardware delivery, system verification and commissioning, as well as the deployment of all the procedures for the start of science operations, are all progressing at the pace required to start Early Science observations in the second half of 2011. Nevertheless, the opening of the observatory to external users will result in additional challenges to meet the

standards expected for ALMA data and run science operations at the same time as construction and commissioning. For these reasons the ALMA science advisory committees have all recommended that the main focus remains on the full ALMA construction and operations and that the Early Science capabilities are focused on a limited set of well-tested modes.

The announcement of opportunity for Early Science observations will be released in the first quarter of 2011 with the deadline for proposal submission before the summer. The precise capabilities that will be available for Early Science will be announced as part of the call for proposals, but it is likely that the array will be offered in two compact configurations of 16 antennas (with the maximum baseline likely to be of the order of 250 metres). The limited instantaneous coverage of the uv -plane will imply that most projects will require Earth rotation synthesis to achieve good imaging capabilities during Early Science. The available observing modes will be limited to single field interferometry using Bands 3, 6, 7 or 9 (84–116 GHz, 211–275 GHz, 275–373 GHz, 602–720 GHz, respectively), full polarisation capabilities and a range of single

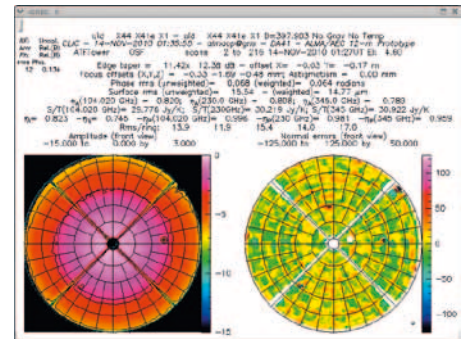



Figure 6. Example results of a holography run after tuning the position of approximately half of the panels on the AEM dish. In this particular case the surface was found to be set to approximately 15 μm rms.

spectral resolution correlator modes. During the first year of operations, scientific observations will be limited to a fraction of the total available time, not exceeding 30%, as the first priority of the project will be to work on completing and commissioning the full ALMA system.

A series of workshops, schools and tutorials have been and are being organised to prepare European astronomers for ALMA. The European ALMA Regional Centre (ARC) and its nodes located in several European countries have put in place a strong effort to support the community uptake of Early Science. On 6 and 7 April 2011, the European ARC will organise a tutorial at ESO Headquarters in Garching focused on the use of the ALMA software for Early Science (see the full announcement on page 49). In particular, the tutorials will focus on the use of the ALMA observing tool, which will be used by ALMA users for the preparation of observing proposals and to set up the approved projects for observation at the telescope.

References

- Nikolic, B. et al. 2009, *The Messenger*, 131, 14
 Testi, L. 2010, *The Messenger*, 139, 52

A detailed astronomical image of the R Coronae Australis star formation region. The central focus is a bright, multi-colored star (R Coronae Australis) surrounded by a dense cluster of younger stars. The scene is filled with dark, dusty molecular clouds and reflection nebulosity, creating a complex and dynamic environment. The background is a vast field of stars, with some appearing as bright, multi-pointed sources.

Colour image of the nearby intermediate—low mass star formation region R Coronae Australis taken with the MPG/ESO 2.2-metre telescope. Images through *B*-, *V*- and *R*-band filters were combined. The star in the centre is R Coronae Australis itself (an Herbig Ae/Be star), which is surrounded by an embedded cluster of young stars, the Coronet. Dark clouds and reflection nebulosity from illuminated dusty molecular clouds encircle the region.

Precise Modelling of Telluric Features in Astronomical Spectra

Andreas Seifahrt^{1,2,3}

Hans Ulrich Käufel³

Günther Zängl^{4,5}

Jacob Bean^{2,6}

Matthew Richter¹

Ralf Siebenmorgen³

¹ University of California at Davis, USA

² Institut für Astrophysik, Göttingen, Germany

³ ESO

⁴ Meteorologisches Institut der LMU, München, Germany

⁵ Deutscher Wetterdienst, Offenbach, Germany

⁶ Harvard–Smithsonian Center for Astrophysics, Cambridge, USA

Ground-based astronomical observations suffer from the disturbing effects of the Earth's atmosphere. Oxygen, water vapour and a number of atmospheric trace gases absorb and emit light at discrete frequencies, shaping observing bands in the near- and mid-infrared and leaving their fingerprints — telluric absorption and emission lines — in astronomical spectra.

The standard approach of removing the absorption lines is to observe a telluric standard star: a time-consuming and often imperfect solution. Alternatively, the spectral features of the Earth's atmosphere can be modelled using a radiative transfer code, often delivering a satisfying solution that removes these features without additional observations. In addition the model also provides a precise wavelength solution and an instrumental profile.

The Earth's atmosphere consists of a rich gas mixture. While its main constituent, nitrogen (N_2), does not exhibit any rotational–vibrational transitions, most other molecules do. Strong absorption line systems from water vapour (H_2O), carbon dioxide (CO_2) and ozone (O_3) shape the well-known photometric band-passes in the near- and mid-infrared. In addition, oxygen (O_2) shows strong absorption bands in the red optical; other molecules such as nitrous oxide (N_2O), carbon monoxide (CO), or methane (CH_4) contribute noticeably to the atmospheric

transmission losses in the near- and mid-infrared, often hampering the observation of important astrophysical lines.

While the Earth's atmosphere absorbs light from astronomical sources at a large number of frequencies from the ultraviolet to radio wavelengths, it also emits light in the same transitions, radiating its thermal energy into space. At wavelengths longer than about 2300 nm, the emission originating from the Earth's atmosphere competes with the signal from astronomical sources. The break-even point depends on many factors, such as the spatial resolution, slit width, and detector characteristics of the spectrograph, but also on the height of the observing site. Since the atmospheric emission is spatially extended, it affects the spectrum of the astronomical target similarly to the nearby sky and can thus be removed by beam-switching (nodding) techniques or by fitting and subtracting the two-dimensional signal along the slit.

Empirical calibration

Removing the telluric absorption features is more difficult since their exact signature is only imprinted in the source spectrum. Traditionally, telluric absorption features are removed by observing a so-called telluric standard star before or after the observation of the science target at the same airmass, subsequently dividing the spectrum of the science target by that of the telluric standard. Typically, early-type stars with spectral types ranging from early B to late A are used for this purpose, since they exhibit rather featureless spectra, except for strong hydrogen lines. Since these stars are often fast rotators, other weak stellar features, for example helium lines, are further suppressed. Alternatively, early-to-mid G-type stars can serve as telluric standards as well, since high resolution Fourier transform spectra (FTS) of the Sun provide the necessary template to compensate for their intrinsic stellar features. The observation of telluric standard stars is a standard procedure and commonly employed for all spectrographs operating on ESO telescopes. It is often part of the calibration plan for the instrument

and, in these cases, is automatically provided for service mode observations. Since telluric lines generally do not scale linearly with airmass and observing conditions are time variable, it is necessary to observe a telluric standard star at the same airmass and close in time to the science target in the same instrumental setup. Special software tools at the telescope allow the efficient selection of an appropriate standard star.

Nevertheless, using standard stars as empirical calibrators has several disadvantages. The observation of standard stars is time-consuming, especially when science targets are bright or high signal-to-noise requirements are to be met. For the brightest standard stars, the time required for telescope and instrument presets ultimately limits the efficiency of this method. Moreover, on instruments like CRIFES, the instrumental profile depends on the performance of an adaptive optics system, and thus, on the observing conditions and source brightness. Changes in the instrumental profile lead to changes in the line shape of unresolved spectral lines. In these cases standard stars rarely provide a perfect match to the science target, effectively limiting the precision with which telluric features can be removed.

Other shortcomings originate from the intrinsic stellar features of the standard stars. Hydrogen and helium lines in early-type standards cannot be perfectly removed and thus affect the line profiles of the same species in the spectrum of the science target. A further complication in removing these lines occurs when the wavelength coverage of the spectrum is shorter than the line widths of broad hydrogen lines, which can easily be the case for CRIFES. Early-type stars can also exhibit other spectral features, such as oxygen or carbon lines in the near-infrared, often as emission features originating under non-local thermodynamic equilibrium (non-LTE) conditions. Similarly, mismatches in the line depths of solar-type standard stars with the solar FTS atlas, attributable to abundance differences or deviating effective temperatures, can leave residuals of the standard star's intrinsic features in the final spectrum.

Modelling telluric features

Alternatively, the telluric absorption spectrum can be synthesised, using a radiative transfer code in combination with a layered model of the Earth's atmosphere and a database containing the transition data for all molecules in consideration. We have successfully used the program LBLRTM (Clough et al., 1992) for this purpose. LBLRTM is a non-commercial layer-by-layer radiative transfer code tailored to produce telluric spectra under various atmospheric geometries. The code is generally available to the community and uses the high resolution transmission molecular absorption database HITRAN (Rothman et al., 2009) as a molecular line database. HITRAN contains energy levels, frequencies, line strengths, pressure-broadening and -shift coefficients, for more than 1.7 million spectral lines of 42 different molecules and their common isotopes from the red optical to the sub-mm.

A layered model of the Earth's atmosphere serves as the primary input for LBLRTM and contains temperature, pressure and molecular abundance information as a function of atmospheric height at the observatory. For a representative, yet accessible model of the atmospheric conditions at the time of the observation, we supplement a static model of the atmosphere with meteorological data for temperature, pressure and humidity of the troposphere and lower stratosphere (surface height ≤ 26 km). LBLRTM converts the atmospheric model into individual isothermal layers and calculates absorption and emission spectra for a given path through the atmosphere, i.e. for a given zenith angle or airmass.

A single model run takes only a few seconds on a standard desktop PC. The resulting spectrum has an intrinsic reso-

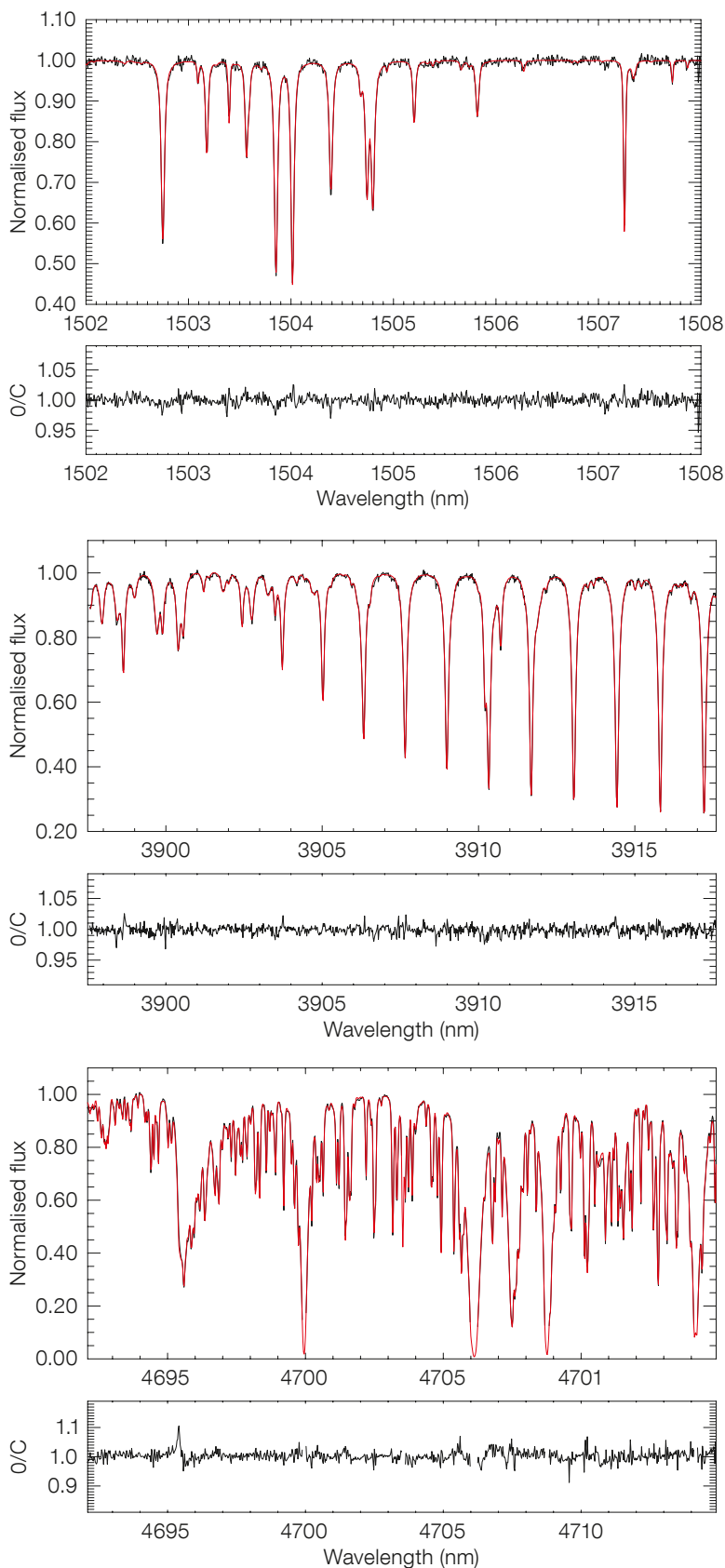


Figure 1. Examples of synthesised telluric spectra fitted to CRIRES observations of standard stars. Each panel shows the measured spectrum in black and the model overplotted in red. We show the residuals after division by the models, i.e., after removal of the telluric absorption lines, at the bottom of each panel. Top panel: Water vapour (H_2O) lines in the *H*-band. Middle panel: Nitrous oxide (N_2O) and water vapour (H_2O) in the *L*-band. Bottom panel: Ozone (O_3), carbon monoxide (CO), carbon dioxide (CO_2), and water vapour (H_2O) lines in the *M*-band.

lution that is set to resolve the narrowest telluric lines in a given spectral region. Resolving powers are thus often of the order of 10^6 and the model spectrum needs to be convolved with the instrumental profile of the spectrograph to match the measured telluric spectrum. To first order, the instrumental profile can be represented by a single Gaussian function. More complex profiles might be used if higher precisions and signal-to-noise ratios need to be achieved. At the same time, the abundance of certain molecules might be over- or underestimated by the atmospheric model, especially for strongly variable species such as water vapour. Given the extreme geographical location of most astronomical observatories, including Cerro Paranal, general meteorological models rarely reproduce the exact water vapour levels on site. Thus, the model data need to be matched to the actual observing conditions. A chi-squared fitting algorithm can be employed to solve for the instrumental profile and to re-adjust the abundance of the molecular species in the atmospheric model while minimising the residuals between the observed spectrum and the spectral model.

We show some example fits to spectra obtained with the CRIRES spectrograph in Figure 1. The resolving power was $R \sim 65\,000\text{--}80\,000$ as measured from the width of the instrumental profile, which was fitted at the same time as a single Gaussian function. More examples and a detailed discussion of the fitting performance can be found in Seifahrt et al. (2010). In all cases, the abundance of most atmospheric species was slightly modified by a few percent during fitting to achieve an optimal result. The fit process also included the wavelength solution for the CRIRES spectra. This step is critical, since narrow and steep telluric lines are sensitive to small wavelength errors and produce notable residuals for wavelength mismatches as small as ~ 30 m/s. A typical fit process, including various runs of LBLRTM takes about two minutes to converge over the spectral coverage of a single CRIRES detector. We have also successfully applied the code to optical high resolution spectra from UVES and to low resolution near-infrared spectra from SINFONI.

Wavelength calibration as added value

Fitting telluric lines to empirical spectra not only provides a model of the telluric absorption, it also delivers a precise wavelength solution. This is an important added value of this method, given that the wavelength calibration for high resolution near- and mid-infrared spectra is often challenging. Rare gas emission line lamps used in low resolution near-infrared spectrographs, such as He, Ne, Xe, and Kr lamps, provide only a sparse line density and are only of very limited use at high spectral resolution (see also Aldenius et al., 2008). Even the rich spectra of ThAr emission line lamps, commonly employed by high resolution optical spectrographs, have a much lower line density in the near-infrared than in the red optical. Typical line densities of ~ 400 lines per 100 nm around $\lambda = 1000$ nm drop quickly to less than ~ 20 lines per 100 nm at $\lambda = 2500$ nm. Given the typical wavelength coverage of $\sim \lambda/200$ per CRIRES detector, many spectral settings remain poorly calibrated. Moreover the dynamic range of the ThAr emission spectrum is very high due to the strong contrast between the Th and Ar lines, leaving weaker lines at low signal-to-noise ratios while nearby stronger lines quickly saturate.

Often atmospheric OH* emission lines (commonly referred to as airglow emission) are used for wavelength calibration in the near-infrared, especially for low- and mid-resolution spectrographs. OH* is a chemical radical and its transitions originate from non-LTE processes in high atmospheric layers. They appear in emission but not in absorption in astronomical spectra and constitute the dominant background source in the near-infrared *J*- and *H*-bands. However, neither the line density nor the line strength of individual OH* lines is high enough to make this species useful for the wavelength calibration of high-resolution spectrographs. For example, the small spatial pixel scale of CRIRES (86 milliarcseconds/pix) makes the use of OH* lines especially challenging, given that each pixel covers less than 10^{-2} arcsecond² on the sky.

In contrast, the atmospheric features of other regular molecules in LTE, as we model them with LBLRTM, show a high density of strong absorption lines and

thus provide a natural *in situ* wavelength calibration. Since they are imprinted in the source spectrum before the light reaches the spectrograph, these lines suffer the same instrumental effects as the intrinsic lines in the stellar spectrum. Hence, in contrast to all emission line sources used to wavelength calibrate long-slit spectra, telluric absorption lines provide an intrinsically more precise calibration source, especially since lamp emission lines are recorded in separate exposures, often hours after the science spectra and thus after potential changes in the spectrograph setup.

Performance and limitations

As can be seen in the examples presented in Figure 1, the modelling of telluric absorption lines is not perfect, but leaves residuals at the 2% level for most lines when observed at high spectral resolution. A few lines exhibit even stronger residuals. The main reasons for these mismatches are imprecise line data in the HITRAN database and insufficient treatment of line coupling (also known as line mixing) in the radiative transfer code. The latter is, for example, responsible for the strong residuals of the CO₂ Q-branch at 4695 nm (see the lower panel of Figure 1). Other limitations may arise from uncertainties in the determination of the instrumental profile and the atmospheric model.

Line data in HITRAN have strongly varying accuracy levels. Typical uncertainties of line positions range from a few to several hundred m/s, but can be as high as several km/s in extreme cases. Line strengths are rarely precise to the 1% level. However, the HITRAN database is constantly updated and the data quality will further improve in the future. Also, individual line data can be re-fitted when comparing synthesised spectra with high resolution spectra of standard stars before applying the code to spectra of science targets.

Despite these limitations, synthesised telluric spectra can provide the same or even better telluric correction than empirical spectra. The question of when to use empirical spectra or a telluric model depends on a number of factors and

should be decided on a case-by-case basis. However, the use of a telluric model should be strongly considered for regions where standard stars have spectral features, when instrumental setups (including the instrumental profile) cannot be reproduced, or when observations encompass a wide range in airmass.

Some recent and ongoing science programmes entirely rely on telluric models for calibration. One example is the CRIRES-POP project, dedicated to providing the community with a high resolution, high signal-to-noise near-infrared spectral atlas of several stars across the Hertzsprung-Russell diagram (Lebzelter et al., 2010). Data reduction for this project employs telluric models to wavelength calibrate settings that lack coverage by ThAr lines or gas cells. CRIRES-POP concentrates on very bright stars and uses a large number of CRIRES settings. Obtaining spectra of telluric standard stars for each science target would be very time consuming, at least doubling the total observing time. Most importantly, the programme

includes observations of early-type stars to map their spectra to search for unaccounted lines. This process would prove impossible if a standard star of similar spectral type was used as an atmospheric calibrator.

Another project utilising telluric models is the CRIRES radial velocity campaign to search for extrasolar planets around mid-to-late M-type stars (Bean et al., 2010a,b). The wavelength calibration for this project relies on a custom-built ammonia gas cell, given the need to determine radial velocities to the m/s level. The telluric features present in all observations obtained by this programme need to be corrected to a high level of precision. Obtaining high signal-to-noise standard star spectra for all science observations would have made the project less time-effective. Also, the instrumental profile between the science observation and the standard star must match; a challenging requirement for CRIRES. Given the sensitivity of the radial velocity method to small changes in the instrumental profile, the use of stand-

ard star observations would have compromised the achievable long-term radial velocity precision, strongly favouring the telluric modelling approach.

Last but not least, telluric models are not only used to wavelength calibrate and to correct for the telluric features in observed spectra, but also to plan observations and predict the atmospheric throughput based on meteorological forecasts. For example, the exposure time calculator for CRIRES employs a telluric model to allow the user to check spectral settings for the impact of telluric absorption under different water vapour levels.

References

- Aldenius, M. et al. 2008, *The Messenger*, 133, 14
 Clough, S. A., Iacono, M. J. & Moncet, J.-L. 1992, *J. Geophys. Res.*, 97, 15761
 Rothman, L. S. et al. 2009, *Journal of Quantitative Spectroscopy and Radiative Transfer*, 110, 533
 Seifahrt, A. et al. 2010, *A&A*, in press, arXiv:1008.3419
 Bean, J. L. et al. 2010a, *ApJ*, 713, 410
 Bean, J. L. et al. 2010b, *The Messenger*, 140, 41
 Lebzelter, T. et al. 2010, *The Messenger*, 139, 33



NGC 3603, shown here in a VLT FORS three-colour composite (from *V*-, *R*- and *I*-band images), is a young Galactic starburst cluster situated at a distance of 6.8 kiloparsecs. With many dozens of massive young hot stars and an age of a few Myr, it is the focus of many studies as a nearby template for extragalactic starburst environments.

Astronomy Meets Biology: EFOSC2 and the Chirality of Life

Michael Sterzik¹
Stefano Bagnulo²
Armando Azua³
Fabiola Salinas⁴
Jorge Alfaro⁴
Rafael Vicuna³

¹ ESO

² Armagh Observatory, United Kingdom

³ Department of Molecular Genetics and Microbiology, Pontificia Universidad Católica de Chile, Chile

⁴ Faculty of Physics, Pontificia Universidad Católica de Chile, Chile

Homochirality, i.e., the exclusive use of L-amino acids and D-sugar in biological material, induces circular polarisation in the diffuse reflectance spectra of biotic material. Polarimetry may therefore become an interesting remote sensing technique in the future search for extraterrestrial life. We have explored this technique and performed a laboratory experiment making an exotic use of an astronomical instrument. During a period when EFOSC2 was detached from the Nasmyth focus to host a visitor instrument at the NTT, we have observed various samples of biotic and abiotic material and measured their linear and circular polarisation spectra. Among the various targets, we have included samples of the hypolithic cyanobacteria species *Chroococcidiopsis* isolated from the Coastal Range of the Atacama Desert. To our knowledge, these are the first and highest precision measurements of circular polarisation using living material and obtained with an astronomical instrument.

Motivation

The building blocks of life are *chiral*. Their molecular structure lacks an internal plane of symmetry, and their mirror image cannot be superimposed on their original image. The term chirality is specifically used when a molecule (or an object) exists in both mirror-symmetric configurations. The human hands are the classic example that illustrates the concept of chirality, and the term *chiral* itself comes from the Greek word for hand, $\chi\epsilon\rho\iota\pi$. In chemistry, the two images of a chiral

molecule are called enantiomers, and the two forms are generally referred to as right-handed and left-handed, or dextrorotatory and levorotatory.

The term *homochirality* is used when a molecule (or a crystal) may potentially exist in both forms, but only one is actually present. Homochirality characterises life as we know it: all living material on Earth contains and synthesises sugars and nucleic acids exclusively in their right-handed form, while amino acids and proteins occur only in their left-handed representation. However, in all these cases, both enantiomers are chemically possible and energetically equal. The reasons for homochirality in living material are unknown, but they must be related to the origin of life. It is still disputed whether bioactive molecules (and with them small enantiomeric excesses) were delivered to Earth (e.g., by meteorites) or whether (pre-)biotic chemistry started on Earth (Bailey et al., 1998). Undoubtedly, however, chemical and biological processes on Earth must have favoured the selection of one-handed biomolecules leading towards homochirality. If similar evolutionary scenarios naturally occur elsewhere in the Universe, homochirality may be a universal hallmark of all forms of life.

Chirality induces optical activity: each enantiomer rotates the reflected (or transmitted) light in opposite directions, and homochirality guarantees that there will be an excess of circularly polarised light in one direction. This opens up the interesting possibility that biosignatures could be sensed remotely by means of polarimetric techniques.

This chain of arguments, which had been raised in various articles in the scientific literature (e.g., Wolstencroft et al., 2004), was also discussed during the workshop Astrobio 2010¹ held in Santiago de Chile last January. For the first time, an international and interdisciplinary conference that aimed to cover major topics in astrobiology was organised and hosted in Chile. The topics covered included the origins of life, the chemistry of the Universe, extrasolar planetary systems, and the search for life in the Solar System. A prominent topic of discussion was the Atacama Desert as an example of an

extreme environment on Earth, and the microbial colonisation of subsurface layers in halites (rock salt) and quartz rocks by specific cyanobacteria. In the most hostile environments (exceptional aridity, salinity, and extreme temperatures), a primitive type of cyanobacteria, *Chroococcidiopsis*, can be the sole surviving organism. This has interesting implications for the potential habitability, and eventual terraforming, of certain areas on Mars (Friedmann & Ocampo-Friedmann, 1995).

The idea of using the ESO Faint Object Spectrograph and Camera (EFOSC2) to investigate samples of *Chroococcidiopsis* extracted from the underside of Atacama Desert quartzes and to measure their circular polarisation in a laboratory experiment arose at this conference. The idea looked appealing, because only limited, and sometimes contradictory, reports about circular polarisation measurements of biotic material as a signature of homochirality are available in the literature. Moreover, the successful use of an astronomical instrument for the first time for that purpose could serve as a benchmark for further applications of this method in astrophysics.

A detailed feasibility study as well as the production of significant quantities of *Chroococcidiopsis* were prepared and initiated in the following weeks. Since there is no formal process in place to obtain “observing time” for laboratory experiments, the ESO Director General was asked for authorisation. He approved the experiment under the condition that it did not pose any risk to the instrument. This could be achieved by using EFOSC2 when it was not attached at its nominal Nasmyth focal station (i.e. during an extended visitor instrument run), but keeping it in a horizontal position (which avoids the possibility of any material falling on the entrance window). Our “laboratory” is shown in Figure 1, left. EFOSC2 is detached from the New Technology Telescope (NTT). A microphotograph of our main target, *Chroococcidiopsis*, is displayed on the right.

Experiment

During one week in June 2010, three of us (Pontificia Universidad Católica

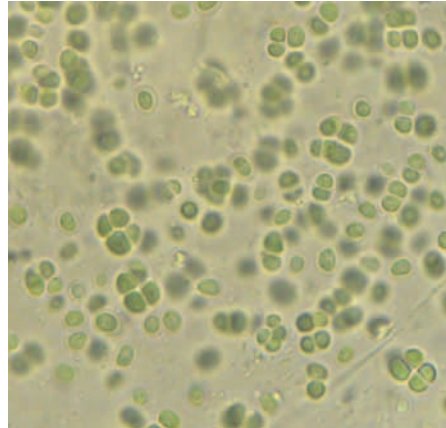
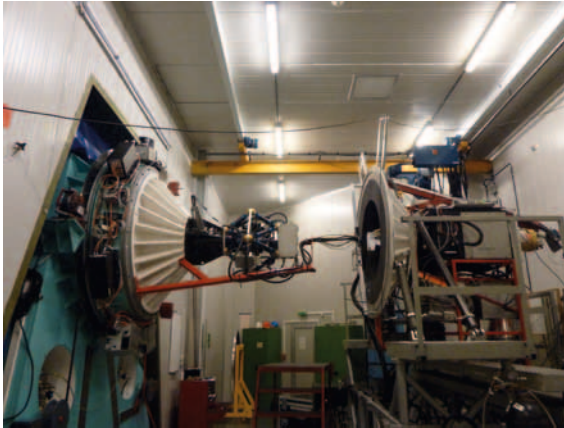


Figure 1. Left: The EFOSC2 instrument is shown detached from the NTT. The instrument attached to the Nasmyth focus (on the left) is ULTRACAM. Right: A microphotograph of the cyanobacteria *Chroococciopsis*, enlarged 100 times.

student Fabiola Salinas, Stefano Bagnulo and Michael Sterzik) were busy using EFOSC2 to observe samples of minerals and paints (quartz, salt, sugar, white flat-field screen), leaves (*Philodendron*, *Ficus*, *Schefflera*) and cyanobacteria films deposited on filter paper. All samples were prepared as thin sheets inserted in the flat-field screen position. An integrating sphere (the usual calibration lamp mechanism for EFOSC2 when attached to the 3.6-metre telescope) was used for diffuse illumination. EFOSC2 covers large spectral regions in the spectropolarimetry mode: we used mostly grism 13 to cover the range 370–930 nm, with a spectral resolution of ~ 2.3 nm (we adopted a 1-arcsecond slit width). Both linear and circular polarisation measurements of the samples were obtained, using the $\lambda/2$ and $\lambda/4$ retarder waveplates, respectively (we note that the $\lambda/4$ retarder waveplate is a recent addition to the instrument, see Saviane et al. [2007]).

Polarimetric measurements were taken by combining several pairs of exposures obtained with different position angles of the retarder waveplates (-45° , 45° , 135° , 225° for circular polarisation, and 0° , 22.5° , 45° , ... 335.5° for linear polarisation measurements, measured from the principal plane of the Wollaston prism). This “beam swapping” technique minimises the instrumental effects — for a detailed description of the measuring strategies, see, e.g., Bagnulo et al. (2009). For inorganic samples and for leaves, the typical observation cycles lasted 20 minutes, dominated in practice by overheads (readout time and retarder waveplate setting), and allowed us

to measure the polarisation level with an error bar of the order of 10^{-4} per spectral bin. Measurements of the cyanobacteria lasted several hours, but for a total integration time of just about 10 minutes. This exposure allowed us to reach an error bar of 10^{-6} per spectral bin. These figures refer only to the statistical errors due to Poisson noise. With our ultra-high signal-to-noise ratio measurements, we have certainly hit the limits imposed by the polarimetric optics and the experimental conditions — we will come back later to this important point. Here we note that the reliability of the error bars (in terms of statistical error) has been validated with the use of so-called null-profiles (i.e. the difference between Stokes profiles obtained from different pairs of exposures). Null profiles were found scattered around zero within the error bars.

Results and outlook

Figures 2 and 3 show the results obtained from our circular polarisation measurements (Stokes V normalised to the intensity) of a *Philodendron* leaf, and a film of *Chroococciopsis* deposited on filter paper, respectively. We also obtained calibration measurements of a white screen flat-field, produced by a barium sulphate based white reflectance coating. The circular polarisation measured for the screen flat-field was found as a negative continuum of about -0.05% , with the absolute value slowly increasing towards shorter wavelengths. No narrow features or signals are present in the polarisation spectra of this reference source.

In the *Philodendron* leaf we detected both broad polarised features (with an amplitude of $\sim 0.5\%$), and, superposed on them, a narrow feature at about 680 nm (with an amplitude of $\sim 0.05\%$ over the continuum), both well above the statistical noise (the green line shows the null profile). The behaviour of Stokes V in the continuum closely follows the reflectivity, shown with a solid black line (this is known as the Cotton effect). This behaviour closely resembles the diffuse reflectance circular dichroism spectra of leaves as seen by Wolstencroft et al. (2004). The narrow feature around 680 nm is very similar to the results shown by Gregory & Raps (1974) in their transmission spectroscopy of chloroplasts and is related to the chlorophyll-a pigment response.

The interpretation of the results for *Chroococciopsis* is the most interesting. In the continuum, Stokes V shows a behaviour similar to that observed for the white screen field, and hence is likely to be of instrumental origin. A number of narrow, low amplitude features appear superposed on the continuum. In order to prove that these features are real (and not spurious signals, e.g., caused by the CCD readout noise) we also obtained ultra-high signal-to-noise ratio measurements with the retarder waveplate at 0° , 90° , 180° and 270° . With these retarder waveplate settings, we would theoretically expect a null signal. The resulting profile, shown with the red line in Figure 3, and arbitrarily rectified to zero for display purposes, shows no high frequency signatures. This curve, together with a consistently flat null profile (shown

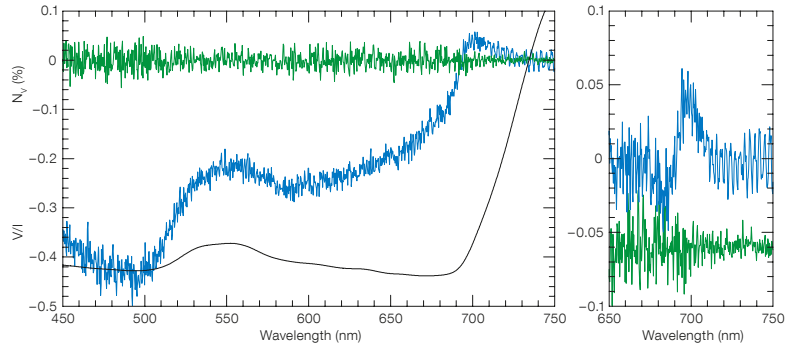


Figure 2. The *Philodendron* leaf is shown at left and its polarised spectrum measured with EFOSC2 at middle and right. The blue lines show the circular polarisation (V/I). In the rightmost panel, V/I is rectified to zero. The green lines show the null profile (offset by -0.06% in the rightmost panel, for display purposes) demonstrating the statistical errors. The black line is the reflectivity (in arbitrary units).

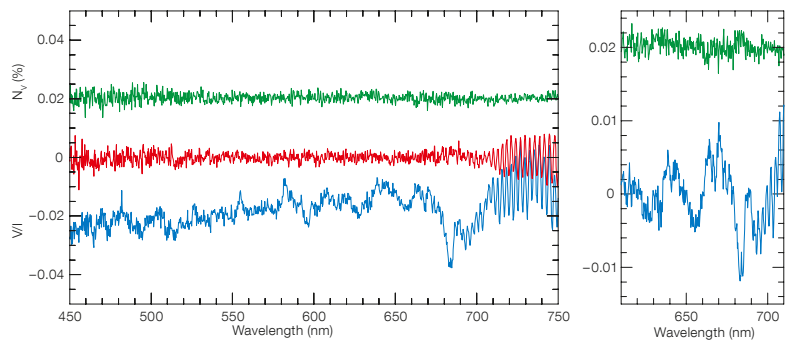


Figure 3. The sample of *Chroococcidiopsis* is shown at left and its polarised spectrum in the middle and right panels. The blue line shows circular polarisation and the green line is the null profile (offset by $+0.02\%$). The red line shows the spectrum obtained with the retarder waveplate at position angles offset by 45° , rectified to zero. In the rightmost panel, V/I is rectified to zero.

with the green line offset to $+0.02\%$ in the right panel) suggests that the narrow features are indeed real. We notice again the prominent chlorophyll-a feature around 680 nm , but may also infer signatures of other pigments like carotenoids and phycocyanins. Our measurements also appear consistent with polarisation spectra obtained from a different type of cyanobacteria by Sparks et al. (2009).

While we kept the noise confidently at a very low level, the polarimetric mode of EFOSC2 is lacking the full characterisation needed to reach ultra-high and absolute precision polarimetric measurements under the conditions of our experiment. Using special calibration techniques, in some astronomical observations it is already possible to achieve a precision of 10^{-6} (e.g., Bailey et al., 2010), but in our experiments we are limited by an instrument setup in which most of the signal comes from off-axis rays. Patat & Romaniello (2006) and Bagnulo et al. (2009) have discussed the spurious polarimetric effects observed off-axis with

the FORS instrument of the VLT. Some of these effects may also play a role in EFOSC2. We must also remark that the prepared samples are not fully reproducible in their configuration, and thus likely introduce some effects due to their different backscattering properties.

In conclusion, the polarised spectra of Figures 2 and 3 show that the polarimetric techniques employed by us are sensitive to the presence of biotic material. We detect chiral signatures of pigments involved in biotic photosynthetic reaction chains. Signatures of chlorophyll pigments can be captured both in samples of leaves and cyanobacteria of species *Chroococcidiopsis*. More accurate measurements of the polarised signal amplitudes require experiments to be carried out with samples prepared under better controlled laboratory conditions. It will also be interesting to observe the polarimetric signatures of *Chroococcidiopsis* in their natural habitat beneath translucent rock surfaces. This will allow the feasibility of detecting this type of

bacteria on other Solar System bodies in the future with extremely large telescopes to be assessed.

We thank all the La Silla staff who supported the setup and execution of this unusual experiment! Stefano Bagnulo acknowledges a grant received as visiting scientist at ESO/Chile.

References

- Bagnulo, S. et al. 2009, PASP, 121, 993
- Bailey, J. et al. 1998, Science, 281, 5377, 672
- Bailey, J., Lucas, P. W. & Hough, J. H. 2010, MNRAS, 405, 2570
- Gregory, R. P. F. & Raps, S. 1974, Biochem. J., 142, 193
- Friedmann, E. I. & Ocampo-Friedmann, R. 1995, Adv. Space Res., 15(3), 243
- Patat, F. & Romaniello, M. 2006, PASP, 118, 146
- Saviane, I. et al. 2007, The Messenger, 129, 14
- Sparks, W. B. et al. 2009, PNAS, 106 (19), 7816
- Wolstencroft, R. D., Tranter, G. E. & Le Peleven, D. D. 2004, Bioastronomy 2002, IAU Symp., 213, 149

Links

¹ <http://www.astro.puc.cl/astrobio2010>

Observations of Multiple Stellar Populations in Globular Clusters with FLAMES at the VLT

Raffaele Gratton¹
 Eugenio Carretta²
 Angela Bragaglia²
 Sara Lucatello¹
 Valentina D'Orazi¹

¹ INAF–Osservatorio Astronomico di Padova, Italy

² INAF–Osservatorio Astronomico di Bologna, Italy

In the last few years, it has become evident that globular clusters, previously accepted as prime examples of simple stellar populations, contain at least two, and in some cases more, stellar generations. Thanks to the superb spatial resolution of the Hubble Space Telescope on one side, and to the forefront spectroscopic and multiplexing capabilities of UVES and FLAMES at the VLT on the other, extensive, high precision datasets are shedding light on cluster formation and evolution. Here, we briefly describe the contribution by our team to these exciting discoveries.

Multiple populations in globular clusters

Globular clusters (GCs) are very massive stellar complexes. As an example, Figure 1 shows an image of the globular cluster 47 Tucanae. All GCs observable in or near the Milky Way are very old, so their formation cannot be observed in detail. These early phases were likely complex, including a variety of dramatic and energetic phenomena such as supernova (SN) explosions, photoionisation, high and low velocity winds from blue and red massive stars, possibly combining in giant expanding bubbles of gas and shock fronts that may have triggered further star formation. The scene where this drama occurred might have been even more diversified — in the core of giant clouds or, for the most massive clusters, even of dwarf galaxies. These dramatic events left a trace — represented by the chemical composition of the stars — that not only can be followed today in quite subtle spectral features, but also can influence their distribution along the main sequence (MS) and the horizontal branch (HB).



Figure 1. Image of the globular cluster 47 Tuc (NGC 104), obtained with the ESO 1-metre Schmidt Telescope at the La Silla Observatory in Chile.

All GCs investigated to date show a peculiar abundance pattern (for a review, see Gratton et al., 2004). They usually appear to be very homogeneous, with a few exceptions like M 54 and Omega Centauri, insofar as the Fe-peak elements are concerned, thus ruling out self-enrichment by SN ejecta. However, many GC stars have an unusual composition, rich in Na and Al and poor in O and Mg, typical of material that experienced H-burning at very high temperatures, while others have a normal O- and Mg-rich but Na- and Al-poor composition, which is virtually identical to that of metal-poor field stars. Within each GC, the abundances of Na and O, or Al and Mg are anti-correlated with each other (see Figure 2). Since the main outcome of H-burning is He, we expect low O/high Na stars also to be He-enriched, which explains the occurrence of multiple HBs and MSs. The connection between O–Na and Mg–Al anti-correlations, variations in He abundances, and the presence of multiple HBs is however likely to be more complex than described here (see Gratton et al., 2010).

This abundance pattern between O–Na and Al–Mg is characteristic of GCs, while it is almost absent among field stars (Gratton et al., 2000). It is not limited to red giants, but is present also in the low-mass MS stars, as demonstrated by the key study with the VLT’s high resolution optical spectrograph, UVES, by Gratton et al. (2001; based on the large programme 165.L-0263). These unevolved stars cannot have sustained the nucleosynthesis chains that deplete O and Mg, and enhance Na and Al, because they cannot reach the required temperatures and have very thin convective envelopes, unable to mix nuclear products into their atmospheres. The UVES large programme excluded early claims that this composition might result from a peculiar evolution of GC stars: all low O/high Na stars originated from matter processed and ejected by stars belonging to a previous stellar generation within the GC, although not by the SNe (or the low-mass stars, which give a different characteristic imprinting) of this earlier population.

Self-pollution models still lag behind the observations and are not yet able to explain convincingly all observed features: candidate first generation (FG) polluters

are either thermally pulsating intermediate-mass asymptotic giant branch (AGB) stars undergoing hot bottom burning (Ventura et al., 2001) or massive rotating stars prior to SN explosion (Decressin et al., 2007).

Our FLAMES survey

Although the star-to-star O–Na abundance anticorrelation had been recognised early on as a pivotal signal of self-enrichment in GCs, significant progress was hindered by the slow acquisition rate of data, due to the use of single object spectrographs. At the time of the Gratton et al. (2004) review, data for a grand total of only about 200 stars, distributed in some ten GCs, were available. The high multiplexing capability of the VLT’s Fibre Large Array Multi Element Spectrograph (FLAMES) allowed us an order of magnitude increase in data collection capability: our survey has already harvested spectra for more than 2000 red giants, analysed individually with a homogeneous procedure. With our work, we intended to answer some fundamental questions: Were GC stars really born in a single instantaneous burst? Did all GCs self-enrich themselves? How do abundance patterns within each individual GC relate to the formation and early evolution of the GC itself and of each individual member?

We selected a large sample of GCs with diverse HB morphology, since, as mentioned, there appears to be a link between the chemical anomalies, the extension of the HB, and the presence of multiple MSs. We obtained FLAMES data on 24 GCs (ESO programmes 072.D-0507, 073.D-0211, 081.D-0286, and 083.D-208). We used the pipeline-reduced spectra to obtain Fe, Na, and O abundances from spectra from the medium-high resolution spectrograph, GIRAFFE, and of more elements, including Mg and Al, from the UVES data. Up to now we have published about 15 refereed papers presenting results for 21 GCs.

With this data, we have confirmed that all GCs contain multiple populations (Carretta et al., 2009a). We even proposed a new definition of *bona fide* GCs as “stellar aggregates showing the Na–O

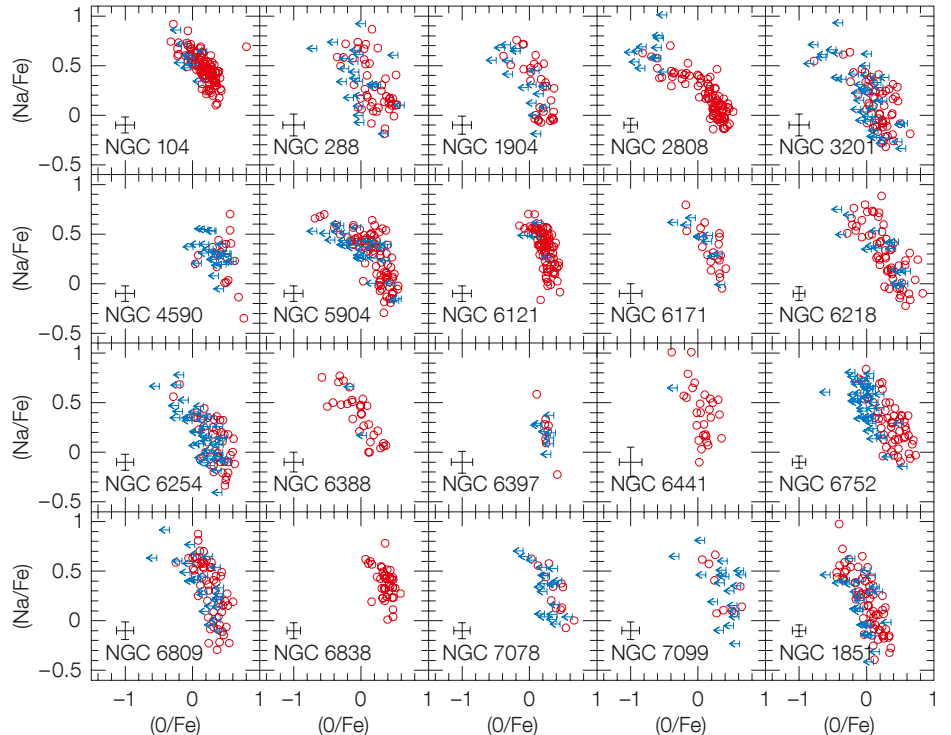


Figure 2. The Na–O anticorrelation is shown as $\log(\text{Na}/\text{Fe})$ vs. $\log(\text{O}/\text{Fe})$ normalised to the solar abundance in 20 GCs as observed with FLAMES (adapted from Carretta et al. [2009a] and Carretta et al. [2010]). The typical error bar for each set of measurements is shown.

anticorrelation”, as distinct from associations and open clusters (Carretta et al., 2010a). In Figure 3, adapted from Carretta et al. (2010a), we show massive stellar clusters (both GCs and open clusters) in the relative age vs. mass plane. Here relative ages are used (see Carretta et al., 2010a): in this scale, a relative age of 1 means an age close to 12.5 Gyr. Different symbols are used for open clusters and GCs, and for those clusters where the Na–O anticorrelation has been found or not (for several clusters, data currently available are not sufficient to clarify this point). From this figure, it seems clear that the presence of multiple populations is the typical result of the formation process of massive stellar clusters and must be explained by their formation scenarios.

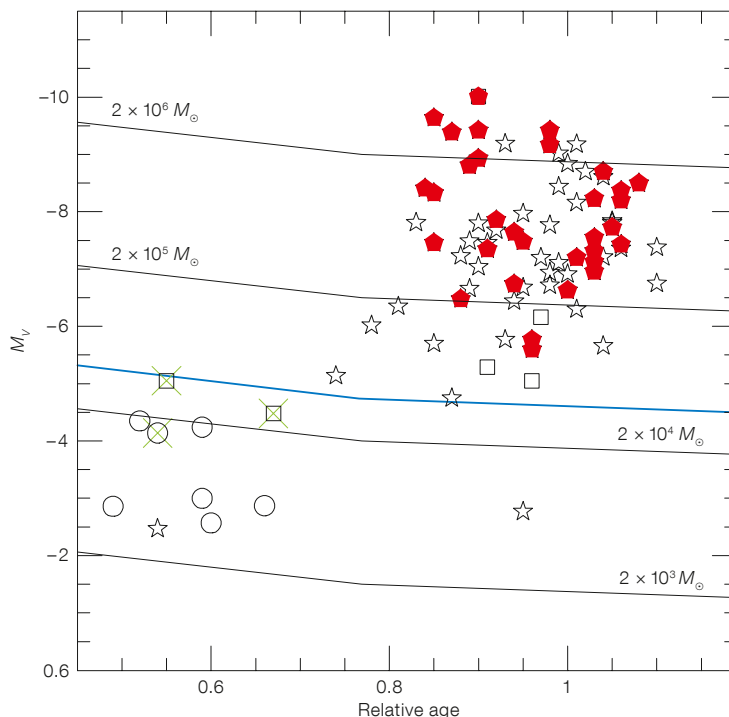
The size of our sample led, for the first time, to a quantitative estimate of the fraction of FG and second generation (SG) stars in GCs (Carretta et al., 2009a). The SG is always dominant, including at

least two thirds of the total population. Since the peculiar chemical composition of the SG stars indicates that only a fraction of FG stars may have produced the right gas mixture, the original clouds from which the GCs formed should have been much more massive than current GCs (likely ten times or even more). Since GCs now account for roughly 1% of the Galactic halo, a large fraction of the halo should have originated in the same episodes that led to the formation of the GCs.

We obtained diverse distributions of the Na–O and Mg–Al anticorrelations for different GCs (Carretta et al., 2009a, Figure 2; Carretta et al., 2009b) in some of the GCs, indicating that some parameter, most likely the typical polluter mass, is varying from cluster to cluster. There is a strong link between the extension of the Na–O anticorrelation and some of the main parameters of GCs, mainly mass and metallicity.

We also confirmed that in spite of these striking star-to-star differences in the light elements, most GCs (with a few notable exceptions) are extraordinarily homogeneous in Fe-peak elements, with upper limits as low as 5% on the root

Figure 3. The relative age parameter is plotted vs. absolute magnitude M_V for globular and old open clusters. Red filled pentagons are for GCs where the Na–O anticorrelation has been observed. Open stars mark GCs for which insufficient data about the Na–O anticorrelation is available. Squares are for the clusters of the Sagittarius dSph galaxy and open circles are for old open clusters (see Carretta et al., 2010a). Green crosses mark those clusters where the Na–O anticorrelation has been searched for but not found. Superimposed are lines of constant mass (light solid lines, see Bellazzini et al., 2008). The heavy blue solid line (at a mass of $4 \times 10^4 M_\odot$) is the proposed separation between globular and open clusters.



mean square dispersion. A by-product of our work is a new metallicity scale for GCs based on homogeneous abundances from high resolution UVES spectra (Carretta et al., 2009c). The homogeneity and good statistics also allowed the first distinction between the He-rich, SG and the He-poor FG populations at the red giant branch (RGB)-bump (Bragaglia et al., 2010a) to be made, as foreseen by models.

Our first extensive study of the chemical composition of M 54 in the nucleus of the disrupting Sagittarius dwarf galaxy showed a metallicity dispersion and Na–O anticorrelation in both the metal-rich and metal-poor component (Carretta et al., 2010b), with similarities with Omega Centauri, probably indicative of a similar origin in dwarf spheroidal galaxies.

The Li abundances offered a complementary approach. Li is easily destroyed in stellar interiors so, if there is no Li production within the polluters, Li and O should be positively correlated and Li and Na anticorrelated. Measures of O, Na, and Li abundances in the same stars are rare, but D’Orazi and Marino (2010) found no Li–O correlation in a sample of about 100 giants in M4. If confirmed in other GCs, this would be explained only with Li production in the polluters, very likely intermediate-mass AGB stars.

Finally, we found that the fraction of Ba-stars (which arise from mass transfer in binaries) is higher among FG stars (D’Orazi et al., 2010). This prompted us to estimate the binary fraction from multi-epoch measurements of radial velocities, available for three of our GCs, finding that the binary fraction of SG stars is much lower than that of FG stars. Binaries are more common in low than in high density

environments: our finding is then a direct probe of the ambient condition at the distant epochs where the bulk of different stellar generations formed in GCs.

These results are unprecedented and were made possible by the large samples of high resolution spectra available, and by the high degree of homogeneity attained by the analysis procedures adopted in our survey.

Future directions

Our results, as well as the discovery of multiple MSs from high precision Hubble Space Telescope photometry, are opening unexpected and fascinating windows on the quest for the formation and evolution of massive stellar clusters. However, several issues remain presently unsolved, like the nature of the polluters, the overall timescale of the self-enrichment, the existence of material with pristine composition diluting the products of the polluters, the relation between the formation of GCs and that of the Galactic Halo, the role of different populations on the dynamical evolution of GCs, the connection between multiple populations and other properties of GCs (e.g., mass, the second parameter on the

HB, or the blue and red sequences of GCs seen in many galaxies), and the relation between GCs and the nuclei of dwarf galaxies, and many more.

With its large set of very competitive instruments, the VLT is likely to play a fundamental role in this game even in the future. UVES and FLAMES observations were essential in revolutionising our view of the GCs. New perspectives are possible with the high sensitivity of X-shooter, revealing the spectra of faint MS stars (see Bragaglia et al., 2010b), or the access to near-infrared spectra provided by CRIRES.

References

- Bellazzini, A. et al. 2008, MSAIt, 79, 663
- Bragaglia, A. et al. 2010a, A&A, 519, 60
- Bragaglia, A. et al. 2010b, ApJL, 720, L41
- Carretta, E. et al. 2009a, A&A, 505, 117
- Carretta, E. et al. 2009b, A&A, 505, 139
- Carretta, E. et al. 2009c, A&A, 508, 695
- Carretta, E. et al. 2010a, A&A, 516, 55
- Carretta, E. et al. 2010b, ApJL, 714, L7
- Decressin, T. et al. 2007, A&A, 464, 1029
- D’Orazi, V. & Marino, A. F. 2010, ApJL, 716, L166
- D’Orazi, V. et al. 2010, ApJL, 719, L213
- Gratton, R. et al. 2000, A&A, 354, 169
- Gratton, R. et al. 2001, A&A, 369, 87
- Gratton, R. et al. 2004, ARA&A, 42, 385
- Gratton, R. et al. 2010, A&A, 517, 81
- Lata, S. et al. 2002, A&A, 388, 158
- Ventura, P. et al. 2001, ApJ, 550, L65

Dissecting the Galactic Super Star Cluster Westerlund 1 — A Laboratory for Stellar Evolution

Simon Clark¹
Ignacio Negueruela²
Ben Ritchie¹
Paul Crowther³
Sean Dougherty⁴

¹ Department of Physics and Astronomy,
The Open University, Milton Keynes,
United Kingdom

² Departamento de Física & Ingeniería,
Universidad de Alicante, Spain

³ Department of Physics and Astronomy,
University of Sheffield, United Kingdom

⁴ National Research Council, Herzberg
Institute for Astrophysics, Penticon,
Canada

Westerlund 1 is the first example of a super star cluster identified within the Galaxy. As such, its proximity allows us to resolve directly and study individual stars down to sub-solar masses, as well as their complex interactions. This in turn permits advances in our understanding of the physics of these stellar powerhouses, which drive evolution in starburst galaxies near and far. Here we provide a brief overview of our current understanding of this cluster, both in terms of its stellar constituents — and the constraints they place on the evolution of massive stars from cradle to grave — and its global properties.

Starburst galaxies and super star clusters

Images of starburst galaxies such as the Antennae, M82 and NGC 1313 (see Figure 1) reveal that the process of star formation appears hierarchical, with stars forming within massive clusters, which in turn are located within larger complexes that reflect the underlying structure of the natal giant molecular clouds. The impact of both these super star clusters (SSCs) and complexes on the wider galactic ecology is immense: the OB stellar population contained within dominates both the ultraviolet (UV) and, via dust re-processing, the infrared (IR) radiative output of the host galaxy, while their post-supernovae (post-SNe) relativistic remnants — neutron stars and black holes within binary systems — are responsible for the high energy emission.



Figure 1. The central region of the vigorous starburst galaxy NGC 1313 is shown in this colour image from VLT FORS data (from Release eso0643). Note the numerous shells of ionised gas excited by young massive clusters similar to Wd1.

Moreover, the same population of massive stars provides significant input of mechanical energy and chemically processed material via their stellar winds and SNe. Indeed, the combination of both radiative and kinetic feedback is thought to be responsible for the initiation of superwinds that may promote or suppress subsequent generations of star formation, as well as enrich the intergalactic medium. Nevertheless, despite their pivotal role in galactic evolution the small physical extent of SSCs in external galaxies means that they must be studied via comparison of their integrated spectral and photometric properties.

But such an approach is based on two unproven hypotheses: (i) that the Initial Mass Function (IMF) of stars within such clusters (and complexes) is identical to that determined locally; and (ii) that stars

within such clusters follow comparable evolutionary paths to those within the Local Group, such that we understand their radiative output, lifetimes and post-SNe endpoints. Without such assumptions we cannot accurately calibrate the population synthesis codes used to determine cluster ages and integrated masses (and hence star formation rates), nor constrain the degree of mechanical and radiative feedback that yields galactic-scale superwinds.

Unfortunately, through the 20th century it had been supposed that the Galaxy lacked spatially-resolved examples of SSCs, with the integrated masses of young (< 20 Myr) massive open clusters typically being less than $10^3 M_{\odot}$ compared to 10^5 – $10^7 M_{\odot}$ for the former. Targeted near-IR observations of the centre of the Galaxy had revealed the presence



Figure 2. Optical image of Wd1 obtained with the Wide Field Imager mounted on the MPG/ESO 2.2-metre telescope. Note the high degree of reddening to the cluster in comparison to the foreground B supergiant (lower right). Image from Release eso1034c.

of the Arches, Quintuplet and Galactic Centre clusters with masses $\sim 10^4 M_{\odot}$; still an order of magnitude smaller than known SSCs. In fact the first known example of a SSC had been identified fully 40 years earlier — indeed before their widespread recognition in external starburst galaxies! — but had subsequently remained in relative obscurity.

Westerlund 1

Located within the constellation of Ara (the Altar) Westerlund 1 (Wd1; see Figure 2) was simply described by Bengt Westerlund in 1961 as a very young, “heavily reddened cluster”. Indeed the high extinction towards Wd1 ($A_V \sim 11$ mag) hampered spectroscopic investigation, with the first such survey following over a quarter of a century later (Westerlund, 1987). Despite revealing an unprecedented population of high luminosity supergiants of both early and late spectral types, Wd1 once again sank back into obscurity until radio observations of

the B[e] supergiant Wd1-9 serendipitously detected a large number of radio sources amongst the evolved stellar population (Figure 3; see Clark et al., 1998 and Dougherty et al., 2010). Unexpectedly, a number of the cool red supergiants (RSGs) and yellow hypergiants (YHGs) were found to be strong radio sources, despite lacking the requisite UV flux to ionise their ejecta.

Prompted by these results we undertook spectroscopic and photometric observations of cluster members between 2001–2; firstly with the ESO 1.52-metre telescope and the Boller & Chivens spectrograph, and subsequently at higher signal-to-noise ratio (S/N) and resolution with the New Technology Telescope and EMMI spectrograph (Clark et al., 2005). Given the reddening towards Wd1, classification spectra were obtained from 600–900 nm, rather than the more common 400–600 nm window. An appropriate classification scheme, based on the occurrence and strength of H I, He I and He II lines in the OBA stars and

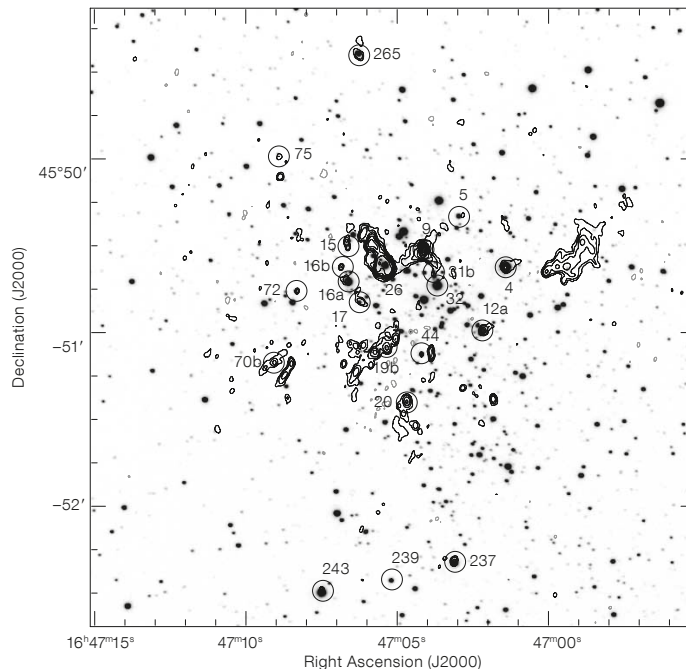


Figure 3. Overplot of radio observations (contours) on an optical image of Wd1. Note the emission associated with the cool hypergiants (Wd1-4, 12a, 16a, 32 & 265 — YHGs; Wd1-20, 26 & 237 — RSGs) indicative of significant ongoing mass loss.

the presence of low excitation metallic and molecular features for cool objects, was constructed from both real and synthetic spectra (Clark et al., 2005; Negueruela et al., 2010). As well as confirming the classifications of Westerlund (1987), these observations also identified large additional populations of OB supergiants and Wolf–Rayet stars (WRs), which had previously escaped detection due to a combination of comparatively low optical luminosity and heavy reddening. Indeed, subsequent observations revealed a population of 25 WRs, composed of both WN and WC subtypes; the richest haul detected within a Galactic cluster at this time (Crowther et al., 2006).

These observations enabled us to determine that Wd1 has an age of $\sim 4\text{--}5$ Myr and appears to be co-eval; conclusions confirmed by later observations (e.g., Negueruela et al., 2010). Moreover, utilising these spectra to calibrate our photometry, we were able to estimate that $\gg 100$ stars within the cluster must have evolved from progenitors with initial

masses $\geq 30 M_{\odot}$. Such a census has two implications. Firstly, it offers an explanation for the anomalous radio emission associated with the YHGs and RSGs, whereby the diffuse UV radiation field from the hot stellar population (OB stars and WRs) provides the ionising photons. Secondly, using this population to normalise a Kroupa-type IMF we were able to infer a total (initial) mass for Wd1 of $\sim 10^5 M_{\odot}$, making it the most massive Galactic cluster yet discovered by an order of magnitude and hence the first SSC within the Milky Way.

Therefore, Wd1 is the first example of an SSC for which its relative proximity permits the resolution and study of individual stars to sub-solar masses — enabling the ecology of such an agglomeration to be decoded for the first time.

Massive stellar evolution — a tale of two pathways

A key driver in massive stellar evolution is mass loss, which strips away the H-rich mantle of O stars to yield H-depleted WRs. Indeed the rate at which this proceeds not only governs the precise evolutionary path trodden by the star, but also its ultimate post-SNe fate. Radio observations had already revealed the characteristic signature of heavy mass loss associated with many stars (Clark et al., 1998; Dougherty et al., 2010), while our new spectroscopy reveals a rich post-main sequence (post-MS) population. Thus Wd 1 presents a unique opportunity to investigate the physics of stellar evolution for some of the largest stars to be found within the Galaxy.

Nevertheless, such a goal is challenging for three reasons. Firstly, sophisticated modelling with non-local thermodynamic equilibrium (non-LTE) atmospheric codes is required to determine accurately physical properties such as stellar luminosity, temperature, mass-loss rate and chemical abundances; all of which are essential to determine accurately the precise evolutionary state of an individual star (see Figure 4; Ritchie et al., 2009b). Secondly, as such stars transit from the MS to H-depleted WR phase they pass through a dizzying variety of short-lived evolu-

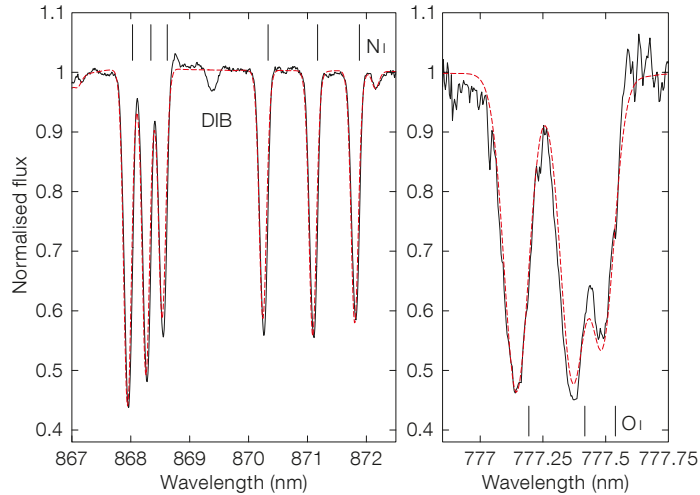


Figure 4. Comparison of observed (black) and synthetic (red) spectra of the LBV Wd1-243, focusing on the Ni and O I triplets and indicating significant chemical evolution of N and O (respectively 12 and 0.1 times solar abundances).

tionary states that include the luminous blue variables (LBVs) and the closely related P Cygni supergiant/B hypergiant, supergiant B[e] stars, YHG and RSG stages. It is thought that mass loss in such phases may play a dominant role in the removal of hydrogen and subsequent formation of WRs, but it appears likely that this process is accomplished via transient outbursts in which mass-loss rates increase by several orders of magnitude over their quiescent values. A prime example of this behaviour in LBVs is the 19th-century eruption of η Car, while similar behaviour has also been inferred for YHGs and RSGs such as ρ Cas and VY CMa. However, such outbursts are rare, with none subject to modern day observational and analytical techniques, meaning that the physical mechanism leading to the extreme mass-loss events has yet to be identified.

Finally, a synthesis of our multi-wavelength observations of Wd1 suggests a very high binary fraction amongst the WR population (Crowther et al., 2006; Clark et al., 2008). Binary-mediated mass loss through Roche-lobe overflow in short period systems offers an additional evolutionary pathway for massive stars, which leads to significantly lower pre-SNe core masses than expected for single stars. The importance of this pathway was dramatically demonstrated by the discovery of a magnetar (a class of neutron star with magnetic field strengths $\sim 10^{15}$ G) within Wd1 (Muno et al., 2006). Conventional wisdom assumes that stars

with initial masses in excess of $\sim 25 M_{\odot}$ give rise to the post-SNe formation of black holes rather than neutron stars. Consequently, with a current MS turnoff mass in excess of $\sim 30 M_{\odot}$ (Clark et al., 2005; Negueruela et al., 2010), it had been expected that only black holes should currently be forming within Wd1. Indeed, given that the pre-SNe mass loss required to yield a neutron star rather than a black hole is greatly in excess of that expected for single star evolution, significant binary driven mass loss appears mandatory to allow for the formation of the Wd1 magnetar.

Quantitative analysis via VLT follow-up

The existing spectral data were insufficient to address these issues, being of too low S/N and resolution to enable non-LTE-model atmosphere analysis and only at a single epoch, thus preventing the identification of either intrinsic (instabilities) or extrinsic (binary) variability. Consequently, throughout the period 2004–9 we obtained multiple epochs of high quality, 600–900 nm spectroscopic data of ~ 100 members of the evolved stellar population of Wd1 with both FORS and FLAMES on the VLT. Full details of the target selection, experimental setup and reduction techniques employed may be found in Ritchie et al. (2009a) and Negueruela et al. (2010). These data enabled us to address each of the challenges described above.

Firstly, the data permit quantitative atmospheric modelling of individual stars in order to determine their stellar parameters. An example of such an analysis is presented in Ritchie et al. (2009b; see Figure 4). By constraining the chemical abundances for the LBV Wd1-243 it was possible to demonstrate unambiguously that it is a highly evolved, likely post-RSG, object. The use of elemental abundances to place the panoply of post-MS stars — LBVs, B/YHGs, RSGs, etc. — in a precise evolutionary scheme is a powerful technique, with mass loss systematically driving down the H/He ratio while simultaneously exposing the products of nuclear burning at the stellar surface. We aim to extend this approach to the remaining population of transitional stars within Wd1 in the immediate future.

Secondly, in combination with existing historical observations, the data enabled a search for variability amongst the subset of bright evolved stars over a ~ 50 -yr baseline. Such an approach had previously allowed for the classification of Wd1-243 as an LBV, while radio observations of the B[e] star Wd1-9 showed an episode of enhanced mass loss that likely ended within the last 200 years (Dougherty et al., 2010). Intriguingly, while significant wind variability and pulsational instability appeared to be ubiquitous for all subtypes of evolved stars observed within Wd1, no further examples of LBVs have yet been identified within the hot super-/hyper-giant population.

However dramatic variations in spectral type, likely reflecting pulsation-driven changes in the stellar photosphere, were identified amongst the Blue-/YHG and RSG populations (c.f. the YHG Wd1-265 shown in Figure 5; Clark et al., 2010); indeed all stars of spectral types later than B1 appear to be pulsationally unstable. Amongst the cool super-/hyper-giants this occurrence is of considerable importance since identical behaviour has been observed in field YHGs such as ρ Cas, where it has been associated with episodes of dramatically enhanced mass loss ($\sim 5 \times 10^{-2} M_{\odot} \text{ yr}^{-1}$; Lobel et al., 2003). When coupled with quantitative

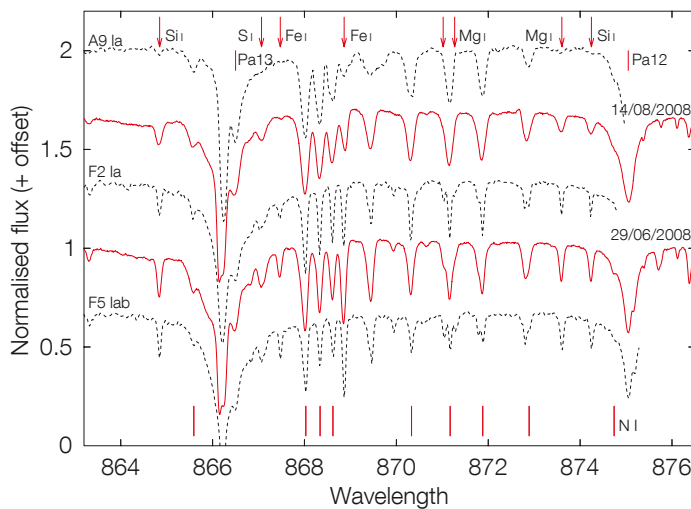


Figure 5. Time-resolved spectra of the pulsating YHG Wd1-265. Comparison with classification spectra (dotted lines) indicates significant variability in spectral type over a period of only 46 days.

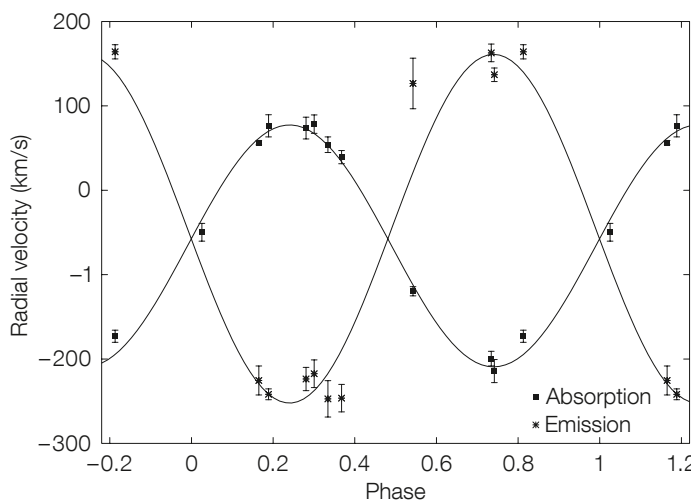


Figure 6. Radial velocity curve for both components of the WNL+OB binary Wd1-13 folded on the ~ 9.27 -day orbital period.

modelling, continued spectral monitoring of these stars raises the prospect of both determining the duty cycle of such mass-loss events as well as providing stringent constraints on the underlying physics driving these instabilities. Likewise, high cadence observations of the hotter supergiants potentially open up their internal structure to scrutiny via asteroseismology studies, while also probing the origin of their highly structured stellar winds.

Finally, we turn to the main science driver for our intensive spectrographic survey — comprising multi-epoch observations of ~ 100 evolved stars over a 14-month baseline utilising the VLT Fibre Large Array Multi Element Spectrograph

(FLAMES) — the identification of radial velocity variables resulting from binary motion. While analysis of the full dataset is currently underway, preliminary results for the first year of observations of the brightest quarter of targets imply a binary frequency of $> 40\%$ amongst the OB-supergiant population (Ritchie et al., 2009a). This finding suggests that single and binary channels may be of comparable importance in the evolution of massive stars, although a determination of the period distribution of the binary population will be necessary to quantitatively confirm this assertion.

A second critical result from this analysis was the identification of Wd1-13 — which had previously been identified as an

eclipsing system — as a *double-lined* WNL+OB supergiant binary (Figure 6). This combination of properties enabled us to determine dynamical masses of 23 ± 3 and $35 \pm 5 M_{\odot}$ for the WNL and OB supergiant components respectively (Ritchie et al., 2010). Comparison to theoretical models of WR binary evolution suggest that the WNL component had an initial mass of $\sim 40 M_{\odot}$, which immediately places a firm lower limit on the mass of the magnetar progenitor. Given that magnetars are also present in clusters with comparatively low-mass MS turnoffs ($< 20 M_{\odot}$; Clark et al., 2008), their progenitors clearly span a range of masses, implying that an additional “ingredient” such as rapid rotation or a high natal magnetic field must be required for their formation.

Moreover, we may also place quantitative constraints on the location of the bifurcation in the canonical “Conti scenario” for stellar evolution, whereby the most massive stars evolve via:

O MS \rightarrow WNLh \rightarrow LBV \rightarrow WNL \rightarrow WNE \rightarrow WC \rightarrow SNe

thus avoiding a cool hypergiant phase, and less massive stars via

O MS \rightarrow OB SG \rightarrow RSG \rightarrow LBV/YHG? \rightarrow WNL \rightarrow WNE(\rightarrow WC?) \rightarrow SNe

(where the WNLh designation means that the star shows hydrogen emission lines in its spectrum). Given the both YHGs and RSGs are currently present within Wd1, the masses implied for the progenitors of these stars by Wd1-13 reveals that the division must occur at $> 40 M_{\odot}$.

Future prospects

In the last decade of study Wd1 has yielded many of its secrets, enabling us to confirm that it is the first SSC to be identified within the Galaxy, as well as permitting us to place powerful observational constraints on the evolution of massive stars in their natural environment for the first time. However, what does the future hold? Our immediate goal is to fully determine the physical properties of

the binary population of Wd1 in terms of frequency, orbital separation and mass ratio, which will be accomplished by comparison of the complete RV dataset to Monte-Carlo simulations. It is hard to overestimate the importance of such a goal — in addition to constraining the relative weighting of single and binary evolutionary channels accurately, such information will also constrain the physics of massive star formation (e.g., Ritchie et al. [2009a] and references therein) as well as the production efficiency of both high- and low-mass X-ray binaries, binary pulsars — a major source of gravitational radiation — and potentially the production of gamma-ray bursts.

Looking further ahead, the presence of RSGs within Wd1 permits a clear and unequivocal test of current theories of massive stellar evolution, which do not permit such stars to exceed $\log(L/L_{\odot}) \geq 5.6$ (e.g., Meynet & Maeder, 2005). Unlike field stars, the well-determined distance to Wd1 permits an accurate determination of the luminosity of the cluster RSGs once an appropriate bolometric correction has been determined via model atmosphere analysis.

Turning to Wd1 as a whole, we have a unique opportunity to investigate the interaction between individual massive stars within an SSC. The motivation for such a study is vividly illustrated by the cometary nebulae associated with the RSGs Wd1-20 & 26 and which are visible in mid-IR and radio images (Figure 3; Dougherty et al., 2010). These appear to be the result of the ablation and entrainment of the outer stellar layers/winds of these stars by the incipient cluster wind driven by the mechanical and radiative feedback from individual stars and SNe. But how do such winds work? Comparison of radio, mid-IR and X-ray data indicate that the intercluster medium appears to be multi-phase, composed of cool, neutral and dust-laden clumps shadowing warmer ionised gas in close proximity to the core, which, in turn, are imbedded in an X-ray-bright component, emitting via both thermal and non-thermal mechanisms. How is momentum imparted to this material to yield a cluster wind and what is the efficiency

of this process? Answers to both questions are essential if we are to understand the impact of SSCs on their wider (extra-) galactic environments.

And finally regarding Wd1 in a wider context — did it form alone? Examination of star-forming regions suggests that such clusters do not form in isolation, but currently there is no evidence for ongoing star formation closely associated with Wd1. Was it born with other siblings which have since dispersed, or did it instead form monolithically in a single starburst event — and if so, why? How many other examples lurk in the Galactic plane? Systematic spectroscopic follow-up of candidates identified via current and future surveys such as the VISTA Variables in the *Via Lactea* survey will enable us to place and understand Wd1 in the context of the recent star formation history of the Milky Way. Clearly the discovery and analysis of Westerlund 1 has answered many questions, but has raised many more.

References

- Clark, J. et al. 1998, MNRAS, 299, L43
- Clark, J. et al. 2005, A&A, 434, 949
- Clark, J. et al. 2008, A&A, 477, 147
- Clark, J. et al. 2010, A&A, 514, 87
- Crowther, P. et al. 2006, MNRAS, 372, 1407
- Dougherty, S. et al. 2010, A&A, 509, 79
- Lobel, A. et al. 2003, ApJ, 583, 923
- Meynet, G. & Maeder, M. 2005, A&A, 429, 581
- Muno, M. et al. 2006, ApJ, 636, L41
- Negueruela, I., Clark, J. & Ritchie, B. 2010, A&A, 516, A78
- Ritchie, B. et al. 2009a, A&A, 507, 1585
- Ritchie, B. et al. 2009b, A&A, 507, 1597
- Ritchie, B. et al. 2010, A&A, 520, 48
- Westerlund, B. 1987, A&AS, 70, 311

AMAZE and LSD: Metallicity and Dynamical Evolution of Galaxies in the Early Universe

Roberto Maiolino¹
 Filippo Mannucci²
 Giovanni Cresci²
 Alessio Gnerucci³
 Paulina Troncoso¹
 Alessandro Marconi³
 Francesco Calara⁴
 Andrea Cimatti⁵
 Filomena Cocchia¹
 Adriano Fontana¹
 Gianluigi Granato⁶
 Andrea Grazian¹
 Francesca Matteucci⁷
 Taro Nagao⁸
 Laura Pentericci¹
 Antonio Pipino⁹
 Lucia Pozzetti¹⁰
 Guido Risaliti²
 Laura Silva⁶

- ¹ INAF–Osservatorio Astronomico di Roma, Monte Porzio Catone, Italy
² INAF–Osservatorio Astrofisico di Arcetri, Firenze, Italy
³ Dipartimento di Fisica e Astronomia, Università degli Studi di Firenze, Italy
⁴ Jeremiah Horrocks Institute for Astrophysics and Supercomputing, University of Central Lancashire, Preston, United Kingdom
⁵ Dipartimento di Astronomia, Università di Bologna, Italy
⁶ INAF–Osservatorio Astronomico di Trieste, Italy
⁷ Dipartimento di Fisica, Università di Trieste, Italy
⁸ Graduate School of Science and Engineering, Ehime University, Japan
⁹ Department of Physics and Astronomy, University of California Los Angeles, USA
¹⁰ INAF–Osservatorio Astronomico di Bologna, Italy

The metal content in galaxies provides important information on the physical processes responsible for galaxy formation, but little was known for galaxies at $z > 3$, when the Universe was less than 15 % of its current age. We report on our metallicity survey of galaxies at $z > 3$ using SINFONI at the VLT. We find that at $z > 3$, low-mass galaxies obey the same fundamental relation between metallicity, mass and star formation rate as at $0 < z < 2.5$; however, at $z > 3$ massive galaxies deviate from this relation,

being more metal-poor. In some of these massive galaxies we can even map the gas metallicity. We find that galaxies at $z \sim 3.3$ have regular rotation, though highly turbulent, and inverted abundance gradients relative to local galaxies, with lower abundances near the centre, close to the most active regions of star formation. Overall the results suggest that prominent inflow of pristine gas is responsible for the strong chemical evolution observed in galaxies at $z > 3$.

The chemical enrichment that we observe in local galaxies has been produced by the nucleosynthesis of stars formed over their cosmic lives. Such enrichment has been modulated by the inflow of pristine gas (which both boosts star formation and dilutes the gas metallicity), enriched gas outflows (driven by the star formation activity itself or by active galactic nuclei [AGNs]) and gas exchange during galaxy merging events. The shape of the initial mass function of star formation also plays an important role, since different stellar masses inject into the interstellar medium different amounts of chemical elements. Clearly, the metal content of galaxies is an important tracer of their star formation history and of the main physical processes involved in galaxy evolution. Indeed, the metallicity of local and distant galaxies is one of the most important tools to constrain galaxy evolutionary models.

Clear observational evidence of a connection between the content of metals and star formation history is given by the tight three-dimensional correlation between metallicity, stellar mass and star formation rate (dubbed Fundamental Metallicity Relation, FMR, Mannucci et al., 2010), as illustrated in Figure 1. More specifically, the gas metallicity is observed to increase as a function of the stellar mass (at a given star formation rate [SFR]) and to decrease with the SFR (at a given stellar mass). Galaxies show a very small metallicity scatter of 0.05 dex around this surface and this suggests that the bulk of galaxy formation occurs through a smooth, long-standing equilibrium between star formation, gas inflow and outflow. Distant galaxies, out to $z < 2.5$, appear to obey the same funda-

mental relation between metallicity, mass and SFR observed in local galaxies. This finding suggests that the same mechanisms of galaxy formation are at work at any epoch in the redshift interval $0 < z < 2.5$.

Until recently, little was known about the metallicity of galaxies at $z > 3$, due to the difficulty of detecting the optical nebular lines (redshifted into the near-infrared) required to measure the metallicity in these faint systems. However, this is a crucial epoch of very fast galaxy evolution, just before the peak of cosmic star formation, which requires thorough investigation to understand the formation of primeval galaxies properly.

The AMAZE and LSD surveys

We have undertaken two major projects using the near-infrared integral field spectrograph SINFONI at the VLT. AMAZE (Assessing the Mass-Abundances redshift [Z] Evolution) is an ESO large programme that was awarded 180 hours of observations. It consists of deep SINFONI, seeing-limited, integral field spectroscopy of about 30 star-forming galaxies (Lyman-break selected), most of which are at $3.0 < z < 3.7$ and a few them at $4.2 < z < 5.2$. In the following we will focus on the sample at $z \sim 3.3$. For these galaxies the nebular lines [O II] 3727 Å and [Ne III] 3869 Å are redshifted into the *H*-band, while H β and [O III] 5007 Å are redshifted into the *K*-band. The flux ratio of these lines allows us to measure the gas metallicity, as discussed in Maiolino et al. (2008).

LSD (Lyman-break galaxies Stellar population and Dynamics) is a companion programme that was awarded 70 hours of observations with SINFONI, assisted by the adaptive optics module, so as to achieve a much higher angular resolution relative to the seeing-limited observations. The sample consists of eight Lyman-break galaxies at $z \sim 3.3$ selected to have a nearby bright star, which is required to guide the adaptive optics system.

In both projects the line emission (especially the strongest one, [O III] 5007 Å) is generally spatially resolved by our data.

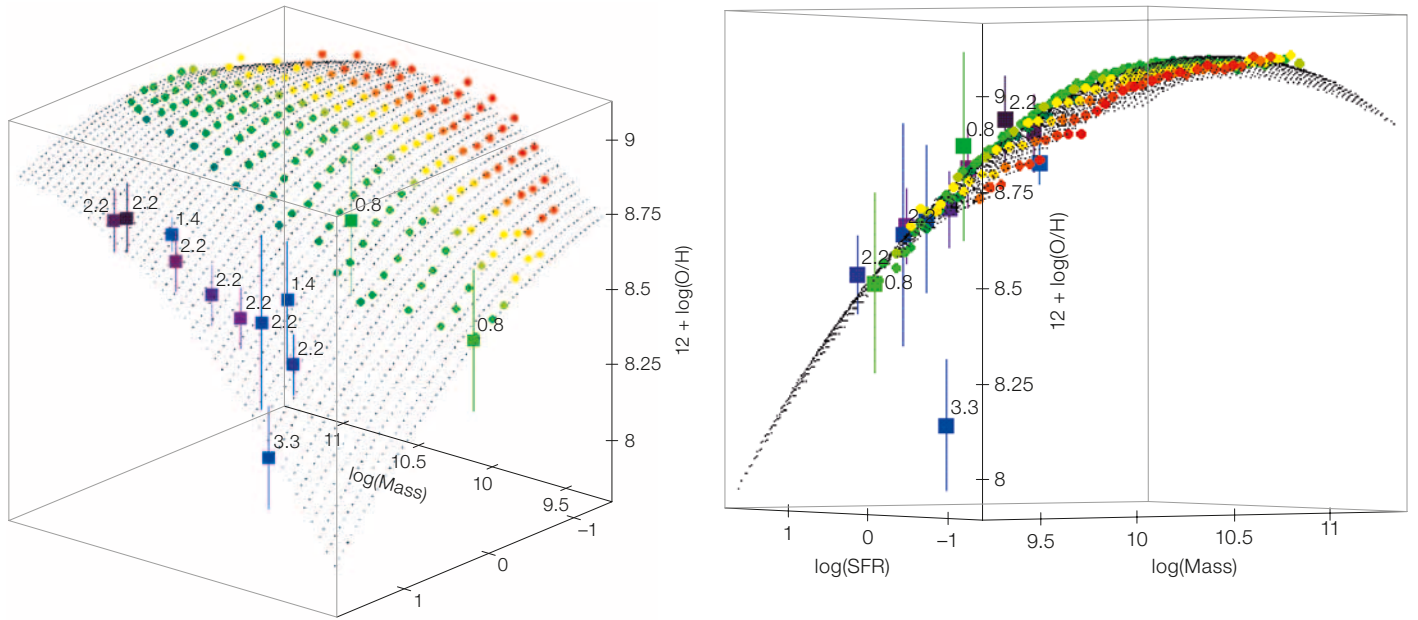


Figure 1. Two views of the fundamental metallicity relation (FMR) between mass, star formation rate and metallicity for local galaxies are shown. The small points, with different colours, indicate different star formation rates. Squares with error bars indicate the average location of distant star-forming galaxies at different redshifts (the latter indicated by the number associated with each point). The point at $z \sim 3.3$ deviating from the FMR was obtained with the first preliminary set of 17 galaxies from AMAZE and LSD. From Mannucci et al. (2010).

The projected spatial resolution is typically about 5 kpc (seeing ~ 0.6 arcseconds) for the AMAZE data and about 1.5 kpc for the (nearly) diffraction-limited data in LSD (point spread function [PSF] ~ 0.2 arcsec-

onds). Also in both samples extensive multiband photometry (including Spitzer data) allowed us to constrain the stellar masses tightly. The star formation rate is inferred by using both the $H\beta$ luminosity and spectral energy distribution (SED) broadband fitting, generally obtaining consistent results.

A detailed description of these two programmes, as well as preliminary results, is given in Maiolino et al. (2008) and in Mannucci et al. (2009). Additional results have been, or are being published in five additional papers (Gnerucci et al., 2010; Cresci et al., 2010; Troncoso et al., 2010;

Troncoso et al., in prep.; Gnerucci et al., in prep.), while follow-up observations are delivering additional results. It is beyond the scope of this paper to give an extensive overview of the various results. Here we only show some of the main highlights that have been obtained by these programmes so far.

Chemical upsizing at $z > 3$

The AMAZE and LSD samples span more than two orders of magnitude in stellar mass ($M_* \sim 10^9 - 10^{11} M_\odot$) and over an order of magnitude in star formation rate

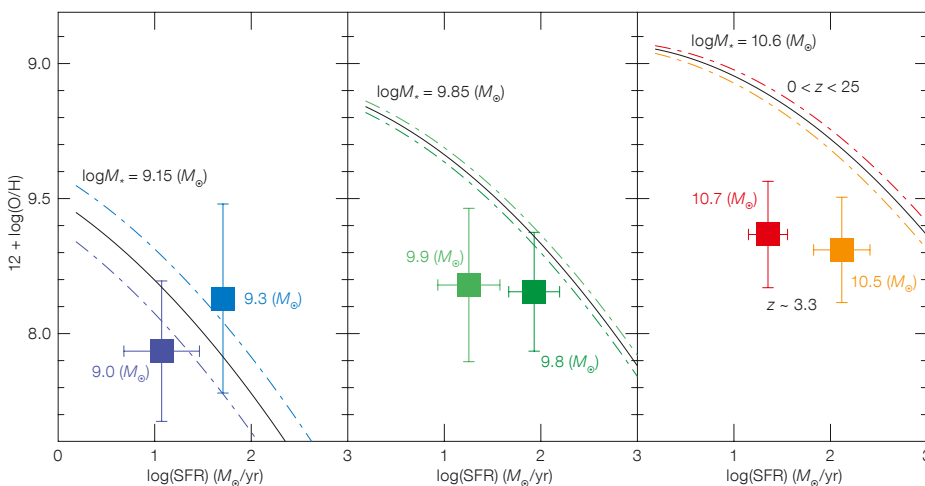


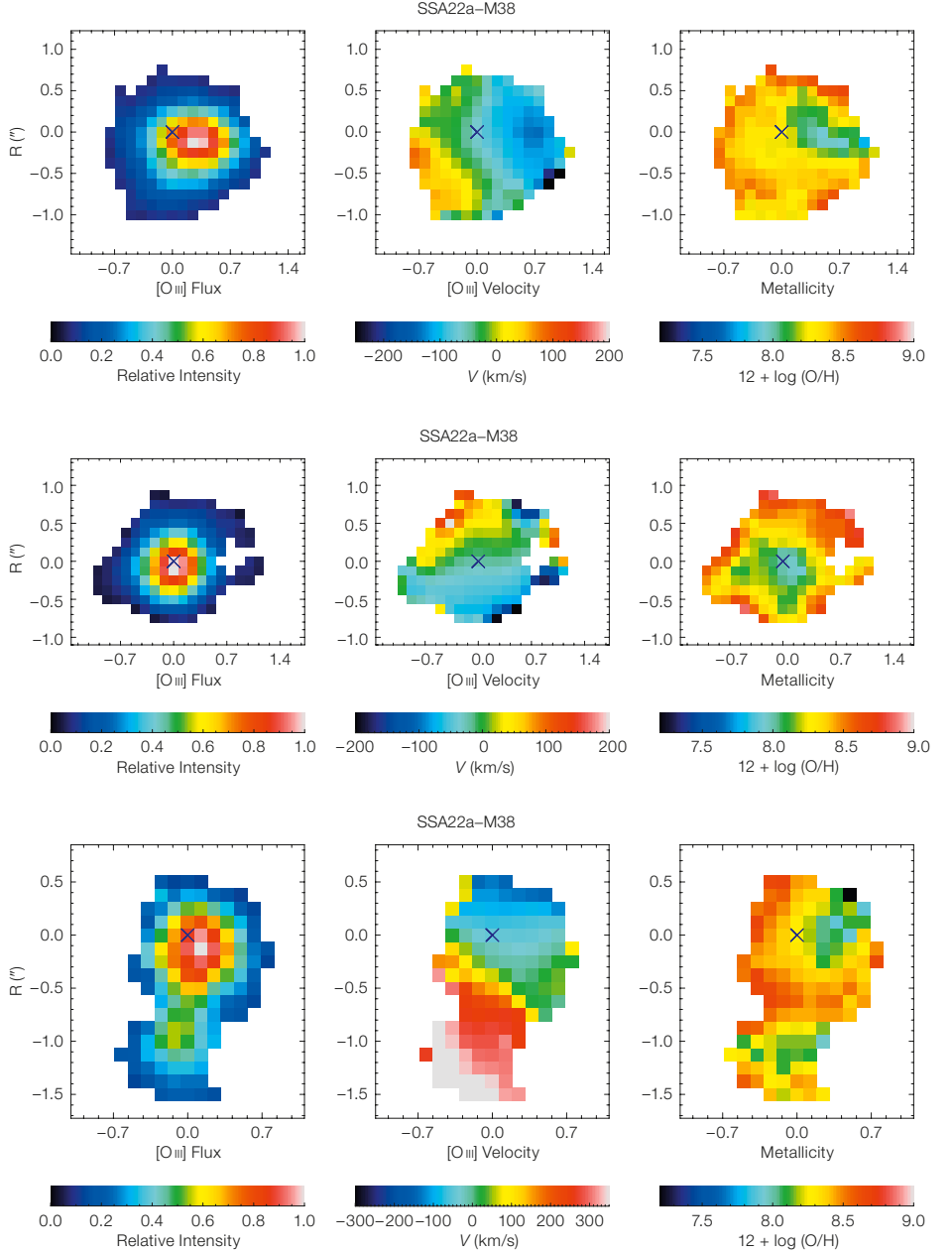
Figure 2. Metallicity versus star formation rate in galaxies at $0 < z < 2.5$ on the FMR (lines) and in galaxies at $z \sim 3.3$ (squares) is shown for three different stellar mass ranges. Within each panel different colours give the metallicity values at exactly the same average stellar mass for galaxies both at $0 < z < 2.5$ and at $z \sim 3.3$. Note that while the metallicity of low-mass galaxies at $z \sim 3.3$ is consistent with local galaxies, massive galaxies at $z \sim 3.3$ are significantly more metal-poor relative to their local counterparts. From Troncoso et al. (2010).

Figure 3. [O III] flux, velocity field and metallicity maps for three massive galaxies at $z \sim 3.3$ characterised by regular rotation patterns. The metallicity has a minimum close to the central peak of star formation (as traced by the maximum of H β emission). From Cresci et al. (2010).

(SFR $\sim 30\text{--}300 M_{\odot}/\text{yr}$). Therefore, the metallicity inferred from the SINFONI spectra allows us to obtain information on the mass–SFR–metallicity relation (FMR) at $z \sim 3.3$. Figure 1 shows the location of galaxies at $z \sim 3.3$ obtained from the average of the first set of 17 galaxies observed in AMAZE and LSD, showing that galaxies at $z \sim 3.3$ clearly deviate from the FMR.

In Figure 2 (from Troncoso et al., 2010a) we exploit the full AMAZE and LSD final samples. The solid and dashed lines show a cut of the FMR (i.e. the metallicity–SFR relation) at three different values of stellar mass. The AMAZE+LSD data at $z \sim 3.3$ are shown with solid squares that, for sake of clarity, give the average of the data in bins of mass and SFR. Low-mass galaxies ($M_{\star} \sim 10^{9.2} M_{\odot}$, leftmost panel) have a metallicity in line with the expectation of the relation observed at $0 < z < 2.5$, indicating that these low-mass galaxies at $z \sim 3.3$ are very much like local galaxies and suggesting that they are regulated by the same evolutionary processes. However, massive galaxies at $z \sim 3.3$, especially at $M_{\star} \sim 10^{10.7} M_{\odot}$ (rightmost panel), are significantly more metal-poor than galaxies at $0 < z < 2.5$ with the same SFR. Taken at face value, this result seems to imply that massive galaxies at $z \sim 3.3$ are in an earlier evolutionary stage relative to their low-mass counterparts, in the sense that they have still to reach the metallicity–mass–SFR relation characterising galaxies at low- z . This is in contrast with the expectations of downsizing scenarios, where massive galaxies should evolve faster and at earlier epochs relative to low-mass systems.

There are a few possible scenarios that could explain the deviation of massive galaxies at $z \sim 3.3$ from the FMR observed at $0 < z < 2.5$. An excess of pristine cold gas inflow in massive galaxies, at such early epochs, may significantly dilute the gas metallicity. Alternatively, galaxy mergers may drive gas from the outer, low metallicity regions into



the central parts of massive galaxies, hence diluting the metallicity of star-forming regions. The latter scenario can be investigated by studying the dynamical properties of these systems, as inferred by our SINFONI data.

Massive rotating discs at $z > 3$

The two-dimensional spectroscopic information delivered by SINFONI allows us to trace the kinematics of the galaxies at

$z \sim 3.3$ in our sample, by measuring the velocity shift of the brightest line, [O III] 5007 Å. About 30% of the galaxies in our sample show ordered rotational motions (Gnerucci et al., 2010a). A few examples of such rotating systems are shown in Figure 3, where the central panels show the rotation curve, along with the [O III] flux map (leftmost panels).

In relation to the chemical upsizing result discussed above, we find that there is no correlation between the dynamical prop-

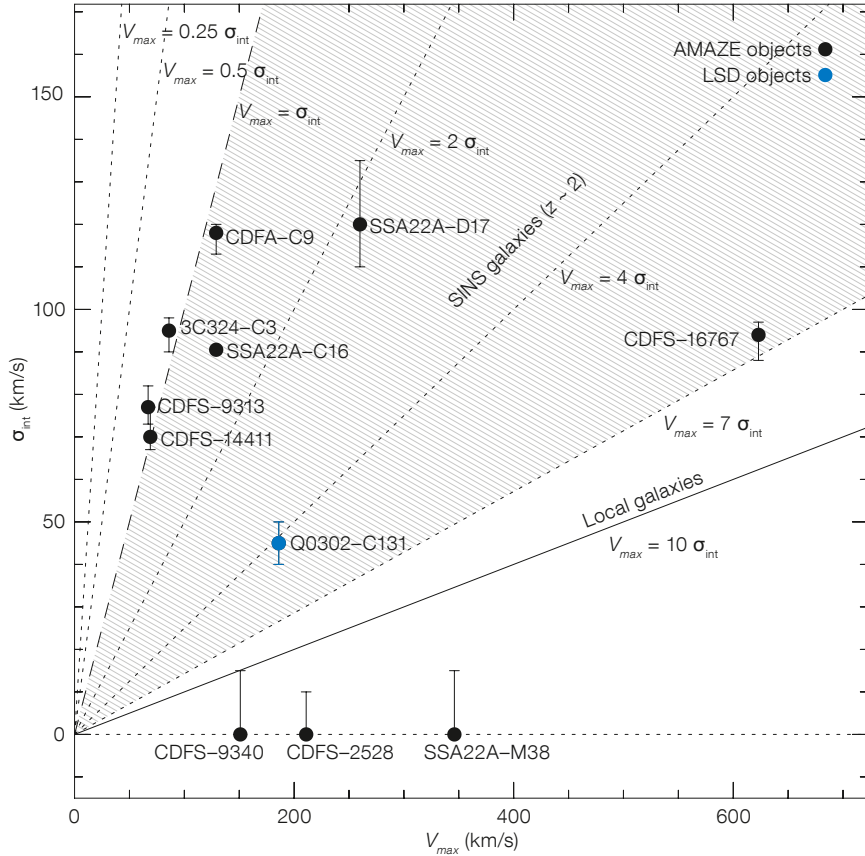


Figure 4. Velocity dispersion (σ) versus rotational velocity (V_{max}) is shown for disc galaxies at $z \sim 3.3$ with a regular rotation pattern. The solid line shows the relation $V_{max}/\sigma = 10$ typical of local galaxies. Note that discs at $z \sim 3.3$ are much more turbulent than local galaxies, many of them having $V_{max}/\sigma \sim 1$. From Gnerucci et al. (2010).

erties of massive galaxies at $z \sim 3.3$ and their deviation from the fundamental metallicity–mass–SFR relation observed at $0 < z < 2.5$. More specifically, among the $z \sim 3.3$ massive galaxies, which are metal-poor relative to the metallicity–mass–SFR relation at $0 < z < 2.5$, we find systems with both irregular kinematics (likely tracing merging systems) and a regular rotation curve, in equal numbers. Therefore, merging cannot be the only process responsible for lowering the gas metallicity in these early galaxies.

From the rotation curve we can also infer dynamical masses, which are in the range $2 \times 10^9 - 2 \times 10^{11} M_{\odot}$. Clearly, some massive rotating discs are already in place at this early epoch in the Universe. However, in contrast to local disc galax-

ies, at $z \sim 3.3$ rotating discs are much more turbulent. Indeed, as illustrated in Figure 4, the velocity dispersion (σ) is generally comparable with the rotational velocity (V_{max}). More specifically, the average ratio between rotational velocity and velocity dispersion is $\langle V_{max}/\sigma \rangle_{z=3.3} = 2.2$, to be compared with the value $\langle V_{max}/\sigma \rangle_{z=0} = 10$ typical of local discs. Galaxies at $z \sim 3.3$ appear to be even more turbulent than those investigated at $z \sim 2$ by the parallel SINFONI programme SINS (Förster Schreiber et al., 2009), which are characterised by $\langle V_{max}/\sigma \rangle_{z=2} = 4.5$.

The highly turbulent nature of $z \sim 3.3$ discs is likely due to very high gas fractions, which make the discs dynamically unstable. In samples at $1 < z < 2.5$ high gas fractions have been confirmed directly through CO observations (Daddi et al., 2010; Tacconi et al., 2010). At $z \sim 3.3$ we have obtained indirect evidence for high gas fractions (even approaching $f_{gas} = M_{gas}/M_{tot} \sim 0.9$) based on the high surface density of star formation (hence exploiting the Schmidt–Kennicutt relation) and on the comparison

between dynamical and stellar masses (Mannucci et al., 2009; Gnerucci et al., 2010; Troncoso et al. in preparation). Such high gas fractions are likely associated with the prominent cold inflows of gas predicted to occur at such early epochs by some theoretical models (e.g., Dekel et al., 2009).

Metallicity gradients and cold flows at $z > 3$

In some galaxies we not only resolve the $[O III] 5007 \text{ \AA}$ emission (used to trace the kinematics), but also the fainter lines of $[O II] 3727 \text{ \AA}$ and $H\beta$, therefore enabling us to map the metallicity. The rightmost panels in Figure 3 (from Cresci et al., 2010) show the metallicity map for three massive galaxies characterised by regular rotation velocity fields. Surprisingly, in contrast to local galaxies, the minimum metallicity is located close to the central regions. However, the most interesting result is that the minimum metallicity is associated with the peak of $H\beta$ flux, which traces the most active star-forming regions. This result supports the scenario where such massive systems at $z \sim 3.3$ drive major inflows of pristine gas towards their central regions. Such pristine gas both boosts star formation and locally dilutes the pre-existing medium, therefore producing the observed spatial anticorrelation between star formation and gas metallicity.

The same (strong) cold flow scenario can explain, more generally for massive galaxies at $z \sim 3.3$, their reduced metallicity relative to the fundamental metallicity–mass–SFR relation observed at $0 < z < 2.5$, as well as the highly turbulent nature of these systems.

References

- Cresci, G. et al. 2010, *Nature*, 467, 811
- Daddi, E. et al. 2010, *ApJ*, 713, 686
- Dekel, A. et al. 2010, *Nature*, 457, 451
- Förster Schreiber, N. M. et al. 2009, *ApJ*, 706, 1364
- Gnerucci, A. et al. 2010, *A&A*, submitted, arXiv 1007.4180
- Maiolino, R. et al. 2008, *A&A*, 488, 463
- Mannucci, F. et al. 2010, *MNRAS*, 408, 2115
- Mannucci, F. et al. 2009, *MNRAS*, 398, 1915
- Tacconi, L. J. et al. 2010, *Nature*, 463, 781
- Troncoso, P. et al. 2010, *A&A*, submitted

His Majesty King Harald of Norway (far right) presents the 2010 Kavli Prize in Astrophysics to, from left to right, Jerry Nelson, Raymond Wilson and Roger Angel.



Credit: Scanpix



The inauguration of the EVALSO (Enabling Virtual Access to Latin-American Southern Observatories) high speed network project held at ESO Offices in Santiago Chile on 4 November 2010. See the article by Filippi (p. 2).

Raymond Wilson Honoured with Two Prestigious Prizes

Jeremy Walsh¹

¹ ESO

Ray Wilson, who retired from ESO in 1993, was awarded two prestigious prizes in September 2010 for his outstanding work on telescope optics: the Kavli Prize in the field of astrophysics and the Tycho Brahe Prize 2010 of the European Astronomical Society.

Announced in June 2010, and awarded in Stockholm in September, the million-dollar Kavli Prizes were awarded to eight scientists “whose discoveries have dramatically expanded human understanding in the fields of astrophysics, nanoscience and neuroscience” (see the Kavli press release¹). The Kavli prize is awarded by the Norwegian Academy of Science and Letters, the Kavli Foundation and the Norwegian Ministry of Education and Research. The Kavli Foundation is funded by Fred Kavli, the Norwegian entrepreneur and philanthropist who later founded the Kavlico Corporation in the US — today one of the world’s largest suppliers of sensors for aeronautical, automotive and industrial applications. There were three recipients in astrophysics, all acclaimed for their work on the development of giant optical telescopes² — Roger Angel of the University of Arizona, Tucson, attached to Steward Observatory; Jerry Nelson of the University of California, Santa Cruz and long associated with the Keck Observatory; and Ray Wilson. The photograph on the facing page (upper) shows the three prize winners at the prize award ceremony in Oslo.

The Tycho Brahe Prize of the European Astronomical Society (EAS) is awarded annually in recognition of the development or exploitation of European instruments, or major discoveries based largely on such instruments. The prize is sponsored by the Klaus-Tschira foundation, based in Heidelberg, Germany. Announced in April, Ray received the prize at the JENAM meeting in Lisbon, Portugal (see the article by Sandu and Christensen, p. 42) and, at the plenary session on 10 September 2010, he delivered a lecture entitled “From the ESO NTT to the



VLT and the 42-metre ELT: the development of active optics as the basis of all modern telescope optics”. Figure 1 shows Ray receiving the Tycho Brahe prize from the retiring president of the EAS, Joachim Krautter.

Ray Wilson, who was born in England and educated at Birmingham University and Imperial College London, arrived at ESO in 1972 from Zeiss at Oberkochen, Germany where he had been head of the Optical Design Department for Astronomical and Analytical Instruments. At ESO, first in Geneva and then in Garching, he was the first head of the ESO Optics and Telescopes Group. The revolutionary active optics of the 3.58-metre NTT, inspired by two years of work at the La Silla Observatory, was the crowning achievement of Ray’s work at ESO. This successful concept, where both the alignment of the optical elements as well as the shape of the flexible primary mirror are controlled in a closed loop based on the measurements of a wavefront sensor, was then also used for the VLT 8.2-metre telescopes. In addition, Ray contributed to telescope designs with more than two powered mirrors, which are now being explored for the next generation of extremely large telescopes, such as the European Extremely Large Telescope (E-ELT) project.

Figure 1. Ray Wilson receiving the Tycho Brahe prize from the president of the EAS at the JENAM meeting in Lisbon, Portugal.

During his last years at ESO he began work on his magnum opus, the two-volume work *Reflecting Telescope Optics*, published by Springer⁵. Volume I: *Basic Design Theory and Its Historical Development*, first appeared in 1996, and Volume II: *Manufacture, Testing, Alignment, Modern Techniques* followed in 1999. Both are currently in their second edition and Ray is working on updates for the third editions. Ray has also been honoured by a number of other prizes, including the Karl Schwarzschild Medal of the German Astronomical Society, an appointment as Chevalier of the French Légion d’Honneur and the Prix Lallemand of the French Academy of Sciences.

Links

- ¹ The Kavli Prize: <http://www.kavlifoundation.org/kavli-prize>
- ² Announcement of Kavli Prize for astrophysics: <http://www.kavlifoundation.org/2010-astrophysics-citation>
- ³ ESO announcement of Kavli Prize: <http://www.eso.org/public/news/eso1022/>
- ⁴ Announcement of Tycho Brahe Prize: <http://www.eso.org/public/announcements/ann1018/>
- ⁵ Wilson, R. N. 2004, *Reflecting Telescope Optics*, Volumes I and II, 2nd edition, (Heidelberg: Springer)

Availability of Reduction Software for HARPS Data at ESO Headquarters in Garching

Gaspare Lo Curto¹
Thierry Beniflah¹
Andrew Burrows¹
Eric Emsellem¹
Kevin Maguire¹
Luca Pasquini¹
John Pritchard¹
Martino Romaniello¹

¹ ESO

From the start of the year 2011 the HARPS data reduction software will be also available at ESO Headquarters in Garching. This new initiative will enable users to apply for access to the system locally in Garching.

The experience of the past few years of operations of HARPS has shown that sometimes the data reduced online at the La Silla Observatory might require further reprocessing and analysis. This is usually because the wrong set of initial parameters have been specified in the observing template (such as stellar spectral type or

initial guess for the radial velocity). In these cases the spectral extraction is not affected, but the precision and the accuracy of the radial velocity measurement are generally not optimal. Although these cases are not frequent, they do happen from time to time and require re-computation of the radial velocities. We aim to address such needs by allowing individual users to visit ESO Headquarters in Garching and give them access to the same data reduction software that is available at the La Silla Observatory site, both in its on- and off-line flavours.

Users wishing to take advantage of this service are encouraged to check the details at the web page¹. The user should then contact ESO giving a brief scientific and technical rationale as to why reprocessing is required, together with the amount of data that needs to be reduced and the intended dates of travel to Garching. ESO, after checking availability, will make available desk space and will grant access from the user's laptop to the data reduction computer. Limited on-site user support will also be provided

(e.g., introduction to the data reduction system, etc.). Regrettably ESO will not be able to cover any expenses (travel, accommodation, etc.) for these "data reduction missions". The visitor will use her/his own laptop to run the data reduction software remotely via the standard GUIs. The raw data will then be transferred to the reduction machine, either from a laptop (i.e. via ftp) or from the archive ftp site after an archive request has been processed. Saving the reduced data is the responsibility of the user. Visitors are expected to spend at most five days on each data reduction mission, and the service will be available during normal office hours from Monday to Friday at ESO Headquarters in Garching.

Users wishing to employ this HARPS reduction service in Garching should send an email to re-harps@eso.org.

Links

¹ Details of the service at: www.eso.org/sci/facilities/lasilla/instruments/harps/tools/reprocess.html

ESO Participation at the Joint European and National Astronomy Meeting in Lisbon, Portugal

Oana Sandu¹
Lars Lindberg Christensen¹

¹ ESO

The Joint European and National Astronomy Meeting (JENAM) that took place in Lisbon, Portugal, during the week of 6–10 September 2010, was the 18th Annual Meeting of the European Astronomical Society (EAS) and the 20th Annual Portuguese Meeting of Astronomy and Astrophysics. JENAM brings European astronomers together to discuss frontline topics in astronomy, space science and instrumentation technology.

ESO was extensively involved in the meeting, highlighting its role as a driving force in ground-based astronomy at the European level, as well as globally. Several key ESO people participated in the meeting and there were also an ESO plenary and special session, an ESO exhibition with free educational and informational material and a book launch.

During the first day of the meeting, ESO participated in the special session on Astronomy Challenges for Engineers and Computer Scientists with talks by Bruno Leibundgut, Director for Science, on science projects at ESO and Andreas Kaufer, Director of La Silla Paranal Observatory, on ESO's infrastructures. Roberto

Tamai, Head of ESO's Technology Division, showcased the technology of the VLT/VLTI, while Roberto Gilmozzi, Head of ESO's Telescope Division, presented the principal technological features of the European Extremely Large Telescope (E-ELT); a project that incorporates many innovative developments. A presentation on control software and data reduction and analysis was delivered by Michèle Péron, Director of Engineering and Software Development.

On Tuesday, 7 September, there was a dedicated ESO plenary session. Bruno Leibundgut gave a comprehensive talk about recent developments at the La Silla Paranal Observatory, including plans for

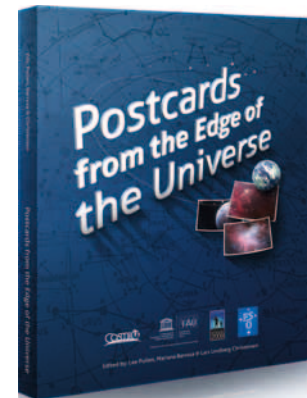
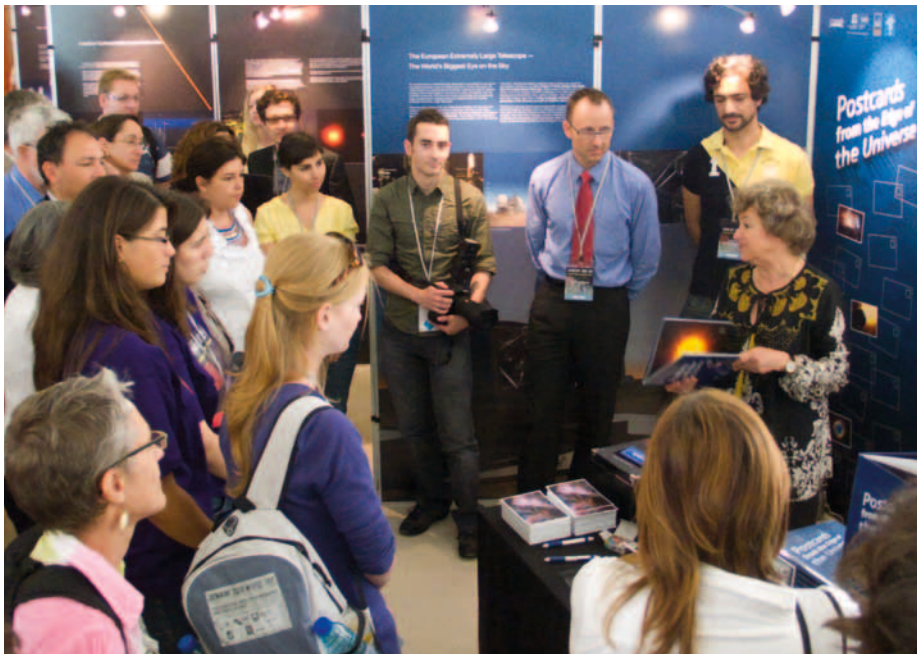


Figure 1. The ESO stand at JENAM in Lisbon, Portugal shown during the launch of the book *Postcards from the Edge of the Universe*. Catherine Cesarsky, former ESO Director General and past President of the IAU, is shown discussing the book.

the E-ELT. He was followed by the leader of the ESO Survey Team, Magda Arnaboldi, who presented the status of the Public Surveys that have recently begun with VISTA.

A special session on ALMA Early Science took place on the same day. The session included presentations on the current status of the construction project, the ALMA development plan and its opportunities, and the European ALMA Regional Centre plans for user support in preparation for Early Science. The session also included a demonstration of the ALMA software that will be used to apply for observing time on ALMA, to prepare observations, interact with the ALMA archive and reduce the data.

ESO also participated in the session dedicated to Education and Outreach after IYA2009 in Europe. Pedro Russo, Global Coordinator for the International Year of Astronomy 2009, talked about his experience in spearheading this project.

During the five days of the conference, ESO exhibited its astronomical discoveries, and the telescopes that made these discoveries possible. The E-ELT project attracted the interest of many passers-by who admired the telescope model and went on to learn more about

the instrument that will be the world's biggest eye on the sky.

In order to encourage interaction between participants and foster debates on topics related to astronomy in a more relaxed environment, ESO ran the ESO Hour at its stand on three days of the meeting. The event proved to be successful, gathering numerous participants from the meeting who engaged in conversation with people from the organisation.

One of the highlights at the ESO stand was the launch of the book *Postcards from the Edge of the Universe*. This book is based on the science carried out by a hand-picked selection of the best bloggers from the Cosmic Diary¹, one of the 12 Cornerstone projects of the International Year of Astronomy 2009. Twenty-four astronomers from all corners of the globe explain their science in articles edited by Lee Pullen, Mariana Barrosa and Lars Lindberg Christensen.

Announced several days in advance and kept as a surprise, the book launch took place on Tuesday, when several of the authors and editors talked about the book (see Figure 1). A special talk was given by a guest of honour — the former ESO Director General Catherine

Cesarsky. A book signing session took place and free postcards signed “Greetings from the Edge of the Universe” were distributed to people, who were encouraged to post them to their family and friends. More information on obtaining PDF copies of the book, or information on how to order a hard copy or send electronic postcards, are available².

Among other highlights of the meeting included the inauguration of the EAS Lodewijk Woltjer Lecture award talks with Woltjer himself giving the first talk. Under his leadership as Director General, ESO signed the VLT contract and established itself as one of the world's leading astronomical institutes. Lodewijk Woltjer also made significant contributions to theoretical astrophysics from his fundamental work on the Crab Nebula and his studies on the energy source of radio galaxies and quasars. Another highlight of the JENAM meeting was the award of the EAS Tycho Brahe Prize for 2010 to telescope designer Ray Wilson (see the article on p. 41).

Links

¹ Cosmic Diary: <http://www.cosmicdiary.org>

² *Postcards from the Edge of the Universe*: <http://www.postcardsfromuniverse.org>

Visiting ESO's Office in Santiago

Michael West¹

¹ ESO

Astronomers travelling to Chile to observe with ESO telescopes are encouraged to include a visit to ESO's office in Santiago. With the recent completion of the new ALMA building (see Figure 1), there is now a vibrant scientific community of more than 100 astronomers, fellows and students at the ESO premises in Santiago. ESO's Office for Science in Chile is happy to provide accommodation and *per diem* for visiting astronomers who wish to give a science talk and interact with ESO and ALMA staff. If interested, please contact Michael West (mwest@eso.org). We look forward to welcoming you to Santiago!



Figure 1. The hand-over ceremony for the new ALMA offices at the ESO premises in Santiago. Tim de Zeeuw (ESO Director General, left) and Thijs de Graauw (ALMA Director, right) exchange the key.

Café & Kosmos Events in Munich

Henri Boffin¹
Hannelore Hämmerle²
Barbara Wankerl³
Silke Zollinger⁴

¹ ESO

² Max-Planck-Institut für extraterrestrische Physik, Garching, Germany

³ Excellence Cluster Origin and Structure of the Universe, Garching, Germany

⁴ Max-Planck-Institut für Physik, Munich, Germany

On a Monday evening such as the 5th of July this year, the trendy bar Café Jasmin in the Schwabing district of Munich is full inside, despite the hot air and blazing Sun that would normally invite people to enjoy a beer outside in a tree-shaded



Credit: A. Griesch/MPP

Figure 1. An interested crowd in lively discussion with the physicist Stefan Stonjek from MPP at the first Café & Kosmos event.

garden. Although we are in the midst of the international football season, these people did not gather to watch another game of the World Cup; oddly enough, these are members of the public interested in science, and in our Universe in particular. They are here to listen and discuss with ESO astronomer Markus Kissler-Patig, the fundamental question: Are we alone in the Universe?

Subsequent science cafés have confirmed the success of the first event that took place on 31 May 2010, when Stefan Stonjek, a physicist from the Max-Planck-Institut für Physik (MPP), discussed *The Big Bang in the Tunnel*, covering the latest details about the CERN Large Hadron Collider (see Figure 1). The complex topic of string theory was aired by Ilka Baumgartl and Marco Baumgartl from the Excellence Cluster in September and the subject of the black hole at the heart of the Milky Way was discussed by Stefan Gillessen from the Max-Planck Institute for Extraterrestrial Physics in November. The series is entitled *Café & Kosmos* and is a joint initiative between ESO, the Excellence Cluster Origin and Structure of the Universe, and the Max-Planck Institutes for Physics, Astrophysics and Extraterrestrial Physics.

The idea is to bring science directly to the general public in the Munich area in the relaxed atmosphere of a bar.

For many, research is “far away” and happens behind the closed doors of laboratories. Admittedly, there are many science magazines in print or on television and some newspapers have a page about science, but the contact between science and the public is often very indirect. Many scientific institutions organise open days, which are often very successful, but these take place only once a year at most. Public conferences on scientific themes are also often popular, but they generally follow the same academic scheme: the scientist speaks and the public listens. Direct exchanges between scientists and the public seldom take place.

The *Café & Kosmos* initiative aims to bring researchers and non-scientists together, and to do so in places where people typically meet, share their thoughts, discuss business and debate about big and small things. Thus a pub in the centre of the city of Munich was chosen for the meetings; a place where communication traditionally takes place. With *Café & Kosmos*, we want to give

people the chance to speak directly with scientists about current fascinating scientific themes.

The proposed themes for *Café & Kosmos* come from astrophysics, cosmology and particle physics, and are on topics of great interest for non-scientists, such as “What are black holes?”, “What do we know about dark matter?”, “Why did CERN build the LHC?”, “What do we know about planets outside our Solar System?”, and so on. The discussions are held in German. These and other topics are discussed in the relaxed atmosphere of a pub — every first Monday of the month. The duration of the discussions is initially about one and a half hours, although our first two experiences have shown us that many people tend to stay for much longer.

For more information on the *Café & Kosmos* series, including the list of future speakers, please go to <http://www.cafe-kosmos.org>.

It is a pleasure to thank Aleks Vulic, owner of *Café Jasmin*, for his permission to use his premises for these interactive sessions, as well as the speakers.

New Staff at ESO

Jean-Philippe Berger

I have been at ESO as a VLT staff astronomer, on leave from the Laboratoire d’Astrophysique de Grenoble (France), for about 10 months. I came to Santiago with my wife Stephanie and our three children Clara, Lucie and Axel.

I remember my very early fascination with ruins that later turned into a deep interest in human civilisations and especially their dawn and dusk. This has never left me. I believe the connection between

my passion for history and astronomy occurred in a remote Spanish village when I was approximately ten years old. My uncle had a TV (our family did not) and I watched an episode of the well-known science fiction series *Cosmos* 1999. It came as a revelation that man could travel into space and reach remote parts of the Universe. I immediately became interested in rockets and space shuttles. Finding and studying new civilisations seemed to be a realistic project and it took me a few years to accept that current technology was

barely capable of flying to the planets in the Solar System. Then at the age of 13 I received a book from my uncle: *Le Ciel* by Jean-Claude Pecker. This was the true revelation that one could “travel” in space thanks to telescopes and an imaginative brain.

Even though I continued to follow history lectures throughout my academic career, my educational path slowly but surely shifted towards science and technology and the final call to become an astronomer came during my short

stay at ENS Lyon for my masters in astrophysics. After a two-year stay in Chad, Africa, as a physics teacher, I joined the Laboratoire d'Astrophysique de Grenoble (LAOG) in 1995 for a PhD on the polarising properties of dusty environments in young pre-main sequence binaries. Towards the middle of my PhD I realised that I wanted to become involved in an instrumentation project. One day, on the stairway, I met a colleague who was also an optical engineer, Pierre Kern, who was very excited by his new idea to use the miniature optical circuits developed by the telecommunications industry to produce interference between the light of two telescopes. I was immediately struck by the potential of this technology for aperture synthesis in the optical and asked him if there was a way for me to contribute to the project. Unfortunately he was applying for a grant to recruit a PhD student and had a good candidate; but fortunately (for me) the grant never arrived and I spent the remaining part of my PhD developing this new and promising technology. Since then the term "Astrophotonics" has been coined to describe the marriage between photonics and astrophysics.

So, eighteen months from the end of my PhD grant I started everything from scratch, and I found myself alone in an empty lab with the task of exploring how to apply photonic technology to astronomical interferometry. Fortunately I married Stephanie almost at the same time as I changed my research path and her presence by my side for all these years has been essential in holding me to this new path. My thesis culminated in resolving the accretion disc of a young star, FU Orionis, for the first time with astronomical unit resolution, working with my unofficial but remarkable advisor and friend Fabien Malbet, who taught me how to use the Palomar Testbed Interferometer, which was then the only instrument with sufficient sensitivity to study protoplanetary discs. At the end of my PhD I realised that my research interests combined challenging astrophysics with challenging instrumentation.



Jean-Philippe Berger

I continued developing integrated optics technology after my thesis, thanks to the support of the French Space Agency (CNES). I dived into the photonics world for two years at LEMO and in 2000 I obtained a NASA/JPL Michelson Fellowship to work with Wesley Traub and his team at the Harvard-Smithsonian Center for Astrophysics. My project was to install an instrument, IONIC3, capable of combining three beams of the IOTA interferometer in Arizona and to use it to generate the first images of the circumstellar environment in a pre-main sequence star. I remember those American years with a lot of affection, and the seemingly countless days and nights spent at IOTA (Mount Hopkins, Arizona) and CHARA (Mount Wilson) still live with me. We expended a huge amount of energy to try to produce the first maps of young stellar objects in the near-infrared. This was partially successful, but clearly limited by the lack of long baselines at IOTA.

In 2002 I took up a permanent position at the Observatoire de Grenoble, where I continued to develop new projects related to astronomical aperture synthesis imaging. I also started to get more and more involved in teaching at the

Université Joseph Fourier and in public outreach and realised that it was an essential part of our mission as "astronomes de la République". Finally, in 2008, at a conference in Marseille, some of my colleagues and myself were impressed by the imaging results coming out from the MIRC instrument at CHARA and became convinced that the VLTI and integrated-optics technology were ready for four-telescope operation. This discussion gave birth to the PIONIER VLTI visitor instrument project that I initiated and led in collaboration with some in December 2008. Since then PIONIER has been built and it received its first stellar photons in October 2010.

Coming to ESO and VLTI was thus a natural move. First I could follow PIONIER and secondly I was keen to join the impressive Paranal astronomical machine and the excellent VLTI team.

Fellows at ESO

Margaret Moerchen

I grew up in central Texas, where city lights frequently obscured the nightly show of constellations. (While we proudly refer to Texas as The Lone Star State, it isn't for this reason!) When it was time for a meteor shower, I could make a short drive into the hill country where a much richer sky was revealed — and perhaps it's because the stars weren't always in plain sight that these glimpses were so inspiring.

These night-time excursions continued while I did my undergraduate coursework at the University of Texas at Austin. I then found an even darker sky in the Davis Mountains, home of McDonald Observatory, where I had my first experience using a “big” (0.75-metre) telescope. After graduating, I took my first step into mid-infrared astronomy by working on the design of EXES (Echelon Cross Echelle Spectrograph), a spectrograph that will soon fly on SOFIA, the Stratospheric Observatory for Infrared Astronomy.

Wanting to continue in the hot field of the thermal infrared, I went to the University of Florida to participate in the building of mid-infrared instruments such as T-ReCS (Thermal Region Camera and Spectrograph) for Gemini South. I spent five monsoon seasons in Gainesville, where my thesis research employed T-ReCS and other mid-infrared cameras to study the architecture of young planetary systems by determining the location of warm dust within them. At the same time, I had the opportunity to become involved in the development of CanariCam (presently in the commissioning phase), the mid-IR facility instrument for the Gran Telescopio Canarias, the 10.4-metre segmented-mirror telescope on La Palma.

After attending the Observing Planetary Systems workshop at ESO Chile in 2007, I thought this would be a fantastic place to combine the pursuits of both scientific research and instrumentation development. I became even more sold on ESO after I had the chance to visit Paranal to assist in a post-intervention characterisation of VISIR. Now, almost three years



Margaret Moerchen

later, I'm back at the VISIR console as instrument fellow and am part of the team working on its exciting upgrade project. My functional duties include support of observations not only with VISIR, but with all instruments at Unit Telescope 3 (UT3) and UT4, and at UT4 I've been able to learn more about adaptive optics and the near-infrared regime. Performing a wide variety of science programmes at the two telescopes has provided a unique perspective on the power of 8-metre telescopes, and welcoming visiting astronomers and hearing enthusiastic detailed descriptions of their projects is one of the most rewarding aspects of the support work. In fact, even driving astronomers up or down the mountain in the middle of the night offers one of the benefits we sometimes forget — to look at the night sky! I've seen the most spectacular crumbling-fireball meteors of my life while on the summit road, and they're an impressive reminder of why I travelled thousands of miles to stay up at night in the middle of the desert.

Davor Krajnović

On a warm summer night, in the company of a dentist, a physician and a manager, in the cockpit of a sailing boat that rocks slowly, while a breeze brings the smell of pine trees and the buzzing sound of a few persistent cicadas, and the stars shine on us with the intensity of a crystal-clear night, the dentist concludes: “What a good job you have: looking at the stars!”

I often ask myself, how many decisions I made to get here. Until I was more than half way through my university physics degree I was not thinking of being a professional astronomer. I had not even looked through a telescope until about that time. One of the first convincing moments was when I joined a group of fellow students on a visit to the observatory in the sleepy town of Višnjan in Croatia, where amateur astronomers were becoming professionals in their achievements of spotting Near Earth Objects. There I had a first glimpse of the life of an astronomer: it was not just star-gazing. There was a lot of careful and patient taking of pictures, comparing them, and working with different image-processing software, and so on, throughout the night, until the rain came. It was fun!

The starting point in my career was the acceptance to do a PhD at the Leiden Observatory. Very early on, I went to observe with the SAURON integral-field unit mounted on William Herschel Telescope on La Palma. The fifth observing run of the SAURON Project was 14 nights long and a number of team members came to share the time, but I stayed for the full run. Two weeks on the mountain, not having to close the dome once, catching as many photons as the detectors allowed, from dusk until dawn, and, just before going to sleep, looking at the shadow of the mountain on the clouds or the Atlantic Ocean, this was something extraordinary. I was hooked.

I spent four wonderful years in Leiden. My thesis consisted of the analysis of the nuclear properties and dynamical modelling of nearby early-type galaxies, as well as developing a method to analyse the two-dimensional kinematic maps coming from instruments such as SAURON. After the PhD, I went to Oxford where I stayed for five years. For the last two I was an Extraordinary Junior Research Fellow of Queen's College (the "Extra" actually means they were not paying my salary, but they did take care of me as a college does). There I started working in the near-infrared and with laser-guided adaptive optics observations, which unfortunately also meant that trips to the telescopes became rarer. A large part of my science, however, concentrated on a new and exciting project, the ATLAS3D survey, which I am co-leading. This is a multi-wavelength survey of a complete sample of nearby early-type galaxies, and it includes a large team of

observers and theoreticians. The first results are coming out right now and it is amazing to see how the initial ideas have turned into science.

It is now about ten years since I left my hometown and I am entering my second year as an ESO fellow. Astronomy really is not just star-watching, and ESO is a prime example of the complexity needed for successful astronomical operations. I feel rather privileged to be able to participate in it. On a warm summer night, however, when a friend says it is a good job, this star watching, one has to make a decision: to agree, or say: "Well, actually I study black holes ..."



Davor Krajnović

In Memoriam Christine Nieuwenkamp

Tim de Zeeuw¹

¹ ESO

Christine (Chris) Nieuwenkamp was born in Belgium and studied at the Higher Institute for Translators in Antwerp. She started her professional career in the purchasing department of a Brazilian mining company stationed in Belgium. She joined ESO in April 1990 as Administrative Assistant for Purchasing in the Contracts and Procurement Service at ESO Headquarters in Garching.

Through her strong motivation and dedication, Chris was able to cope with a constantly high workload, especially related to calls for tender, contracts and contract administration, and interacted with a large number of staff in both Garching and Chile. In addition Chris successfully trained and integrated new staff in the Contracts and Procurement Department. For several years Chris was an active and respected member of the ESO Staff Association in Garching. Her excellent performance as a Procurement Officer was well-recognised both inside and outside ESO and she was a pleasure to work with. She died on 18 October 2010. Chris will be remembered by her friends and colleagues at ESO and missed by her husband and two children.



Announcement of the

ALMA Community Days: Towards Early Science

6–7 April 2011, Garching, Germany

ALMA, the Atacama Large Millimeter/submillimeter Array, is expected to be the leading observatory at millimetre and submillimetre wavelengths over the coming decades. It is the result of a global collaboration involving Europe, North America, East Asia and the host country Chile. When completed, it will comprise at least 66 high precision antennas equipped with receiver and digital electronics systems to observe in the frequency range from 30 GHz to 1 THz and achieve angular resolutions as high as 5 milliarcseconds. Dynamic scheduling and innovative calibration strategies will ensure the most efficient use of the unique atmospheric qualities encountered at the 5000-metre high site on the Chajnantor plateau in the northern Andes.

While Full Science Operations are estimated to begin in 2013, the increasing capabilities of the growing array will become available to the astronomical community following the start of Early

Science Operations in the second half of 2011. During the first phase of Early Science, an array of 16 antennas will be offered for interferometry with four frequency bands and a limited range of baselines. Early Science observations are currently estimated to be scheduled for at most one third of the available time, the remainder being reserved for continuing commissioning and science verification activities.

Scientific users will interact with the ALMA facility through their local ALMA Regional Centre (ARC), which will provide user support on all aspects related to observing with ALMA and assist observer teams throughout the lifecycle of their project. The European ALMA community is supported by a network of regional ARC nodes that are coordinated by the central European ARC hosted at ESO Headquarters in Garching, Germany.

With the ALMA Community Days, the ESO ARC aims to prepare the European astronomical community for ALMA Early Science operations. The first day will be dedicated to a series of scientific and technical presentations related to ALMA and Early Science capabilities, while the second day will be taken up by interactive tutorials on the preparation of ALMA observing proposals using the ALMA Observing Tool (OT). This should help novice and advanced ALMA users alike to create observing projects that optimally exploit the unique capabilities of ALMA during Early Science operations.

Further information can be found at www.eso.org/sci/meetings/2011/alma_es_2011.html or by emailing alma_es@eso.org.



Announcement of the ESO Workshop

Fornax, Virgo, Coma et al.: Stellar Systems in Nearby High Density Environments

27 June–1 July 2011, Garching, Germany

This workshop will provide an overview of recent observational results on the stellar systems in nearby galaxy clusters, i.e. Fornax, Virgo, Coma et al., and a forum for discussion and comparison of theoretical models for the evolution of galaxies and larger-scale structures with observational properties of stellar systems in high density environments at redshift zero. The aim is also to identify those questions that can be tackled by the European Extremely Large Telescope (E-ELT), as the exceptional high angular resolution and collecting power of an extremely large telescope are essential ingredients for the study of resolved stellar populations at distances larger than 10 megaparsecs. The nearby clusters Fornax, Virgo, Coma et al. will be the first obvious targets of this exciting new era in extragalactic astronomy.

Topics to be covered include:

- 1) the faint end of the galaxy luminosity function in clusters: dwarf galaxies, ultra-compact dwarfs and globular clusters;
- 2) the bright end of the galaxy luminosity function: stellar populations and dynamics — observation and theory;
- 3) surveys of nearby clusters and their follow-up with the ESO Very Large Telescope (VLT) and future facilities (E-ELT, Atacama Large Millimeter/Submillimeter Array, ALMA); and
- 4) the 3D structure of nearby galaxy clusters and the morphological transformation of galaxies.

The number of participants is limited to the capacity of the ESO auditorium (about 90 participants).

Scientific Organising Committee:

Magda Arnaboldi (chair), Nobuo Arimoto, Michele Cappellari, Eric Emsellem, Bill Harris, Ken Freeman, Ortwin Gerhard, John Kormendy, Harald Kuntschner, Claudia Maraston, Lucio Mayer, Simona Mei, Bianca Poggianti, Sadanori Okamura, Tom Richtler.

Local Organising Committee:

Magda Arnaboldi, Lodo Coccato, Luca Cortese, Michael Hilker, Marina Rejkuba, Christina Stoffer.

Web page for registration and further details will appear soon at <http://www.eso.org/sci/meetings.html>.

Personnel Movements

Arrivals (1 October–31 December 2010)

Europe	
Ascenso, Joana (P)	Fellow
Beccari, Giacomo (I)	Fellow
Boissier, Jérémie (F)	Fellow
Bressert, Eli (USA)	Student
Coccatto, Lodovico (I)	Fellow
Gabasch, Armin (I)	Software Engineer
Heidecke, Thies (D)	Student
Kains, Noé (B)	Fellow
Lablanche, Pierre-Yves (F)	Student
Longmore, Steven (GB)	Fellow
Lützgendorf, Nora (D)	Student
Pettazzi, Lorenzo (I)	Control Engineer

Chile	
Alvarez, Fernando (RCH)	Head of the Maintenance Department
Gonzalez, Jaime (RCH)	Optical Technician
Jones, Matias (RCH)	Student
Miccolis, Maurizio (I)	System Engineer
Rodrigues, Myriam (P)	Fellow
Vanderbeke, Joachim (B)	Student
Vega, Florine (RCH)	Procurement Clerk

Departures (1 October–31 December 2010)

Europe	
Beniflah, Thierry (F)	Head of Information Technology
Bois, Maxime (F)	Student
Cortesi, Arianna (I)	Student
Frank, Matthias (D)	Student
Guidetti, Daria (I)	Student
Hansen, Camilla Juul (DK)	Student
Hewitson, Jennifer (D)	Secretary/Assistant
Larsen, Jonas (DK)	Software Engineer
Lombardi, Marco (I)	Astronomer
Naets, Thomas (B)	Internal Auditor
Neumayer, Nadine (D)	Fellow
Penuela, Tania Marcela (CO)	Student
Ruiz Velasco, Alma (MEX)	Student
Russo, Pedro Miguel (P)	Astronomer
Seemann, Ulf (D)	Student
Taylor, Luke (GB)	Laser Physicist
Unterguggenberger, Stefanie (A)	Student
Williams, Michael (GB)	Student

Chile	
Asmus, Daniel (D)	Student
Kaminski, Adrian (D)	Student
Raffi, Gianni (I)	Head of the Computing IPT
Thomas, Alexis (RCH)	Network Specialist
Varas, Oscar (RCH)	Dome Mechanic



Credit: ESO/V. Beletsky

A wide field image of the southern hemisphere constellations Crux and Centaurus which make up part of the Scorpius Centaurus Association (Sco OB2), the nearest region of recent massive star formation.

This OB association was studied by Adriaan Blaauw in his PhD thesis (1946) and published in Bulletin of the Astronomical Institutes of the Netherlands (Blaauw 1952, BAN, 11, 414).

In Memoriam Adriaan Blaauw

Adriaan Blaauw, the European Southern Observatory's second Director General, and a key figure in ESO's early history, died on 1 December 2010, at the age of 96.

"Adriaan Blaauw was one of the most influential astronomers of the twentieth century. I had the privilege to be amongst his students when he returned to Leiden from his position as Director General. He continued to remain keenly interested in everything to do with ESO, and still had his characteristic twinkle in the eye when he visited La Silla and Paranal earlier this year. It is hard to grasp that he is no longer with us," said ESO's current Director General, Tim de Zeeuw.

Adriaan Blaauw was born in Amsterdam, the Netherlands, in 1914. He studied astronomy at Leiden University, under de Sitter, Hertzsprung and Oort, and obtained his doctorate with van Rhijn at the Kapteyn Laboratory in Groningen in 1946, with a thesis entitled, "A study of the Scorpio–Centaurus cluster". During his career, Blaauw studied the properties of OB associations (groups of young, hot stars) which contain the fossil record of their star formation history. Perhaps his most famous work explained why some of these stars are found to be travelling unusually rapidly — so-called run-away stars. Blaauw proposed that these stars had originally been members of binary systems, but that when one star in the binary experiences a supernova explosion, its companion suddenly ceases to feel the gravitational pull that keeps it in its orbit and hence it "runs away" at its orbital velocity. This work was published in his 1961 paper, "On the origin of the O- and B-type stars with high velocities (the 'run-away' stars), and some related problems".

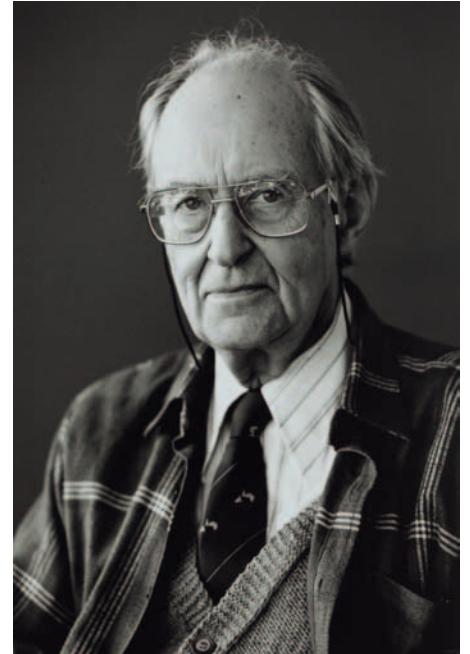
In addition to his distinguished research career, Blaauw played a central role in setting up ESO. In 1953, the astronomers Walter Baade and Jan Oort proposed the idea of pooling European resources and funding to create an astronomical

research organisation that could compete on the international level. Blaauw had returned to Leiden in 1948, moved to Yerkes Observatory in 1953, becoming its associate director in 1956, and moved back to Groningen in 1957, where he was in a key position to contribute to putting the idea of Baade and Oort into practice.

ESO was founded in 1962, and Blaauw took up the position of Scientific Director in 1968 and subsequently became the organisation's second Director General from 1970 until 1974. During that time, several telescopes, including the ESO 0.5-metre and 1-metre Schmidt telescopes, began operating at ESO's first observatory site, La Silla, in Chile. This was also a key period for the design and construction of the ESO 3.6-metre telescope, which had its first light in 1976. Blaauw decided that it was crucial for this project to move ESO Headquarters from Hamburg to Geneva, to benefit from the presence of the CERN engineering group. Today, the 3.6-metre telescope remains at the forefront of research, hosting the HARPS spectrograph — the world's foremost exoplanet hunter.

"The early years for any organisation, particularly one in which half a dozen countries and their governments are involved, can provide many challenges. But with Adriaan Blaauw's leadership, preceded by Otto Heckmann, ESO started off on a strong footing," said de Zeeuw.

After stepping down as Director General of ESO, Blaauw returned to Leiden, and continued to play a very important role in international astronomy. He was President of the International Astronomical Union from 1976 to 1979, during which period he managed to convince China to rejoin the IAU. Blaauw retired in 1981 and moved back to Groningen, but stayed active. He served as Chairman of the Scientific Evaluation Committee for the European Space Agency satellite Hipparcos, advising on many aspects of its scientific programme.



Blaauw was well known for his legendary patience and wisdom, and for his genuine interest in astronomy and astronomers, including the most junior students. He liked to bring order quietly to most topics that he turned his attention to. This included the archives of ESO and of the IAU — work which resulted in two books, *ESO's Early History* and *History of the IAU*. His personal account of his life entitled *My Cruise Through the World of Astronomy*, published in the 2004 *Annual Reviews of Astronomy and Astrophysics*, provides an extraordinarily accurate picture of a truly remarkable person, who influenced the lives of many others in a very positive way.

Tributes to Adriaan Blaauw will appear in the next issue of *The Messenger*.

Based on the text of the ESO Announcement ann1090.

ESO, the European Southern Observatory, is the foremost intergovernmental astronomy organisation in Europe. It is supported by 14 countries: Austria, Belgium, the Czech Republic, Denmark, France, Finland, Germany, Italy, the Netherlands, Portugal, Spain, Sweden, Switzerland and the United Kingdom. ESO's programme is focused on the design, construction and operation of powerful ground-based observing facilities. ESO operates three observatories in Chile: at La Silla, at Paranal, site of the Very Large Telescope, and at Llano de Chajnantor. ESO is the European partner in the Atacama Large Millimeter/submillimeter Array (ALMA) under construction at Chajnantor. Currently ESO is engaged in the design of the 42-metre European Extremely Large Telescope.

The Messenger is published, in hard-copy and electronic form, four times a year: in March, June, September and December. ESO produces and distributes a wide variety of media connected to its activities. For further information, including postal subscription to The Messenger, contact the ESO education and Public Outreach Department at the following address:

ESO Headquarters
Karl-Schwarzschild-Straße 2
85748 Garching bei München
Germany
Phone +49 89 320 06-0
information@eso.org
www.eso.org

The Messenger:
Editor: Jeremy R. Walsh
Design: Jutta Boxheimer; Layout, Typesetting: Mafalda Martins and Jutta Boxheimer; Graphics: Roberto Duque
www.eso.org/messenger/

Printed by Peschke Druck
Schatzbogen 35, 81805 München
Germany

Unless otherwise indicated, all images in The Messenger are courtesy of ESO, except authored contributions which are courtesy of the respective authors.

© ESO 2010
ISSN 0722-6691

Contents

The Organisation

G. Filippi – Enabling Virtual Access to Latin-American Southern Observatories	2
---	---

Telescopes and Instrumentation

G. Witzel et al. – On the Instrumental Polarisation of NAOS–CONICA	5
P. Hammersley et al. – Upgrading VIMOS	8
R. Arsenault et al. – Progress on the VLT Adaptive Optics Facility	12
L. Testi et al. – ALMA Status and Progress towards Early Science	17

Astronomical Science

A. Seifahrt et al. – Precise Modelling of Telluric Features in Astronomical Spectra	21
M. Sterzik et al. – Astronomy Meets Biology: EFOSC2 and the Chirality of Life	25
R. Gratton et al. – Observations of Multiple Stellar Populations in Globular Clusters with FLAMES at the VLT	28
S. Clark et al. – Dissecting the Galactic Super Star Cluster Westerlund 1 – A Laboratory for Stellar Evolution	31
R. Maiolino et al. – AMAZE and LSD: Metallicity and Dynamical Evolution of Galaxies in the Early Universe	36

Astronomical News

J. Walsh – Raymond Wilson Honoured with Two Prestigious Prizes	41
G. Lo Curto et al. – Availability of Reduction Software for HARPS Data at ESO Headquarters in Garching	42
O. Sandu, L. L. Christensen – ESO Participation at the Joint European and National Astronomy Meeting in Lisbon, Portugal	42
M. West – Visiting ESO's Office in Santiago	44
H. Boffin et al. – Café & Kosmos Events in Munich	44
New Staff at ESO – J.-P. Berger	45
Fellows at ESO – M. Moerchen, D. Krajnović	47
T. de Zeeuw – In Memoriam Christine Nieuwenkamp	48
Announcement of the “ALMA Community Days: Towards Early Science”	49
Announcement of the ESO Workshop “Fornax, Virgo, Coma et al.: Stellar Systems in Nearby High Density Environments”	49
Personnel Movements	50
In Memoriam Adriaan Blaauw	51

Front cover: Colour image of the barred spiral galaxy NGC 1365 (type SBb) in the near-infrared, taken with HAWK-I on the VLT. NGC 1365 is at a distance of about 18 megaparsecs and hosts an active galactic nucleus. The picture was created from exposures through Y, J, H and K filters with exposure times of 4, 4, 7 and 12 minutes respectively. See Photo Release eso1038 for more details.